Topics in Field Theory and Particle Phenomenology

Sichun Sun

A dissertation
submitted in partial fulfillment of the
requirements for the degree of

Doctor of Philosophy

University of Washington

2014

Reading Committee:

David B.Kaplan, Chair

Andreas Karch

Ann E.Nelson

Program Authorized to Offer Degree:
UW Physics department

University of Washington

Abstract

Topics in Field Theory and Particle Phenomenology

Sichun Sun

Chair of the Supervisory Committee:
Professor David B.Kaplan
Department of physics

In this thesis, I focus on a few different applications of modern quantum field theory. I start with a model beyond the standard model: Little Flavor Theory and its related collider phenomenology. This model combines a flavor theory with Little Higgs theory, to explain the origin of flavor and little hierarchy problem at the same scale.

The field theory on intersecting D-brane has a monopole. The θ vacuum interface could support an electron-monopole dyon system. A certain configuration of D-branes is dual to Wilson lines on the field theory side. These are the other special topics in this thesis. I also include a chapter on a finite temperature field theory method to calculate the corrections to the equation of state.

TABLE OF CONTENTS

Page

LIST OF FIGURES

GLOSSARY

SM: Standard model

LHC: Large hadron collider

ILC: International linear collider

ADS: anti de sitter space

CFT: conformal field theory

CKM: Cabibbo-Kobayashi-Maskawa

PMNS: Pontecorvo-Maki-Nakagawa-Sakata

ACKNOWLEDGMENTS

First I would like to thank my advisor David B.Kaplan. He taught me a lot of details of physics with clear explanations. I always found myself understanding more after talking to him. He also showed me how to start and work through a project through the three papers on which we collaborated.

I would also like to thank Andreas Karch and Ann E. Nelson. It was a great pleasure to work with them. Andreas gave me my very first lesson about AdS/CFT, and topological insulators. Without him, more than half of my papers would have gone differently. Ann is the person who guides me into phenomenology, which seems to be my field after graduation. Their doors were always open if I had any questions. I thank Joe Polchinski at KITP, Santa Barbara, who taught me an intuitive way of thinking of string theory.

I wish to thank the other members in my committee, Anton Andreev, Robin Graham and Gorden Watts. Thank you to the other members in the particle theory and nuclear theory groups: Stephen Sharpe, Larry Yaffe, Stephen Ellis, Dam T. Son and Martin Savage, for the conversations we had.

The postdocs and fellow graduate students are the good company through this long Ph.D journey, and nice people to talk to and to hang out with. Life as a physics graduate student would be different without them.

I would like to thank all my friends from college, now they are scattered around the world, in physics or not. It was fun to get in touch sometimes.

Finally I would like to thank my parents, who have always been supportive of my career choice.

.

DEDICATION

To my parents

Chapter 1

INTRODUCTION

In this chapter I review some background knowledge of this thesis, addressing the problems that I want to solve. Start with two problems of the standard model, and one of its solutions: Little Higgs theory. Then going into three specific topics in particle theory: monopoles, D-brane and finite-temperature field theory. The rest of the thesis, from chapter 2 through 4 are the reprints of published papers which I authored or co-authored [107, 108, 124, 141, 172, 173].

1.1 The standard model: Hierarchy problem and new physics flavor problem

The Standard model of particle physics works really well so far with only a couple of problems, especially with the latest running result from LHC. There are things that the standard model cannot explain, including dark matter and neutrino mass. Moreover there are things that look unnatural.

Among unnatural things, the fine tuning of the Higgs mass, known as the hierarchy problem, has been a major concern. The problem is that the mass of Higgs boson, 126 GeV, is so small compared with the Plank scale. There are three fundamental constants in modern quantum physics: Planck's constant h, the building block of energy, the speed of light, c and Newton's gravitational constant G, and the Planck scale being $M \equiv \sqrt{hc/G} \approx 10^{19} GeV$. In the standard model, we would expect dimensional constant such as the Higgs mass that are not protected by a symmetry to be large. Especially in quantum field theory, there is nothing protecting scalar masses from getting a quadratic divergent correction. The one-loop diagrams yields:

$$\lambda^2/(4\pi)^2 \int^{M_{planck}} \frac{d^4p}{p^2} \sim \lambda^2/(4\pi)^2 M^2_{planck} \tag{1.1}$$

As the quantum correction for the Higgs mass squared. The coupling λ is an order one constant. This implies that to get the right Higgs mass, which is 36 order of magne-

tude smaller than the correction, it requires precise cancellation with no explanation. This generically called the gauge hierarchy problem.

This problem also implies that the scale of new physics beyond the standard model is around TeV, to have the new particle/symmetry to protect the Higgs mass. There are three major kinds of theories around to solve this gauge hierarchy problem, supersymmetry, extra dimensions and composite Higgs/Little Higgs. At current colliders none of them has been seen. All those extensions of SM have become increasingly constrained. In the next section I am going to focus on introducing one of these theories, the Little Higgs.

When constructing physics beyond the standard model, the flavor sector constrains the new physics. There are three generations of leptons and quarks in nature. Different generations of fermions have the same quantum numbers, just different masses. The mass eigenstates are not aligned with flavor eigenstates, which are defined by the couplings to the gauge bosons. The similarities among generations imply the flavor unification at some higher scale. However, these mixings are only through CKM matrix for quarks and PMNS matrix for neutrinos, while the other possible mixing processes (flavor changing neutral current) are highly suppressed. This suppression could come from the high scale of flavor origin, or some new symmetry to protect these processes from happening.

In the next chapter, I am going to present one of the major parts of my thesis work, Little Flavor theory. It is a theory that combines Little Higgs theory and a flavor theory, to solve the gauge hierarchy problem and flavor problem at the same time.

1.2 Little Higgs theory

Little Higgs types of theories have a long history dating back to the 80s [58,68,69,114,115], long long before Higgs being discovered, when people first attempted to treat Higgs boson as a composite object like pions and describe it by a chiral Lagrangian. The interest of this approach has been re-ignited in the 2000s, along with the line of 'deconstruction', a type of extra dimensional theory, and called Little Higgs [16,17,20,169].

There are a lot of similarities between these two theories, especially they both have some extra heavy fermions to cancel the quadratic divergence of top loop contributions to the Higgs mass, and some global symmetry, broken at higher loop level to protect the Higgs

mass. The major difference would be that composite Higgs normally has a much lower scale for 'pions', with a cut-off around TeV, while most of Little Higgs theory have a cut-off around 10 to 20 TeV. This difference is due to the details of how this top partner couples. Comparing to supersymmetry, which has a different spin partner, little Higgs/Composite Higgs has the same spin partner.

To illustrate this cancellation between the same spin partners, here is an example of SU(3) symmetries Little Higgs theory: Parametrize the order parameter as:

$$X = \begin{pmatrix} \eta & 0 & h \\ 0 & \eta & \\ h^\dagger & & -2\eta \end{pmatrix}, \text{With} \quad \phi = e^{iX/f} \tag{1.2}$$

$$L_{yuk} = \lambda_1/\sqrt{2} t_1^c \phi \Psi + \lambda_2/\sqrt{2} t_2^c \phi^\dagger \Psi \tag{1.3}$$

With $\Psi = (t, b, T)$ being the extended $Q = (t, b)$ left-handed quarks, and t_1^c and t_2^c being the right-handed singlets,$(0, 0, t_1^c)$,$(0, 0, t_2^c)$. Expanding this interaction,taking $\lambda_1 = \lambda_2 = \lambda$, one gets,

$$\lambda/\sqrt{2}[fT(t_1^c + t_2^c) + ih^\dagger Q(t_2^c - t_1^c) - \tfrac{1}{2f} h^\dagger h T(t_1^c + t_2^c) + ...] \tag{1.4}$$

$$= \lambda f(1 - \tfrac{1}{2f^2} h^\dagger h) T T^c + \sqrt{2}\lambda h^\dagger Q t^c \tag{1.5}$$

With $T^c = (t_2^c + t_1^c)/\sqrt{2}$, $t^c = i(t_2^c - t_1^c)/\sqrt{2}$. One can see explicitly the quadratic divergence cancel between two of them. From Figure 1.1:

$$\frac{\lambda^2}{(4\pi)^2}\Lambda^2 h^\dagger h + \frac{\lambda^2 f^2}{(4\pi)^2}(1 - h^\dagger h/f^2)\Lambda^2 + O(h^4) \tag{1.6}$$

From the equations above one can see the quadratic divergence indeed cancels between the same spin partners.

One could also see it more easily from a global symmetry perspective. ϕ has an unbroken $SU(3)_L \times SU(3)_R$ that rotates it around. When it couples as Yukawa coupling above, since Ψ has an unbroken $SU(3)$, this $SU(3)_L \times SU(3)_R$ only gets broken down to a different single $SU(3)$ in one λ_1 or λ_2 couplings. Each coupling preserves a different $SU(3)$, and the symmetry is only completely broken when both couplings are included, the remaining $SU(3)$

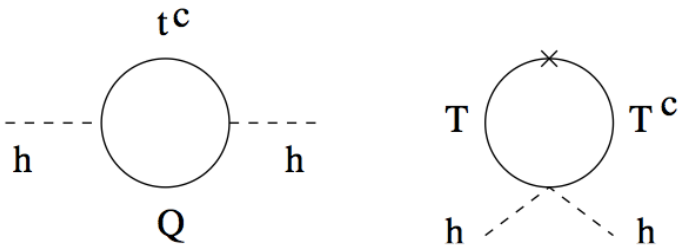

Figure 1.1: Top loop quadratic divergence is canceled by its partner, the extra fermion T

symmetry of ϕ protect the potential from generating for this non-linear sigma field ϕ at one loop order. The only way to generate the potential is to insert both λ_1 and λ_2, but that would result in contribution from higher loops, thus smaller and finite, or single loop with only finite piece but no quadratic divergence. This is called "collective symmetry breaking mechanism" of protecting the mass of the Little Higgs, which means literally demanding a collective of terms to completely break the symmetry of pseudo Nambu-Goldstone boson.

This is a simple example to show how the Little Higgs mechanism works. There are many different ways to construct this type of theory in the same spirit. Many phenomenological issues could arise from it, such as:

1. Top partner structures: which could give rise to different decay processes, and have an impact on detection schemes.

2. electroweak precision tests: s and t parameter, W, Z masses and coupling to quarks could severely constrain Little Higgs theory

3. new gauge boson searches put bounds on the extended gauge group.

4. new Nambu-Goldstone bosons decays in Higgs related processes.

1.3 Monopoles in field theory

A magnetic monopole is a solitonic object, which is the solution of classical field equations with an energy density that is localized in three spatial directions.The solution does not

change shape or dissipate with time. It is a topologically non-trivial field configuration, related to the homotopy group of the map from the boundary of space to the set of vacua.

The known monopoles are the 't Hooft and Polyakov monopole and its generalizations. The set of vacua is classified by the symmetry breaking of the gauge group, in the case of 't Hooft and Polyakov, it is $SU(2)$ spontaneously breaking down to $U(1)$, and the boundary of the space is a 2-sphere. $\Pi_2(SU(2)/U(1)) = Z$ indicates the existence of the monopole.

In the case of 't Hooft and Polyakov monopole, the topologically non-trivial soliton solution to the classical field equation for the scalar field has a non-trivial winding number n, which will result in the magnetic flux, $\Phi = -4\pi n/e$. This flux implies that it is a monopole with magnetic charge $Q_M = \Phi$. There is also the Dirac charge quantization condition, $Q_E Q_M = 2\pi k$, with k being an integer. This comes from the fact that the smallest electric charge in this $SU(2)$ gauge theory is $\frac{1}{2}e$.

In high energy theory, people also talked about a electron-monopole dyon system. One could define a statistical angle $\theta = \frac{Q_E Q_M}{2}$, in the unit of $h = c = 1$. Then this angle can only be 0 or π modular 2π in $3+1$ dimension, corresponding to the Bose-Einstein statistics for bosons or Fermi-Dirac statistics for fermions. The statistical angle shows that when one exchanges two particles, the phase $e^{i\theta}$ is acquired in this two-particle state. In the dimensions higher than two, it could only take values 0 or π. In two-dimensional space, when θ could take more values it is called anyon statistics. Anyonic wavefunctions are 1-dimensional representations of the braid group, while the fermion and boson wavefunctions in a three-dimensional space are 1d representations of the permutation group

In the Chapter 3 I will talk about the work on constructing a $U(1)$ monopole from D-branes and some effect on the anyons from a theta-vacuum interface.

1.4 D-branes in AdS space

Around time from 1995 to 1999, the so-called 'second string revolution' happened, which completely changed the landscape of string theory. Among all the things is the appreciation of the important role of extended objects rather than just 2 dimensional strings in these theories. The bosonic string and both type II and I superstring theories have fundamental objects, called D-branes (Dirichlet-branes), which are stringy solitons that carry Ramond-

Ramond charge [155].

Originally, people knew that this p-brane is a $p+1$ dimensional surface where open strings end, could arise in T-duality in superstring theory. It was also known that they arise as solutions to supergravity field equations. As supergravity is the low-energy limit of full string theory, p-branes can also be extended to the solution of the full Type IIA/B string equation.A D-brane has dynamics,and the open strings which end on it become supersymmetric U(1) gauge theory. One can describe the dynamics of D-branes by the Dirac-Born-Infeld action (DBI):

$$S_{DBI} = -T_P \int d^{p+1}\sigma(e^{-\phi}\sqrt{-det(P[G+B]_{ab} + 2\pi l_s^2 F_{ab})}) \tag{1.7}$$

T_p is the brane tension. The transverse locations of the D-brane are described by the $9-p$ real scalars ϕ in $U(1)$ supersymmetric gauge theory, with position $\Delta x^i = 2\pi l_s^2 \phi^i$. The $P[...]$ is the pull-back of the bulk spacetime metric G and antisymmetric tensor B to the D-Brane world-volume, B is the closed string field:

$$P[G(\sigma)]_{ab} = \frac{\partial X^\mu}{\partial \sigma^a}\frac{\partial X^\nu}{\partial \sigma^b} G_{\mu\nu}(X(\sigma)) \quad P[B(\sigma)]_{ab} = \frac{\partial X^\mu}{\partial \sigma^a}\frac{\partial X^\nu}{\partial \sigma^b} B_{\mu\nu}(X(\sigma)) \tag{1.8}$$

while $F_{\mu\nu}$ is made of the open string field A_μ, part of the $U(1)$ supersymmetric gauge theory.ϕ is the dilaton factor.

One of the interesting properties of D-branes is that this $U(1)$ gauge symmetry of one single D-brane will get enhanced to a non-abelian $U(N)$ symmetry when N D-branes are coincident. When N D-brane are coincident, the strings stretching between them become massless, those extra massless states become the extra representation in the $U(N)$ supersymmetric gauge theory.

Sometimes, it is interesting to compare the semi-classical solutions of string theory with solitons in quantum field theory, the 't Hooft-Polyakov magnetic monopole from last section could actually arise from 2 paralleled D3-branes. One can see it from the same symmetry breaking structure $SU(2) \to U(1)$ when one is seperating 2 D3-branes.

One of the interesting cases is N coincident D3-branes. From solving the supergravity field equation one has the 10d metric solution:

$$ds^2 = \left(1 + \frac{L^4}{y^4}\right)^{-\frac{1}{2}} \eta_{ij} dx^i dx^j + \left(1 + \frac{L^4}{y^4}\right)^{\frac{1}{2}} (dy^2 + y^2 d\Omega_5^2) \tag{1.9}$$

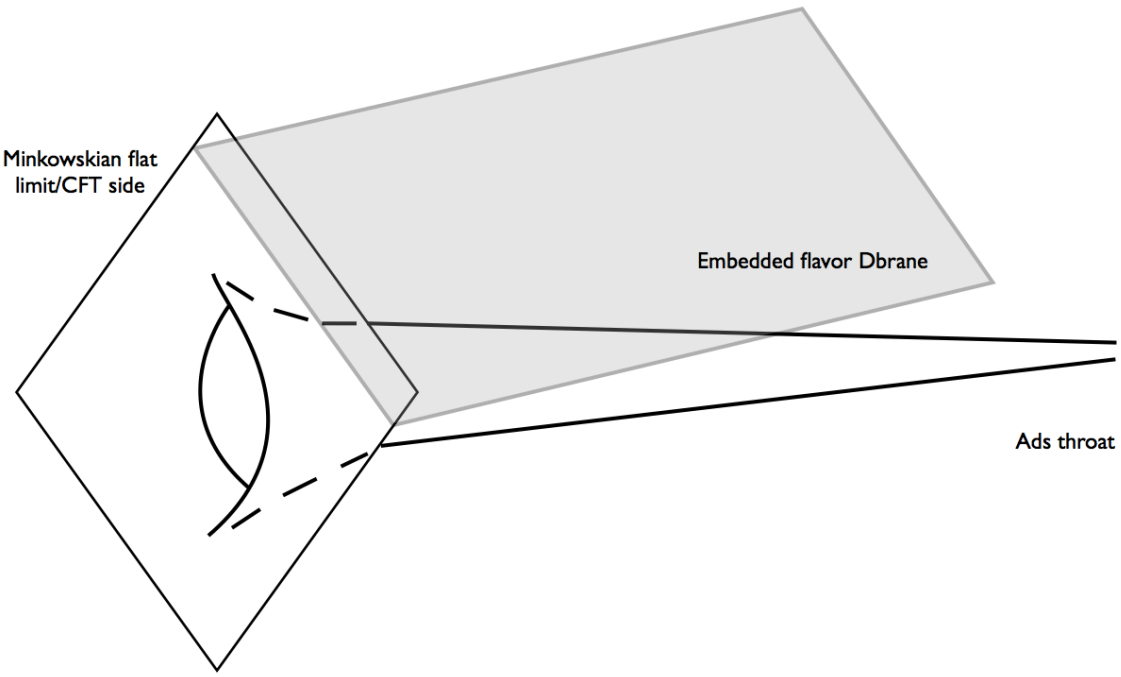

Figure 1.2: Asymptotic AdS space and embedded flavor brane as a defect in CFT side

where the radius L of the D3-brane is given by

$$L^4 = 4\pi g_s N l_s^4 \tag{1.10}$$

This geometry has two limits, as $y \gg L$, we recover flat ten dimensional space-time. When $y < L$, the geometry is often referred to as the AdS throat and would at first appear to be singular as $y \ll L$, as in figure 1.2. Redefining the coordinate:

$$u \equiv L^2/y \tag{1.11}$$

The large u limit is:

$$ds^2 = L^2\left[\frac{1}{u^2}\eta_{ij}dx^i dx^j + \frac{du^2}{u^2} + d\Omega_5^2\right] \tag{1.12}$$

which corresponds to a familiar geometry, one part is the five-sphere S^5 with metric $L^2 d\Omega_5^2$, with the other part being the hyperbolic space AdS_5 with constant negative curvature metric: $L^2 u^{-2}(du^2 + \eta_{ij}dx^i dx^j)$. N D-branes locate $y \sim 0$ or $u \sim \infty$, around AdS throat.

This geometry is regular and symmetrical, it is the familiar $AdS_5 \times S^5$ with the same radius L in the AdS/CFT correspondence.

In Maldecena's limit, $l_s \to 0$ while keeping the other parameters fixed, the N D3 brane metric will become effectively $AdS_5 \times S^5$. It may not be obvious from the first sight, but notice that:

$$ds^2 = \left(1 + \frac{L^4}{y^4}\right)^{-\frac{1}{2}} \eta_{ij} dx^i dx^j + \left(1 + \frac{L^4}{y^4}\right)^{\frac{1}{2}} (dy^2 + y^2 d\Omega_5^2) \tag{1.13}$$

$$= L^2 \left[(1 + \tfrac{L^4}{u^4})^{\frac{-1}{2}} \tfrac{1}{u^2} \eta_{ij} dx^i dx^j + (1 + \tfrac{L^4}{u^4})^{\frac{1}{2}} (\tfrac{du^2}{u^2} + d\Omega_5^2) \right] \tag{1.14}$$

And there is one more factor of $\frac{1}{4\pi l_s^2}$ in front from Nambu-Goto action, taking $l_s \to 0$ implies $L \to 0$ and yields a smooth limit to $AdS_5 \times S^5$ background. Then the $N = 4$ $SU(N)$ supersymmetric gauge theory on N D3-brane becomes the conformal field theory in asymptotic $3+1$ Minkowski spacetime. This is the famous Maldecena's AdS/CFT conjecture, the practical details include taking more limits of different parameters.

People have also tried to put probe D-branes in this $AdS^5 \times S^5$ background, the matter the probe brane carries becomes the fundamental representation of $SU(N)$ supersymmetrical gauge theory, the flavor fermions and their superpartners. Taking probe limits means those probe flavor D-branes will not backreact and curve the $AdS_5 \times S^5$ background.

1.5 Topological insulator in particle physics

The field of topological insulators/orders has grown into the hottest field in condensed matter over the past 10 years [159]. The field theory behind them is topological. It is different from the most states or phases of condensed matter, which have local parameters and the associated broken symmetries. The first example of topological states of matter is the quantum Hall effect (QHE). Topological states of matter have long range parameters. The physics of most of these could be described by different forms of topological field theory.

The low energy effective theory of bulk physics of QHE can be described as below, in terms of a single $U(1)$ gauge theory:

$$S_{eff} = \frac{C_1}{4\pi} \int d^2x \int dt \epsilon^{\mu\nu\tau} A_\mu \partial_\nu A_\tau \tag{1.15}$$

This is the 3-d Chern-Simon theory. This term also gives rise to a Hall current according to $\delta S_{eff}/\delta A_\mu = j^\mu$:

$$j^\mu = \frac{C_1}{2\pi}\epsilon^{\mu\nu\tau}\partial_\nu A_\tau \tag{1.16}$$

From this one can derive the Hall conductivity $\sigma_{xy} = C_1\frac{e^2}{h}$. The coefficient C_1 is an integer for integer quantum hall effect.

One can also write down a 5d Chern-Simon theory, which can be used in the particle theory flavor model in the next Chapter.

$$S_{eff} = \frac{C_2}{24\pi^2}\int d^4x \int dt\epsilon^{\mu\nu\rho\sigma\tau}A_\mu\partial_\nu A_\rho\partial_\sigma A_\tau \tag{1.17}$$

Here C_2 is the second Chern number, one can get it from looking at fermions band structure:

$$C_2 = -\frac{\pi^2}{15}\int \epsilon^{\mu\nu\rho\sigma\tau}\frac{d^4kd\omega}{(2\pi)^5}Tr[(G\frac{\partial G^{-1}}{\partial q^\mu})(G\frac{\partial G^{-1}}{\partial q^\nu})(G\frac{\partial G^{-1}}{\partial q^\rho})(G\frac{\partial G^{-1}}{\partial q^\sigma})(G\frac{\partial G^{-1}}{\partial q^\tau})] \tag{1.18}$$

With G being the fermion propagator in a compact momentum space, which can have multiple poles.

$$iG^{-1}(p_\mu, p_5) = Z_\mu(p)\gamma^\mu + iZ_5(p_5)\gamma^5 - \Sigma(p, p_5) \tag{1.19}$$

One can also get $3+1$ dimensional topological insulator from dimension reduction of $4+1$ topological insulator above [159].For $3+1$ dimensional TI, the Lagrangian can be written down as:

$$S_\theta = \tfrac{\theta}{2\pi}\tfrac{1}{4\pi}\int d^3xdt\partial_\rho(\epsilon^{\rho\mu\nu\tau}A_\mu\partial_\nu A_\tau) \tag{1.20}$$

$$= \tfrac{\theta}{2\pi}\tfrac{1}{16\pi}\int d^3xdt\epsilon_{\rho\mu\nu\tau}F^{\rho\mu}F^{\nu\tau} \tag{1.21}$$

One could see that on the boundary, it reduces to $2+1$ dimensional QHE.

1.6 Finite-temperature field theory

In particle physics people use quantum field theory to calculate dynamic processes at zero temperature, using Feynman diagram in perturbation theory, calculating interacting effects order by order.

In statistical mechanics, the partition function of a statistical system sometimes cannot be evaluated exactly. One way to do it is to evaluate the partition function perturbatively using diagrammatic methods similar to Feynmann diagrams [132]. The Matsubara formalism, or imaginary time formalism is a way of doing it, by identifying time in zero temperature QFT $t = -i\tau$, with τ having the same unit as $\beta = 1/kT$ (T being the temperature), and replacing the integral over energy by sum over n with energy $\frac{2n\pi}{\beta}$ for bosons and $\frac{(2n+1)\pi}{\beta}$ for fermions. This way one switches from evaluating a $3+1$ dimensional process, to a 3 dimensional system in equilibrium.

Including interactions, one could then calculate the correction to the free system in the expansion of Feynman diagram, and to derive the thermal variables like energy, pressure, etc. In Chapter 4, I am going to introduce a work developed based on imaginary time formalism, extracting the correction to the ideal gas relation $PV = kT$ from two-body interactions.

Chapter 2

LITTLE FLAVOR THEORY AND PHENOMENOLOGY

2.1 Extra dimension model for fermion generation: spacetime as a topological insulator

2.1.1 Introduction

It remains a mystery why there are three particle generations in the standard model and why they have the observed pattern of masses and mixing angles, despite many attempts at explanation, experimental evidence for flavor physics beyond the standard model being limited to neutrino masses. The smallness of neutrino masses and the absence of flavor-changing neutral currents and electric dipole moments all suggest that the origin of flavor lies enigmatically at very short distance. A well explored theoretical program is to assume the existence of three generations and guess at textures for the mass matrices which can be justified by a hierarchy of flavor symmetry breaking — an ambiguous exercise given the lack of experimental flavor probes in the right-handed fermion sector. After pioneering work involving abelian flavor symmetries [67], numerous models were also introduced with non-abelian flavor symmetries possessing three dimensional irreducible multiplets to justify the existence of three generations of quarks and leptons. While this general approach can boast of qualitative successes, no models have emerged that are particularly compelling.

Composite and extra dimension models are a natural place to look for an explanation for flavor and the number of generations: both generically contain towers of states, and one can arrange that only three generations are light. Composite models must typically rely on gauge dynamics to explain the origin of three generations, as in Ref. [116], while extra dimension models often rely on the Dirac equation having three zero modes in certain background fields of nontrivial topology Ref. [8, 28, 87]. In composite models, the Yukawa matrices of the standard model are due to complex interactions between constituents, and at best their texture can be predicted; in extra dimension models, the Yukawa matrices can

be computed from wave function overlap integrals in the transverse space (see, for example, [8, 28, 29, 62, 71, 82, 87, 88, 93, 129, 154, 163]). To the extent a gauge/gravity duality pertains, it is possible that these two very dissimilar descriptions could be related. In this Letter we consider an interesting phenomenon observed with lattice domain wall fermions, where the number of massless fermions bound to the surface of a semi-infinite fifth dimension depended discontinuously on the fermion dispersion relation, and hence on coupling constants in the action [100, 110]. It was subsequently shown that the number of light "families" could be understood as a topological property of the five-dimensional (5D) fermion dispersion relation in momentum space [78]. That is because the number of 4D massless surface modes is directly related to the quantized coefficient of the Chern-Simons operator obtained by integrating out the heavy bulk fermions, following the analysis in Ref. [38]; and this coefficient is obtained from a one-loop Feynman diagram which computes a momentum-space winding number associated with the fermion propagator. This phenomenon was first discussed in the classification of fermion modes in liquid helium [80] and is the same phenomenon that defines topological insulators [91, 104, 159]. We consider here that the replication of quark and lepton families we observe in the standard model arise in such a manner (see [176] for related speculations); an attractive feature of the mechanism is that while the number of light families is determined topologically, their transverse wave functions in the extra dimension are all different and dynamically determined, allowing interesting mass mixing without overly restrictive family symmetries. As topology in momentum space depends on the large momentum behavior of the fermion dispersion relation, such models are forced to confront UV physics, and cannot simply rely on an effective field theory description. Therefore after describing the general mechanism and providing a phenomenological toy example, we look at various UV completions that can give rise to a well-defined low energy theory.

2.1.2 Multiple zero modes

We start by considering fermions in 5D, with an inverse Euclidian propagator which respects 4D Lorentz invariance

$$iG^{-1}(p_\mu, p_5) = iZ_\mu(p)\gamma^\mu + iZ_5(p_5)\gamma^5 - \Sigma(p, p_5) \ , \tag{2.1}$$

corresponding to a plane wave $u(p)\exp(ip_a x^a)$, where $p_a = \{p_\mu, p_5\}$ is the 5-momentum and u is a Dirac spinor. We assume Hermitean gamma matrices with Z_μ and Z_5 being real, odd functions of momentum, and Σ a real, even function, so that G^{-1} corresponds to Hermitean derivative interactions in the fermion action. G^{-1} will typically have one or more zeros for real p^μ and some complex value for p_5, and a u spinor which is an eigenstate of γ_5. For the generic case $\Im[p_5] \neq 0$, this pole in G implies a wave function growing exponentially in one of the x_5 directions; because of the symmetry of Z and Σ under $p_5 \to -p_5$, if there is chiral solution to $G^{-1} = 0$ with one sign for $\Im[p_5]$, there is also a solution with the opposite chirality and the opposite sign for $\Im[p_5]$. Such solutions are not normalizable; however, if translation invariance in x_5 is destroyed, either by a boundary or explicit localized x_5 dependence in the action, it is possible that some chiral solutions are normalizable and retained in the Hilbert space — confined to the boundary or defect — while modes of the opposite chirality remain non-normalizable and are discarded. The result is an effective 4D theory at low energy with chiral fermions; this is just a generalization of the domain wall fermion zero mode discovered by Jackiw and Rebbi [96]. If there are multiple solutions to $G^{-1} = 0$, then the 4D theory will have multiple families, distinguished by different transverse wave functions in the extra dimension. While these wave functions will depend continuously on parameters in the 5D Lagrangian, the number of families can only depend discontinuously on those parameters; this makes the number of families look like a topological number, as indeed it is [78]. For example, for 5D lattice domain wall fermions one finds $\Sigma = [m + r\sum_{a=1}^{5}(\cos p_a - 1)]$, $Z_a = \sin p_a$, r being a free parameter. It was shown in Ref. [100] that when the extra dimension is made semi-infinite, chiral zero modes exist at the boundary, where the number of families jumps through the binomial coefficients $\{1, 4, 6, 4, 1\}$ as the ratio (m/r) is tuned through multiples of two, alternating in chirality with each jump. We suggest here that the three families observed in nature might arise in such a manner.

A toy model

For a toy model with three generations we start with the simple and unjustified assumption that the dispersion relation eq. (2.1) is given by

$$iG^{-1} = p_\mu \gamma^\mu + ip_5(1 + c_1 p_5^2)\gamma_5 - m(1 + c_2 p_5^2) \tag{2.2}$$

where m, c_1 and c_2 are real and chosen so that for $p_\mu = 0$, G^{-1} has three roots, all of a given chirality, occurring at $p_5 = i\kappa$ with $\kappa_1 = a$, $\kappa_2 = (b + ic)$, $\kappa_3 = (b - ic)$, where a, b, c are real, positive numbers. These three roots correspond to transverse wave functions for the zero modes of the form $\phi_i(y) = \exp(-\kappa_i y)$. For now we consider the extra dimension to be semi-infinite, and we ignore gravity.

Expanding the 5D fields in this non-orthonormal set of transverse zero mode wave functions yields the low energy 4D theory with off-diagonal kinetic terms, $\mathcal{Z}_{ij}\psi_i^\dagger D_\mu \sigma^\mu \psi_j$, where $\psi_i(x)$ is the chiral spinor associated with the i^{th} zero mode, $i, j = 1, 2, 3$, and the wave function mixing matrix $\mathcal{Z}$ is given by the overlap of transverse wave functions,

$$\mathcal{Z}_{ij} = \int_0^\infty dy\, \phi_i^*(y)\phi_j(y) = \frac{1}{\kappa_i^* + \kappa_j}\ . \tag{2.3}$$

4D gauge invariance requires there to be a y-independent mode for the W bosons, and so weak currents and $\mathcal{Z}$ will both be diagonal in the flavor basis. This is more apparent if one discretizes the extra dimension and considers it as a flavor index, so y-independence of the W is equivalent to the statement that the W couples to each flavor in the UV theory with the same coupling constant.

The natural starting point for construction of a low energy description of the world is to assume one Dirac field in the 5D theory for each Weyl field of the standard model: Q, U, D, L, E with $SU(3) \times SU(2) \times U(1)$ quantum numbers $(3,2)_{1/6}$, $(3,1)_{2/3}$, $(3,1)_{-1/3}$, $(1,2)_{-1/2}$ and $(1,1)_{-1}$ respectively. We assume that Q and L only has left-handed chiral zero modes q_i, ℓ_i, while U, D and E have only right-handed zero modes, u_i, d_i, e_i. These fields can then couple to the Higgs in the 5D theory as $\overline{U}HQ$, etc. (Alternatively one could replace U, D, E by conjugate fields U^c, D^c and E^c with Higgs couplings $U^c H C_5 Q$, etc, where C_5 is the 5D charge conjugation matrix, and assume a 5D dispersion relation where all zero modes are left-handed.)

A problem with the above implementation is that, with a single Yukawa coupling for each 5D field, it is not possible to include weak CP violation. We therefore make the Higgs sector the origin of CP violation in the UV theory, which requires introducing additional scalars. We assume a two-doublet model with a relative CP-violating phase in their vacuum expectation values (vevs) arising from explicit CP-violation in the Higgs potential. To avoid large flavor changing neutral currents, the theory is given a discrete symmetry (softly broken) to ensure that H_u and H_d couple solely to up-type and down-type quarks respectively [74]. Furthermore we must assume that these are bulk fields and that Higgs vacuum expectation values are y-dependent; this is the same model and mechanism commonly used to introduce CP violating bubble walls in theories of electroweak baryogenesis [44]. The Yukawa interactions of the quarks in the 5D theory are given by $(y_U \overline{U} H_u Q + y_D \overline{D} H_d Q + \text{h.c.})$, In principle there could be higher derivative Yukawa-like interactions, but we assume they are zero at the UV scale.

As with the fermion zero modes, we assume an exponential form for the 5D profile of the Higgs vevs. By means of a hypercharge gauge transformation we can make H_d vev to be real and put all the CP violating phase into the H_u: $\langle H_d \rangle = v e^{-y} \sin\beta$, $\langle H_u \rangle = v e^{-(h_r + i h_i) y} \cos\beta$, where we have chosen the scale of the coordinate y so that the exponent in the profile of $\langle H_d \rangle$ equals one, while the real parameters h_r and h_i characterize the profile of $\langle H_u \rangle$. Integrating over the coordinate y then gives rise to conventional 4D mass matrices, such as $[M_U]_{ab} \propto (y_U v \cos\beta/\sqrt{2})(\kappa_{Q,a} + \kappa_{U,b} + h_r + i h_i)^{-1}$.

In our model we choose Higgs couplings to the leptons of the form

$$y_E \overline{L} \widetilde{H}_u E + \frac{1}{\Lambda} (L \widetilde{H}_d)^T C_5 (L \widetilde{H}_d) + \text{h.c} \tag{2.4}$$

where $\widetilde{H} = \sigma_2 H^*$; Λ has dimensions of mass and controls the size of the resulting Majorana neutrino masses. After integrating over the coordinate y the Yukawa interactions give rise to mass matrices which are simple functions of the phenomenological κ parameters; from these and the wave function matrices eq. (2.3) it is straightforward computation to determine all the masses and mixing angles.

The point of this toy model is not to present a full theory of 5D physics, but only want to see whether a model based on this topological insulator mechanism could agree

with experimental data on flavor physics to high accuracy. The model described has 21 real parameters: a, b and c for the Q, U, D, L and E fields, h_r and h_i for $\langle H_u \rangle$, the three Yukawa couplings y_U, y_D, y_E, and the scale Λ characterizing the neutrino coupling to the Higgs. These are fit to 18 data: the nine quark and charged lepton masses, three CKM angles and one phase, two neutrino Δm^2 values, and three neutrino mixing angles. Ignoring uncertainties in the data, in general one would expect some number of disconnected three-dimensional manifolds in parameter space where the model agrees with all the data — that number possibly being zero; lower dimensional spaces of solutions would generally require fine tuning. In searching for solutions, we ignore radiative corrections in our model (such as running of the Yukawa couplings and masses, or radiative generation of higher derivative operators), and fit the parameters to data currently available from the Particle Data Group [144], augmented with recent evidence for nonzero θ_{13} in the neutrino sector [64].

One might think that this model, with more parameters than data, could not be predictive. However, when we numerically map out the manifold of solutions consistent with the data (including experimental and theoretical errors quoted in the PDG) we find (i) we always get a normal, nondegenerate hierarchy, with m_3 in the narrow range $0.048\ \text{eV} \leq m_3 \leq 0.051\ \text{eV}$; (ii) solutions do not favor maximal mixing for $\nu_2 - \nu_3$; (iii) we find J_ν in the narrow range $-0.023 \leq J_\nu \leq -0.014$. What has happened is just that the three-dimensional manifold of predictions form this constrained model maps onto a narrow range of physical properties, so that it is in fact somewhat predictive. Nevertheless, one would like to understand how to construct a model which is both more predictive and is well defined in the UV.

2.1.3 UV completion: Little Flavor

A general method for constructing a UV completion for extra dimension models is to discretize the extra dimensions while keeping the 4D world continuous (deconstruction) [19,20]. In such an approach, the extra coordinate for bulk fermions essentially becomes a flavor index. A 4D deconstructed version of a free theory with dispersion relation similar to eq. (2.2) is readily obtained by discretizing an infinite extra dimension with defect at site

$n = 0$. In this case we have an infinite number of flavors of 4D fermions with the mass matrix $\mathcal{L}_m = (\bar{\psi}_L M \psi_R + \text{h.c.})$, where M is an infinite matrix representing the fifth dimension differential operator. For example:

$$(Mv)_n = \begin{cases} (cv_{n-3} + bv_{n-2} + av_{n-1} + v_n) & n < 0 \\ [(cv_{-3} + bv_{-2} + av_{-1} + v_0) & \\ \quad +(v_0 + av_1 + bv_2 + cv_3)] & n = 0 \\ (v_n + av_{n+1} + bv_{n+2} + cv_{n+3}) & n > 0 \end{cases} \tag{2.5}$$

has the solution $Mv = 0$ with $v_n = x^{|n|}$, where x is any of the three roots of the equation $1 + ax + bx^2 + cx^3 = 0$. The vector is normalizable if $|x| < 1$, and three normalizable zero modes may be found over a range of parameters a, b, c. The topological nature of the underlying theory is manifested by the fact that the the number of normalizable zero mode solutions does not change with small local excursions of M away from the above form. When such a system is gauged, however, the gauge fields couple to an infinite number of flavors in such a theory, and so the theory has a Landau pole and is ill-defined. To cure this, one must work with a finite discretized extra dimension.

With finite continuous extra dimensions, both exponentially growing and falling zero mode solutions are normalizable and to obtain a chiral theory one must perform an orbifold projection [56, 157]. A well-known example is to compactify the extra dimension as a circle parametrized by $\theta \in [-\pi, \pi)$ with the action respecting a Z_2 symmetry $\psi(\theta) \to \gamma_5 \psi(-\theta)$. This symmetry requires mass terms to be odd in θ, and so domain wall defects exist at the fixed points of the reflection, $\theta = 0$ and $\theta = \pi$ where the zero modes of opposite chirality are located, and projecting out modes which are either even or odd under this Z_2 will result

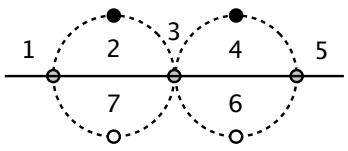

Figure 2.1: A discretized Z_2 orbifold with three zero modes; $\mathcal{R}$ reflects about the horizontal axis.

in a chiral theory. A true UV completion of our topological insulator model for families is possible if a discretized version of this orbifold projection exists and is compatible with the survival of multiple chiral zero modes. In this case M is a finite dimensional matrix, and we assume the action respects a Z_2 symmetry $\psi \to \gamma_5 \mathcal{R}\psi$, where $\mathcal{R}$ is the "reflection" operator in flavor space with $\mathcal{R}^2 = 1$. It is possible to prove an index theorem

$$(\mathcal{N}_L^- - \mathcal{N}_R^-) = -(\mathcal{N}_L^+ - \mathcal{N}_R^+) = \mathrm{Tr}\,\mathcal{R}\ , \tag{2.6}$$

where $\mathcal{N}_L^\pm$ are the number of left-handed zero modes of M with Z_2 charge ± 1, and $\mathcal{N}_R^\pm$ is the same for right-handed zero modes. Evidently we would like $|\mathrm{Tr}\,\mathcal{R}| = 3$ to obtain three chiral families, ruling out discretization of the Z_2 orbifold of a circle, and leading us to consider instead the discretization of an extra dimension consisting of two circles sharing a point. A simple example is the 7-site lattice shown in Fig. 2.1, where we take $\mathcal{L}_m$ to be

$$\begin{aligned} &\bar{L}_1(R_2 - R_7) + \bar{L}_2(R_3 - R_1) + \bar{L}_3(R_4 - R_2) \\ &+\bar{L}_3(R_7 - R_6) + \bar{L}_4(R_5 - R_3) + \bar{L}_6(R_3 - R_5) \\ &+\bar{L}_7(R_1 - R_3) + \text{h.c.} \end{aligned} \tag{2.7}$$

where L_i and R_i are ψ_L and ψ_R respectively at site i. This has the simple interpretation of hopping terms for fermions around the circles, with fermions at the shared point (site 3) being able to hop onto either circle. In this example, $\mathcal{R}$ reflects sites about the horizontal axis in Fig. 2.1, and the action is invariant under $\psi \to \gamma_5 \mathcal{R}\psi$. The theory has three massless Dirac fermions, and if we project out all states with negative Z_2 charge, then we are left with three left-handed zero modes. The important point of this model is not that M has three zero mode solutions, but that the zero modes persist even if M is perturbed in any random way which respects the Z_2 symmetry — although the eigenvectors ("transverse wave functions") will be altered under this perturbation— exactly as one would expect from the topological origin of this model.

This mechanism in general — and the deconstructed model in particular — naturally suggests a number of interesting directions to pursue, most interestingly whether it imposes inescapable constraints on Higgs and CP physics that might be probed by the LHC, as well as observable flavor changing neutral currents or lepton flavor violation, which would be characterized by the scale of the extra dimension.

2.2 little flavor: weak-scale flavor physics

2.2.1 Introduction

The standard model (SM) is extremely successful at predicting what we do not see — namely flavor changing neutral currents (FCNC), lepton family violation among charged leptons, proton decay or neutron oscillations, and (with the exception of the strong CP problem) large CP violating effects. These all follow from the fact that such processes require irrelevant operators in the SM and are therefore suppressed by the high energy scale associated with new heavy particles. By assuming a desert for many decades of energy above the electroweak scale, all of the above processes are strongly suppressed, providing a simple explanation for what we (don't) see. The SM is unsatisfying at the same time, as the hierarchical structure of fermion families is put in by hand with no explanation. An interesting generic explanation for flavor structure was posited long ago by Froggatt and Nielsen [67], in which large approximate flavor symmetries are broken hierarchically by multiple spurions, which individually break the flavor symmetry, but none by itself sufficiently breaking the symmetry to provide Yukawa couplings for all the SM fermions. Since then, many models of flavor have been built on this premise; however, with a desert above the electroweak scale to explain the absence of FCNC and electric dipole moments, it would appear that experimental clues to the origins of fermion family structure would be well beyond the reach of any foreseeable experiment, and so this scientific program has remained inconclusive and unconvincing.

There is tension in the SM, however, between the natural explanation of a desert for the absence of FCNC, lepton and baryon number violation, and CP violation on the one hand, and the fine tuning of the Higgs sector that comes with a desert on the other. There have been numerous attempts to modify the SM to remove this tension. Walking technicolor, for example, maintains the desert while replacing the Higgs sector of the SM with dynamical symmetry breaking — but is no longer viable with the discovery of the Higgs. Another approach, such as in Effective Supersymmetry [47], is to populate the desert while maintaining enough approximate symmetries that suppress the dangerous FCNC and symmetry violating processes. These theories all attempt to extend the viability of the SM up to the GUT

scale. However an interesting and relatively recent alternative is the Little Higgs Mechanism, which extends naturalness in the SM only up to the ~ 10 TeV scale [16, 17, 20, 169]. In these models, composite Higgs theories [58, 68, 69, 114, 115] are designed with large nonlinearly realized symmetries broken by sparse spurions, none of which by themselves break the symmetries sufficiently to allow a Higgs potential to be radiatively generated at one loop[1].

It is intriguing that the underlying mechanism of the Little Higgs Mechanism is similar in spirit to the Froggatt-Nielsen program for flavor structure, even if applied in a different way to a different problem. In this paper we present an effective theory valid up to the ~ 20 TeV scale model that exhibits a large approximate global symmetry broken by means of sparse spurions which combine to give rise to both electroweak symmetry breaking, as well as the observed hierarchies of quark masses and mixing angles. Although we hope this approach may lead to a deep understanding of flavor, the model we present is less ambitious, reproducing the SM quark masses and mixings without predicting them, and not addressing the leptonic sector of the SM. The point of the model is to demonstrate that flavor physics can lie just beyond the electroweak symmetry breaking scale — and can be intimately related to it — without giving rise to FCNC or electric dipole moments in conflict with experiment, and without assuming Minimal Flavor Violation [43]. We show that such a theory, fit to give the observed quark masses and CKM angles to within a few percent, has rich phenomenology with exotic quarks, mesons and massive gauge bosons at the few TeV scale.

We begin by explaining the general structure and symmetries of the model, which consist of an approximate $U(3)$ flavor symmetry times a product of approximate $SU(4)$ symmetries in which is embedded the $SU(2) \times U(1)$ gauge group of the SM. Some of the $SU(4)$ symmetries are nonlinearly realized, and two Higgs doublets appear as pseudo Nambu-Goldstone

[1] A previous model which addressed the origin of fermion masses at the TeV scale without invoking minimal flavor violation, ref. [148], invoked a very large global symmetry group and sparse set of spurions to achieve a flavor hierarchy. This model demonstrated that the same symmetries that produced a fermion mass hierarchy could suppress FCNC. In ref. [22], the extra-dimensional mechanism of "shining" was introduced to produce the fermion masses at the TeV scale without FCNC. Extra-dimensional theories, deconstructed [19] automatically provide the very large approximate symmetry group and sparse set of spurions which can be useful for flavor models, as well as for little Higgs models.

bosons of an $SU(4) \times SU(4)/SU(4)$ nonlinear sigma model. Although the $SU(4)$ groups are not family symmetries, explicit $SU(4)$ breaking by spurions is required before the SM quarks can obtain nonzero Yukawa couplings to the Higgs, with a nontrivial structure arising from the simultaneous breaking of the $U(3)$ family symmetry. After discussing the structure of quark masses and mixing angles, we provide an explicit fit to existing data and show how FCNC in this fit are well within experimental limits. Next we turn to the Higgs potential; by construction the Little Higgs mechanism is at work in eliminating divergent radiative corrections from one-loop fermion contributions. We then briefly explain how our model is inspired by the deconstruction of the extra dimension domain wall fermion/topological insulator model of flavor of reference [121], and conclude with a discussion of how our approach might be extended.

2.2.2 The $SU(4) \times U(3)$ Little Flavor Model

Our model is characterized by the moose diagram in Fig. 2.2, consisting of six sites, three white and three black, connected by oriented links. Fermions live on the sites and mesons on the links, while some gauge bosons reside only on the white sites and others only on the black sites.

Gauge symmetries and the Higgs

The gauge symmetry of the model is $SU(3) \times G_w \times G_b$, where $SU(3)$ is color and $G_{w,b}$ are independent $SU(2) \times U(1)$ groups associated with white (w) and black (b) sites respectively. The SM electroweak gauge group is the diagonal subgroup of $G_w \times G_b$, and we take the the gauge couplings to be

$$g_{1,w} = \frac{g'}{\cos\gamma_1} \ , \qquad g_{1,b} = \frac{g'}{\sin\gamma_1} \ , \qquad g_{2,w} = \frac{g}{\cos\gamma_2} \ , \qquad g_{2,b} = \frac{g}{\sin\gamma_2} \ . \tag{2.8}$$

where $g = e/\sin\theta_w$ and $g' = e/\cos\theta_w$ are the usual SM gauge couplings and the angles $\gamma_{1,2}$ are free parameters.

The gauge fields are coupled to an $SU(4) \times SU(4)/SU(4)$ nonlinear σ-model, parametrized by the field Σ, an $SU(4)$ matrix which transforms under $SU(4) \times SU(4)$ as the $(4, \bar{4})$ representation. The $G_w \times G_b$ gauge symmetry is embedded in the $SU(4) \times SU(4)$ so that the

covariant derivative acts on Σ as

$$D_\mu \Sigma = \partial_\mu \Sigma + i \left(g_{2,w} A^a_\mu T_a + g_{1,w} B_\mu Y \right) \Sigma - i \Sigma \left(g_{2,b} \tilde{A}^a_\mu T_a + g_{1,b} \tilde{B}_\mu Y \right) \ , \tag{2.9}$$

where $\{A^a_\mu, B_\mu\}$ and $\{\tilde{A}^a_\mu, \tilde{B}_\mu\}$ are the gauge bosons of G_w and G_b respectively, while the generators can be written in a 2×2 block notation as

$$T_a = \tfrac{1}{2} \begin{pmatrix} \sigma_a & 0 \\ 0 & 0 \end{pmatrix} \ , \qquad Y = \begin{pmatrix} 0 & 0 \\ 0 & T_3 \end{pmatrix} \ . \tag{2.10}$$

The Σ field breaks $G_w \times G_b$ gauge symmetry down to a diagonal subgroup; if $\langle \Sigma \rangle = 1$, the unbroken subgroup is the diagonal $SU(2) \times U(1)$, which is identified with the electroweak gauge group of the SM, and it has the correct couplings g and g'. The spectrum then contains two exotic Z bosons and an exotic W boson, whose masses are given by

$$M_{Z'} = M_{W'} = \frac{g f}{\sin 2\gamma_2} \ , \qquad M_{Z''} = \frac{g' f}{\sin 2\gamma_1} \ . \tag{2.11}$$

Electroweak symmetry breaking will correct these relations at $O(M_Z^2/f^2)$; in the model we consider in this paper we fix the Goldstone boson decay constant to be $f = 1.5$ TeV; thus the corrections are $O(M_Z^2/f^2) \simeq 1\%$.

The Σ field describes fifteen pseudo Goldstone bosons with decay constant f, to be set to 1.5 TeV in the phenomenological model we describe below. It can be conveniently parametrized as

$$\Sigma = \xi \, \xi_\eta \, \xi_\pi \, \Sigma_H \, \xi_\pi \, \xi_\eta \, \xi \ , \tag{2.12}$$

where

$$\xi \ = \ \exp \left[\frac{i}{2f} \begin{pmatrix} \vec{\pi}\,' \cdot \vec{\sigma} & 0 \\ 0 & \pi_3 \sigma_3 \end{pmatrix} \right] \tag{2.13}$$

$$\xi_\eta = \exp \left[\frac{i}{\sqrt{8} f} \begin{pmatrix} \eta & \\ & -\eta \end{pmatrix} \right] \ , \tag{2.14}$$

$$\xi_\pi = \exp \left[\frac{i}{\sqrt{2} f} \begin{pmatrix} 0 & \\ & \Pi \end{pmatrix} \right] \ , \quad \Pi \equiv \begin{pmatrix} 0 & \pi^+ \\ \pi^- & 0 \end{pmatrix} \ . \tag{2.15}$$

$$\Sigma_H = \exp\left[(i\sqrt{2}/f)\begin{pmatrix} 0 & -i\mathcal{H}^\dagger \\ i\mathcal{H} & 0 \end{pmatrix}\right] , \tag{2.16}$$

The field ξ contains the Goldstone bosons eaten when $G_w \times G_w$ is broken to the diagonal $SU(2) \times U(1)$, and in unitary gauge it is rotated away. The η and $\pi^\pm$ fields correspond to exotic $SU(2)$ singlets which are neutral and charged respectively. Finally, $\mathcal{H}$ contains two electroweak doublets which will be identified with the two SM Higgs doublets, H_u and H_d:

$$\mathcal{H} = \begin{pmatrix} -H_u^T\epsilon \\ H_d^T\epsilon \end{pmatrix} = \begin{pmatrix} h_u^0 & -h_u^+ \\ -h_d^- & h_d^0 \end{pmatrix} . \tag{2.17}$$

The potential for Σ will cause a small misalignment away from the $SU(2)\times U(1)$ preserving vacuum $\langle\Sigma\rangle = 1$, corresponding to nonzero vevs of the Higgs doublets, an example of the composite Higgs mechanism [58, 68, 69, 114, 115] (see references [6, 25, 152] for some more recent developments in composite Higgs theories). Assuming $\langle h_u^0\rangle = v_u/\sqrt{2}$ and $\langle h_d^0\rangle = v_d/\sqrt{2}$, the electroweak breaking vacuum corresponds to

$$\langle\Sigma\rangle = \begin{pmatrix} c_u & 0 & s_u & 0 \\ 0 & c_d & 0 & s_d \\ -s_u & 0 & c_u & 0 \\ 0 & -s_d & 0 & c_d \end{pmatrix} , \qquad c_{u,d} = \cos\frac{v_{u,d}}{f} , \quad s_{u,d} = \sin\frac{v_{u,d}}{f} . \tag{2.18}$$

In the special case $v_u = v_d = v$, (or $\tan\beta = 1$) obtaining the correct W and Z masses requires

$$\sin\frac{v}{f} = \frac{M_Z \sin 2\theta_w}{\sqrt{2}ef} , \tag{2.19}$$

with additional corrections of size $O(M_Z^2/f^2) \simeq 1\%$.

The interactions of the mesons are described by a chiral Lagrangian defined with a momentum cutoff at the scale $\Lambda \sim 4\pi f \sim 19$ TeV in the model we describe here. The leading operator is given by

$$\frac{f^2}{4}\mathrm{Tr}\,(D_\mu\Sigma)^\dagger D^\mu\Sigma , \tag{2.20}$$

which gives canonically normalized meson fields for $\langle\Sigma\rangle = 1$, but care must be taken to account for $O(v/f)$ corrections to the wavefunction normalization in the electroweak symmetry breaking vacuum eq. (2.18).

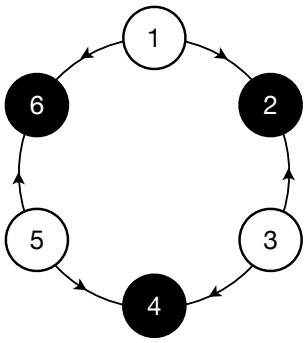

Figure 2.2: The moose describing the $SU(4)$ model. Chiral fermions reside at white sites, and vector fermions at black sites.The links correspond a nonlinear Σ field which contains H_u and H_d Higgs fields, although in the model we construct, Σ fields only live on three of the six possible links pictured here. The gauge symmetry of the theory is $SU(3) \times [SU(2) \times U(1)]^2$, where $SU(3)$ is color; the two $SU(2) \times U(1)$ groups are associated with the white sites and the black sites, and the conventional electroweak gauge group resides in their diagonal subgroup.

Before describing the potential for Σ and its vacuum alignment, we must first discuss the fermions in the model and their Yukawa couplings to Σ.

Fermions

Our model is described by the moose diagram of Fig. 2.2, where the oriented links represent Σ and $\Sigma^\dagger$, while the white and black sites represent fermions transforming nontrivially under G_w and G_b respectively. The fermions are all color triplet (we only consider quarks in this model, not leptons) and consist of $SU(2)$ doublets $Q = (u, d)$ and $SU(2)$ singlets (U, D). The fermions on the black sites are Dirac fermions and are grouped together as the quartets of approximate $U(4)_b$ symmetries

$$\psi_b = \begin{pmatrix} Q \\ U \\ D \end{pmatrix}_b , \qquad \text{black sites: } b = 2, 4, 6 \ . \tag{2.21}$$

The fermions on the white sites are chiral fermions, conveniently packaged as incomplete quartets of independent approximate $U(4)_w$ symmetries:

$$\chi_{w,L} = \begin{pmatrix} Q \\ 0 \\ 0 \end{pmatrix}_{w,L} , \qquad \chi_{w,R} = \begin{pmatrix} 0 \\ U \\ D \end{pmatrix}_{w,R} , \qquad \text{white sites: } w = 1,3,5 \ . \tag{2.22}$$

In the above expressions, the subscripts $b = 2,4,6$ and $w = 1,3,5$ refer to the site numbers in Fig. 2.2.

The G_w and G_b gauge generators are embedded within $U(4)_{w,b}$ exactly as in eq. (2.10), except that Y is extended to include a term $\frac{1}{2}(B-L) = \frac{1}{6}$ for all the fermions, vanishing for the mesons,

$$Y = \begin{pmatrix} 0 & 0 \\ 0 & T_3 \end{pmatrix} + \frac{1}{2}(B-L) = \begin{pmatrix} 0 & 0 \\ 0 & T_3 \end{pmatrix} + \frac{1}{6}\begin{pmatrix} 1 & 0 \\ 0 & 1 \end{pmatrix} \qquad \text{(fermions)} \tag{2.23}$$

where the colored fermions all carry $(B-L) = \frac{1}{3}$. Thus the covariant derivatives act on the fermions as

$$\begin{aligned} D_\mu \chi_{L,w} &= (\partial_\mu + i g_{2,w} A^a_\mu T_a + i g_{1,w} B_\mu Y)\chi_{L,w} \ , \\ D_\mu \chi_{R,w} &= (\partial_\mu + i g_{1,w} B_\mu Y)\chi_{R,w} \ , \\ D_\mu \psi_b &= (\partial_\mu + i g_{2,b} \tilde{A}^a_\mu T_a + i g_{1,b} \tilde{B}_\mu Y)\psi_b \ . \end{aligned} \tag{2.24}$$

Yukawa couplings and masses

The masses and Yukawa terms in our model come in two types: those that preserve an $SU(4) \times U(3)$ symmetry, and those where that symmetry is partially broken by spurions. The $SU(4)$ is the symmetry of the degenerate massive vector fermions on the black sites, which is identified with the $SU(4)_R$ symmetry of the nonlinear σ-model; the $U(3)$ will be identified as a family symmetry and contains the S_3 permutation symmetry of the moose of Fig. 2.2.

The $SU(4) \times U(3)$ symmetric terms

To make the $U(3)$ symmetry manifest it is useful to consider the "unit cell" of our moose digram Fig. 2.2 to consist of an adjacent pair of black and white sites, the moose consisting of three such pairs. We label the cells by $n = 1, 2, 3$, with cell n associated with sites $\{2n-1, 2n\}$, and then an index $\alpha = 1, 2$ will specify the white and the black site respectively within the cell. The fermions are all labeled then as $\Psi_{n,\alpha}$ with

$$\Psi_{1,1} = \chi_1 \ , \quad \Psi_{1,2} = \psi_2 \ , \quad \Psi_{2,1} = \chi_3 \ , \quad \Psi_{2,2} = \psi_4 \ , \quad \Psi_{3,1} = \chi_5 \ , \quad \Psi_{3,2} = \psi_6 \ , \tag{2.25}$$

where the χ are the four-component chiral fermions on the white sites in eq. (2.22), and the ψ are the four component Dirac fermions on the black sites in eq. (2.21).

The symmetric fermion mass and Yukawa terms are given by

$$\mathcal{L}_{\rm sym} = \overline{\Psi}_{m\alpha,L} \left[\mathcal{M}_{m\alpha,n\beta} + \Sigma\, \mathcal{Y}_{m\alpha,n\beta} - \Sigma^\dagger\, \mathcal{Y}^\dagger_{m\alpha,n\beta} \right] \Psi_{n\beta,R} + h.c. \ , \tag{2.26}$$

where $\mathcal{M}^{(0)}$, $\mathcal{Y}$ and $\overline{\mathcal{Y}}$ are independent and take the form

$$\mathcal{M}_{m\alpha,n\beta} = M \begin{pmatrix} 1 & & \\ & 1 & \\ & & 1 \end{pmatrix}_{mn} \otimes \begin{pmatrix} 0 & 0 \\ 0 & 1 \end{pmatrix}_{\alpha\beta} \tag{2.27}$$

$$\mathcal{Y} = \lambda\, f \begin{pmatrix} 1 & & \\ & 1 & \\ & & 1 \end{pmatrix}_{mn} \otimes \begin{pmatrix} 0 & 1 \\ 0 & 0 \end{pmatrix}_{\alpha\beta} \ , \tag{2.28}$$

where all unmarked matrix elements are zero. We have written the mass and Yukawa couplings in a direct product notation to make manifest the $U(3)$ symmetry acting on the unit cell indices m, n. The $\mathcal{M}$ term is a common mass term for the black site Dirac fermions; the $\mathcal{Y}$ term is a nearest neighbor hopping interaction involving Σ in the direction of the link arrow, from white site to black site within the cell, and the $\mathcal{Y}^\dagger$ term is a hopping interaction against the link arrow, from black to white, involving $\Sigma^\dagger$; combined these hopping terms look like a covariant derivative in a fifth dimension, with Σ playing the role of the fifth component of a gauge field. Having the hopping strength be the same in the forward and

backward directions is protected by a discrete Z_2 symmetry. Note though that the Σ field only acts on the three links that connect black and white sites within a cell; in this model we do not have Σ fields acting on the links between cells.

Less obvious in this notation is that $\mathcal{L}_{\rm sym}$ is invariant under a nonlinearly realized $SU(4)_L \times SU(4)'_R$ symmetry which is the $SU(4)_L$ symmetry of the σ-model, times the diagonal subgroup of the σ-model's $SU(4)_R$ and the vector $SU(4)$ symmetry of the black site Dirac fermions. A remarkable consequence of this $SU(4)'_R$ symmetry is that even when the electroweak symmetry is broken spontaneously by the Higgs vev in eq. (2.18), there remain three exactly massless families of SM quarks. This is easy to see if one redefines the Ψ_{n2} fields at each of the black sites as $\Psi_{n2} = \Sigma^\dagger \Psi'_{n2}$; then $\mathcal{L}_{\rm sym}$ is independent of Σ, which means that the mass and Yukawa terms know nothing of electroweak symmetry breaking. In effect, the SM families are forced to only have derivative couplings to the Higgs. Therefore the three surplus RH singlet quarks cannot pair up with the three surplus LH doublet quarks, and one is left with three massless SM families. This mechanism differs from the flavor models in which an approximate chiral flavor symmetry is responsible for keeping the SM families light — such as Minimal Flavor Violation models which start with a $U(3)^3$ symmetry among the quarks [43]. To give the SM families mass requires breaking the $SU(4)$ symmetry, and to have mixing angles and nondegenerate quarks requires breaking the $U(3)$ symmetry; we do both with the same spurions at tree level. However, the $SU(4)$ symmetry is also broken by radiative corrections in the form of G_b gauge boson loops; this is an important issue but we defer discussion of that to § 2.2.4.

The $SU(4) \times U(3)$ symmetry breaking terms

To give the SM quarks masses we introduce two spurions to break the $SU(4) \times U(3)$ symmetry, defined by the traceless 4×4 matrices which can be thought of as transforming as

elements of the adjoint of $SU(4)$:

$$X_u = \begin{pmatrix} 1 & & & \\ & 1 & & \\ & & -3 & \\ & & & 1 \end{pmatrix} , \qquad X_d = \begin{pmatrix} 1 & & & \\ & 1 & & \\ & & 1 & \\ & & & -3 \end{pmatrix} \tag{2.29}$$

Both of these matrices break the $SU(4)$ symmetry down to $SU(3) \times U(1)$ and will allow the light fermions to acquire masses; the X_u matrix splits off the U quark from the $SU(4)$ multiplet, while X_d distinguishes the D quark. We take for our symmetry breaking mass terms

$$\mathcal{L}_{\text{asym}} = \overline{\Psi}_{m\alpha,L} \left[\mathcal{M}^u_{m\alpha,n\beta} + \mathcal{M}^d_{m\alpha,n\beta} \right] \Psi_{n\beta,R} + h.c. \tag{2.30}$$

where

$$\mathcal{M}^u_{m\alpha,n\beta} = M^u_{mn} \otimes \begin{pmatrix} 0 & 0 \\ 0 & 1 \end{pmatrix}_{\alpha\beta} \otimes X_u \ , \qquad \mathcal{M}^d_{m\alpha,n\beta} = M^d_{mn} \otimes \begin{pmatrix} 0 & 0 \\ 0 & 1 \end{pmatrix}_{\alpha\beta} \otimes X_d \ . \tag{2.31}$$

The $M^{u,d}$ matrices act on the $U(3)$ indices of the fermions, the structure of the $\{\alpha\beta\}$ matrix shows that only the Dirac fermions on black sites are involved, and the X matrices act on the implicit $SU(4)$ indices carried by each fermion. By having the X spurions each leave intact an $SU(3)$ subgroup of the black-site $SU(4)$ symmetry, we ensure that the fermions will not contribute any one-loop quadratically divergent mass contributions to the Higgs boson (the Little Higgs mechanism). In fact, log divergences to the Higgs potential from one fermion loop also vanish in this model.

The $M^{u,d}$ matrices in the above expression act on the indices of the three cells of our moose, explicitly breaking the $U(3)$ flavor symmetry, and we take them to have the textures

$$M^u = \begin{pmatrix} \mathcal{M}^u_{11} & \mathcal{M}^u_{12} & 0 \\ 0 & \mathcal{M}^u_{22} & 0 \\ \mathcal{M}^u_{31} & 0 & \mathcal{M}^u_{33} \end{pmatrix} \quad , \qquad M^d = \begin{pmatrix} \mathcal{M}^d_{11} & 0 & 0 \\ \mathcal{M}^d_{21} & \mathcal{M}^d_{22} & 0 \\ 0 & \mathcal{M}^d_{32} & \mathcal{M}^d_{33} \end{pmatrix} \ . \tag{2.32}$$

This choice has been made empirically, and we do not claim it to be unique, but these textures suggests the spurions could arise from a simple symmetry breaking scheme, which

we do not pursue here. We will constrain all of the mass parameters to be real, except for M^u_{31}, whose phase will be the source of CP violation in this model. The diagonal elements break the $U(3)$ down to $U(1)^3$, allowing a nontrivial quark spectrum to emerge but no mixing angles; the off-diagonal terms will generate flavor mixing.

2.2.3 A phenomenological fit

In order to study rare processes in a model which reproduces correctly the SM quark masses and mixing angles, we now fix

$$M = 5000 \text{ GeV} , \qquad f = 1500 \text{ GeV} , \qquad \tan\beta = \frac{v_u}{v_d} = 1 , \tag{2.33}$$

and fit the 11 real parameters plus one phase (λ, and the $\mathcal{M}^{u,d}$ matrices) to the six quark masses, as well as the three mixing angles and one phase in the Cabibbo-Kobayashi-Maskawa matrix, a total of 10 data; our fit is neither unique, nor predictive in the SM quark sector, and the assumption of $\tan\beta = 1$ is for simplicity, not following from any particular Higgs potential. In fact, one would expect $\tan\beta > 1$ in these models, as discussed below, but considering different values for $\tan\beta$ will not alter our analysis significantly. The point of this exercise is to produce a concrete model consistent with the SM in which we can accurately analyze low energy flavor phenomenology from new TeV physics.

The fit we find has

$$\lambda = 1.49794 , \tag{2.34}$$

while the $\mathcal{M}$ matrices (in GeV) are given by

$$M^u = \begin{pmatrix} 1189.54 & 15.4904 & 0 \\ 0 & 6.96490 & 0 \\ 3.50799e^{-i1.224428} & 0 & 0.01441071 \end{pmatrix} , M^d = \begin{pmatrix} 45.7769 & 0 & 0 \\ -1.60269 & 0.600984 & 0 \\ 0 & 0.137582 & 0.0336607 \end{pmatrix} \tag{2.35}$$

These parameters allow us to reproduce the accepted values of the quark masses (in GeV), RG scaled to $\mu = 1$ TeV [181]:

$$\begin{aligned} m_t &= 153.2 & m_c &= 5.32 \times 10^{-1} & m_u &= 1.10 \times 10^{-3} \\ m_b &= 2.45 & m_s &= 4.69 \times 10^{-2} & m_d &= 2.50 \times 10^{-3} \end{aligned} \tag{2.36}$$

and give rise to the CKM matrix

$$|V_{\rm CKM}| = \begin{pmatrix} 0.974 & 0.226 & 0.00385 \\ 0.226 & 0.973 & 0.0423 \\ 0.00892 & 0.0415 & 0.998 \end{pmatrix} \tag{2.37}$$

and unitarity triangle angles

$$\sin(2\alpha) = 0.052 \ , \qquad \sin(2\beta) = 0.72 \ , \qquad \sin(2\gamma) = 0.68 \ , \tag{2.38}$$

all values being within a few percent or better of the values given in Ref. [34].

The wave functions for the SM quarks (i.e., their distribution over the six sites of the moose in Fig. 2.2) can be visualized in Fig. 2.3, where we provide a density plot of the $\ln|\psi|^2$. In this plot, light squares are where most of the support of the wavefunction is, and we see a clear pattern where each of the three families resides mainly within its own cell of the moose. This localization does not explain the mass hierarchy we achieve in this model: that occurs because the $SU(4)$ symmetry in eq. (2.28) allows the Higgs dependence to rotated out of the Yukawa couplings in $\mathcal{L}_{\rm sym}$, causing the Higgs to only couple through the $SU(4)\times U(3)$ violating spurion operators $\mathcal{M}^{u,d}$ in $\mathcal{L}_{\rm asym}$, which have the hierarchy built into them (eq. (2.35)). However, the localization of families with small overlap in the extra dimension explains the smallness of FCNC in this model, since gauge boson couplings are local, and there are no large spurions breaking locality in this extra dimension which can be used to construct dangerous short-distance operators from physics above the cutoff — only the off-diagonal components of $\mathcal{M}^{u,d}$ communicate between cells, and they are small.

In addition to the SM quarks, the model contains six heavy exotic up and down quarks with masses given in (in TeV)

$$\begin{aligned} U: &\qquad 6.628,\ 5.489,\ 5.482,\ 5.482,\ 5.463,\ 2.684 \\ D: &\qquad 6.628,\ 6.456,\ 5.489,\ 5.486,\ 5.482,\ 5.482 \ . \end{aligned} \tag{2.39}$$

All of these masses are well below the cutoff of the effective theory, $\Lambda \sim 4\pi f \simeq 19$ TeV.

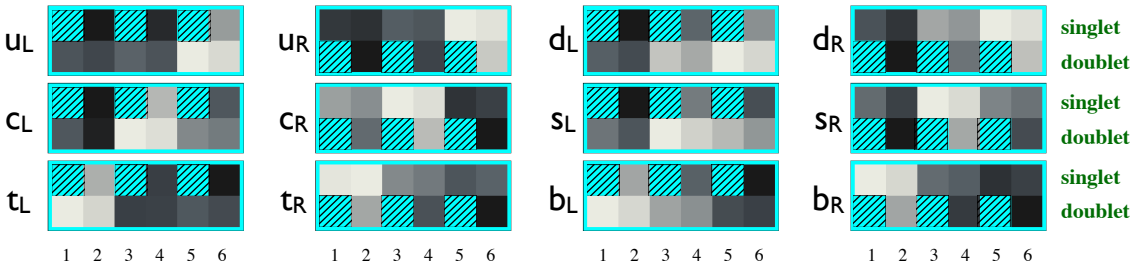

Figure 2.3: A density plot of $\ln|\psi|^2$, where the ψ are the eigenvectors of the LH and RH SM quark wavefunctions; the darker the square, the smaller the wavefunction. Numbers $1,\ldots,6$ along the bottom indicate the site number in the moose of Fig. 2.2; upper and lower rows indicate electroweak singlet and doublet components respectively. One can see, for example, that families are mostly localized in different cells, with the LH down-type quarks being the most spread out, and that RH quarks have a little admixture of doublet, while LH quarks contain some singlet components. Hatched squares indicate combinations that do not exist in the model, such as a LH $SU(2)$-singlet up quark at site #1.

Tree-level FCNC from the Z, Z', and Z'' bosons

We next consider the flavor properties of the neutral gauge bosons in the theory, the Z, Z' and Z''. All exotic gauge boson parameters depend on our choice for the angles $\gamma_{1,2}$, where γ_i parametrizes the relative strength of the gauge interactions on the white and black sites respectively, as in eq. (2.8), and this section we make the somewhat arbitrary choice $\gamma_1 = \gamma_2 = \pi/8$. The Z' and Z'' masses are then given by (eq. (2.11))

$$M_{Z'} = 750 \text{ GeV} , \qquad M_{Z''} = 1400 \text{ GeV} \qquad (\gamma_1 = \gamma_2 = \pi/8) . \tag{2.40}$$

Such masses would be ruled out by direct searches for new heavy neutral gauge bosons if the Z' and Z'' had Z-like couplings to leptons; as we do not consider leptons in this paper, we simply assume that these two exotic gauge bosons are leptophobic; a more complete theory will have to address this issue. Constraints on the flavor changing quark couplings of such bosons are relevant to this model, however, and we consider here the $\Delta F = 1$ and $\Delta F = 2$ processes arising from tree level neutral gauge boson exchange.

It is straightforward to compute the couplings of the gauge bosons for the phenomenological fit discussed above; it simply requires computing the currents coupling to the gauge boson mass eigenstates, and then substituting the light flavor eigenvectors for the $\Psi_{n\alpha a}$

fermions. The results for the couplings of Z, Z', Z'', W and W' are given in the appendix, § A.1.

The off-diagonal neutral gauge boson couplings contribute to tree-level $\Delta S = 2$ operators; in the case of the Z we also have a tree-level contribution to the $\Delta S = 1$ $K^0 \to \mu^+\mu^-$ decay; however, from eq. (A.1) we see that the $\Delta S = 1$ coupling to LH currents equals 10^{-6} , which is sufficiently small to give a branching ratio several orders of magnitude below the observed branching ratio in this channel for the K_L^0.

Squaring the largest $\Delta S = 1$ couplings from eq. (A.1)-eq. (A.3) allows us to compute the coefficients of the $\Delta S = 2$ operators resulting from tree level Z, Z' and Z'', with the results

$$\frac{1\times 10^{-12}}{M_Z^2} \simeq \frac{1}{(10^5\ \text{TeV})^2}\ , \qquad \frac{4\times 10^{-10}}{M_{Z'}^2} \simeq \frac{1}{(4\times 10^4\ \text{TeV})^2}\ , \qquad \frac{1\times 10^{-8}}{M_{Z''}^2} \simeq \frac{1}{(1.3\times 10^4\ \text{TeV})^2} \tag{2.41}$$

The Z and Z' contributions are sufficiently small to have immeasurable effects on kaon phenomenology; the Z'' contribution would be close to the current bounds if it were maximally CP violating, but in fact the phase in the $\bar{s}d$ coupling of the Z'' is found to be 0.06 in a basis where V_{us} is real, so that its $\Delta S = 2$ contributions are likewise compatible with experiment. The product of left currents time right currents receives a chiral enhancement relative to left-left or right-right, but we find that the product of these couplings is very small in each case and not relevant.

FCNC from physics above the cutoff

As our theory is an effective theory for physics below the cutoff $\Lambda \simeq 4\pi f \simeq 19$ TeV, we need to consider whether dangerous FCNC effects can arise from contact operators arising from physics above the cutoff. The generic power counting for operators in the effective theory is [46]: (i) start with an overall factor of $\Lambda^2 f^2$; (ii) include a factor of $1/(\Lambda f^2)$ for each fermion bilinear in the operator; (iii) include a factor of $1/\Lambda$ for each derivative or $\mathcal{M}$ spurion; (iii) include a factor of $1/f$ for each gauge field A and a factor of $g/4\pi$ for each gauge generator T; (iv) include an overall dimensionless coupling assumed to be $O(1)$. We first consider the example of operators contributing to $b \to s\gamma$ which are not a threat but

which are simpler to analyze, before considering more sensitive $\Delta S = 2$ operators for which there are stringent constraints.

Example: tree level contributions to $b \to s\gamma$

We first consider the most symmetric contact operators which could contribute to $b \to s\gamma$,

$$\frac{c_1}{\Lambda^2}\left[(1+\delta)\overline{\Psi}_{m\alpha,L}\mathcal{M}_{m\alpha,n\beta}\left(g_{2b}\tilde{W}^{\mu\nu}\sigma_{\mu\nu}\right)\Psi_{n\beta,R} + (1-\delta)\overline{\Psi}_{m\alpha,L}\mathcal{M}_{m\alpha,n\beta}\left(g_{1b}Y\tilde{B}^{\mu\nu}\sigma_{\mu\nu}\right)\Psi_{n\beta,R} + h.c.\right] \quad (2.42)$$

These operators require an insertion of the $\mathcal{M}$ spurion from eq. (2.27) which gives mass to the vectorlike fermions on the black sites and breaks their chiral $SU(4)$ symmetry down to the diagonal subgroup, as well as insertions of the gauge boson charges which break the vector $SU(4)$ symmetry further down to the gauged $SU(2) \times U(1)$. The coefficients of the two operators should be the same up to radiative corrections, so we expect $c_1 = O(1)$ while δ terms must actually arise from radiative corrections and involve three powers of the gauge generators instead of one, and hence be $O(\alpha/4\pi)$ by the power counting rules.

We can match the above interaction at tree level to the low energy operators

$$\frac{1}{\Lambda^2}\left[\beta_1\frac{em_b}{16\pi^2}\bar{b}_L\sigma_{\mu\nu}s_R F^{\mu\nu} + \beta_2\frac{em_b}{16\pi^2}\bar{b}_R\sigma_{\mu\nu}s_L F^{\mu\nu} + h.c.\right] \quad (2.43)$$

by expressing the Ψ fields and the gauge fields in terms of mass eigenstates, and keeping only the light degrees of freedom of interest. Using the solutions from §2.2.3 we find

$$\begin{aligned} |\beta_1| &= |c_1|\left|(0.0129328 - 0.0331439i) - (56.9843 - 145.866i)\delta\right| \\ |\beta_2| &= |c_1|\left|(0.0267052 - 0.0638978i) + (32.3686 - 83.9222i)\delta\right| , \end{aligned} \quad (2.44)$$

where the phases are a result of our choice of basis. It is apparent from the above expression that the radiative correction proportional to $\delta = O(\alpha/4\pi)$ is comparable to the "leading" term. In either case, both contributions will be far smaller than SM contributions, since $\Lambda \simeq 19$ TeV.

Similarly, we can also consider operators involving insertions of $\mathcal{M}^{u,d}$ instead of $\mathcal{M}$ in the above operator, or operators that involve Ψ on both black and white sites, such as

$$\frac{\lambda f}{\Lambda^2}\overline{\Psi}_{m\alpha,L}\left(g_{1w}YB^{\mu\nu} + g_{2w}W^{\mu\nu}\right)\Sigma\mathcal{Y}_{m\alpha,n\beta}\sigma_{\mu\nu}\Psi_{n\beta} + \ldots \quad (2.45)$$

where the ellipses refers to related terms involving the gauge fields at the black sites, as well as $(\mathcal{Y}\Sigma)^\dagger$ insertions. In every case, the $1/\Lambda^2$ suppression makes these operators uninteresting compared to SM contributions.

Contact operators contributing to $\Delta S = 2$

Next we consider $\Delta S = 2$ four fermion operators, which will involve sums of products of two bilinear $\Delta S = 1$ operators. Therefore we perform the matching of $\Delta S = 1$ bilinears of the form

$$\overline{\Psi}_{m\alpha a}\, S_{m\alpha a, n\beta b}\, \Gamma\, \Psi_{n\beta b} \to c\, \bar{s}\, \Gamma\, d\ , \tag{2.46}$$

where S is any spurion in the theory carrying both site and $SU(4)$ indices which are contracted with the fermion indices, made dimensionless with the appropriate powers of Λ so that c is dimensionless. Γ is a Dirac matrix, and we do not specify whether the operator is color singlet or color octet. The $\Delta S = 2$ operators will then be proportional to the square of such bilinears, with coefficient c^2/Λ^2. We give here a list of such a matching calculation of c for a variety of the largest contributions:

$\bar{s}_L d_R$

$$\begin{aligned}
&\frac{1}{\Lambda}\overline{\Psi}_L \mathcal{M} \Psi_R : && |c| = 2\times 10^{-11}\\
&\frac{1}{\Lambda}\overline{\Psi}_L \mathcal{M}^u \Psi_R : && |c| = 8\times 10^{-11}\\
&\frac{1}{\Lambda}\overline{\Psi}_L \mathcal{M}^d \Psi_R : && |c| = 6\times 10^{-12}\\
&\frac{1}{\Lambda}\overline{\Psi}_L (\mathcal{Y}\Sigma - \mathcal{Y}^\dagger\Sigma^\dagger) \Psi_R : && |c| = 5\times 10^{-11}
\end{aligned} \tag{2.47}$$

$\bar{s}_R d_L$

$$\begin{aligned}
&\frac{1}{\Lambda}\overline{\Psi}_R \mathcal{M}^\dagger \Psi_L : && |c| = 5\times 10^{-10}\\
&\frac{1}{\Lambda}\overline{\Psi}_R (\mathcal{M}^u)^\dagger \Psi_L : && |c| = 8\times 10^{-10}\\
&\frac{1}{\Lambda}\overline{\Psi}_R (\mathcal{M}^d)^\dagger \Psi_L : && |c| = 6\times 10^{-12}\\
&\frac{1}{\Lambda}\overline{\Psi}_R (\mathcal{Y}\Sigma - \mathcal{Y}^\dagger\Sigma^\dagger) \Psi_L : && |c| = 3\times 10^{-10}
\end{aligned} \tag{2.48}$$

$\bar{s}_L\gamma^\mu d_L$

$$\begin{aligned}
&\frac{1}{\Lambda^2}\overline{\Psi}_L\mathcal{M}\mathcal{M}^\dagger\gamma^\mu\Psi_L: && |c| = 8\times10^{-6}\\
&\frac{1}{\Lambda^2}\overline{\Psi}_L\mathcal{M}^u\mathcal{M}^\dagger\gamma^\mu\Psi_L: && |c| = 5\times10^{-6}\\
&\frac{1}{\Lambda^2}\overline{\Psi}_L\mathcal{M}^d\mathcal{M}^\dagger\gamma^\mu\Psi_L: && |c| = 3\times10^{-7}\\
&\frac{1}{\Lambda^2}\overline{\Psi}_L\mathcal{M}^u(\mathcal{M}^u)^\dagger\gamma^\mu\Psi_L: && |c| = 2\times10^{-7}\\
&\frac{1}{\Lambda^2}\overline{\Psi}_L(\mathcal{Y}\Sigma-\mathcal{Y}^\dagger\Sigma^\dagger)\mathcal{M}^u\gamma^\mu\Psi_L: && |c| = 5\times10^{-6}
\end{aligned} \tag{2.49}$$

$\bar{s}_R\gamma^\mu d_R$

$$\begin{aligned}
&\frac{1}{\Lambda^2}\overline{\Psi}_R\mathcal{M}^\dagger\mathcal{M}\gamma^\mu\Psi_R: && |c| = 1\times10^{-6}\\
&\frac{1}{\Lambda^2}\overline{\Psi}_R(\mathcal{M}^u)^\dagger\mathcal{M}\gamma^\mu\Psi_R: && |c| = 2\times10^{-7}\\
&\frac{1}{\Lambda^2}\overline{\Psi}_R(\mathcal{M}^d)^\dagger\mathcal{M}\gamma^\mu\Psi_R: && |c| = 9\times10^{-7}\\
&\frac{1}{\Lambda^2}\overline{\Psi}_R(\mathcal{M}^u)^\dagger\mathcal{M}^u\gamma^\mu\Psi_R: && |c| = 2\times10^{-9}\\
&\frac{1}{\Lambda^2}\overline{\Psi}_R(\mathcal{Y}\Sigma-\mathcal{Y}^\dagger\Sigma^\dagger)\mathcal{M}^u\gamma^\mu\Psi_R: && |c| = 2\times10^{-7}
\end{aligned} \tag{2.50}$$

Given that the $\Lambda \simeq 19$ TeV in our model, and that the four fermion $\Delta S = 2$ operators have a coefficient of c^2/Λ^2 (neglecting RG running effects) we find that all $\Delta S = 2$ effects from short distance physics have a coefficient of $\sim (2\times10^6 \text{ TeV})^{-2}$ or smaller, and pose no problem for phenomenology. The smallness of these operators cannot be attributed to having each family well localized within its own cell on the moose, since there exists sufficient overlap for a realistic Cabibbo angle.

2.2.4 Radiative $SU(4)$ breaking corrections

In section § 2.2.2 we discussed the important role played by the nonlinearly realized $SU(4)'_R$ symmetry of $\mathcal{L}_{\text{sym}}$ in eq. (2.26), which enforced that the standard model families could only have derivative couplings to the Higgs. This allowed us to introduce $SU(4)$ breaking soft spurions $\mathcal{M}^{u,d}$ to give the families mass and distinguish between u-type and d-type quarks, along with $U(3)$ symmetry breaking which allowed us to generate nontrivial hierarchies and mixing angles. A potential problem with this mechanism in the present model is that the G_b gauge interactions explicitly break the $SU(4)'_R$ symmetry as well, and therefore we will

have radiative corrections which spoil the symmetry. In particular, we expect at one loop an $SU(4)'_R$ breaking radiative corrections to the mass $\mathcal{M}$ in eq. (2.27) of form

$$\delta\mathcal{M} \simeq M \times \left[\frac{\alpha_{2b}}{4\pi} \begin{pmatrix} 3/4 & & & \\ & 3/4 & & \\ & & 0 & \\ & & & 0 \end{pmatrix} + \frac{\alpha_{1b}}{4\pi} \begin{pmatrix} 1/36 & & & \\ & 1/36 & & \\ & & 4/9 & \\ & & & 1/9 \end{pmatrix} \right] , \qquad (2.51)$$

where we took $M = 5$ TeV in our fit. One finds that even before turning on the $\mathcal{M}^{u,d}$ spurions in eq. (2.30), this $SU(4)$ violating shift in $\mathcal{M}$ gives a common mass to the standard model quarks of about 25 MeV or higher, depending on the strength of the G_b gauge couplings, as parametrized by the angles $\gamma_{1,2}$ in eq. (2.8). This mass scales as $\sim 1/M$ for larger values of M, but is not very sensitive to reductions in M.

These radiative corrections are very interesting despite being bad news for our phenomenological model. It provides a concrete example how particle masses can be generated radiatively, a dream of theorists since the discovery of the muon with mass $m_\mu \sim m_e/\alpha$. However, since 25 MeV is roughly ten times larger than the up quark mass, this correction invalidates our phenomenological model as it stands. There are several ways to address the problem in the model:

1. We could extend the black site gauge symmetry to $G_b = SU(2) \times SU(2) \times U(1)$ with a discrete symmetry forcing the two $SU(2)$ gauge couplings to have the same value. At one loop the radiative corrections to $\mathcal{L}_{\rm sym}$ would be then be $SU(4)$ symmetric. The Σ field would spontaneously break $G_w \times G_b$ down to $SU(2) \times U(1)$ as before, but now there would be an additional massive W'' gauge boson which would eat the π Goldstone boson. The spurions $\mathcal{M}^{u,d}$ would then have to actually be vacuum expectation values of fields also spontaneously breaking $G_b \to SU(2) \times U(1)$. In this case we would expect the $SU(4)$ violation to be communicated to the SM families with an additional $M^2_{W''}/M^2$ suppression, making the radiative contribution to quark masses at the ~ 1 MeV level or smaller. The extended the G_b gauge symmetry would also impact how the Higgs potential was constructed, but would not be hard to work around.

2. Because of the see-saw nature of SM quark masses in our model, mixing through heavy Dirac families, raising the mass M reduces the effect of radiative corrections. Therefore we could make the $\mathcal{M}$ operator $U(3)$ violating (but still $SU(4)$ symmetric) with larger values corresponding to sites where the lighter families sit. In this way, $SU(4)$-violating radiative corrections contributing to the lighter family masses would be reduced. Presumably with such a hierarchy put in by hand in $\mathcal{L}_{\rm sym}$, the hierarchy in the $\mathcal{M}^{u,d}$ spurions could be less pronounced, but we have not pursued this.

3. It might also be possible to devise related models where the analogue of the radiative $SU(4)$ violation occurred only at two loops, which would render the effect negligibly small.

We do not pursue these ideas further here, since the radiative correction problem does change the two most interesting features of this model: that a symmetry which is not a chiral family symmetry ($SU(4)'_R$ here) can enforce light SM family masses, and (ii) that it is possible to have a phenomenologically sensible model with flavor at the TeV scale which does not invoke minimal flavor violation, and yet still does not have unacceptable FCNC.

2.2.5 The Σ field potential and vacuum alignment

The pseudo-Nambu-Goldstone bosons (pNGBs) in this model parametrize the alignment of the vacuum, which determines whether or not the weak gauge bosons obtain mass via the Higgs mechanism. Some of the pNGBs are "little", meaning that their masses do not receive quadratically divergent one loop contributions from order one interactions, and are naturally light compared with the scale f. The little doublets, H_u and H_d, serve as our little Higgs fields. In a successful little Higgs model these little Higgs doublets obtain a vev v which is parametrically small compared with the compositeness scale f. Obtaining such symmetry breaking pattern with a natural separation between f and v requires competing terms: larger terms, which are minimized in the $\Sigma = 1$ vacuum, but which begin at quartic powers of the little Higgs fields, and smaller terms, which begin at quadratic order in the little Higgs fields, whose net effect is to slightly misalign the vacuum away from $\Sigma = 1$.

In general the Yukawa interactions radiatively produce one loop finite, negative quadratic terms and the gauge interactions produce smaller positive quadratic terms with a one loop log divergence.

Radiative corrections and quadratic terms

The divergence from the gauge loops may be absorbed into the counterterm for the effective interactions

$$\begin{aligned} V_{\text{eff}} \supset c_{\text{gauge}} \frac{f^4}{16\pi^2} \Big[& \quad g_{2,w}^2 g_{2,b}^2 \sum_{a,c=1}^{3} \text{Tr}\left(T_a \Sigma T_c \Sigma^\dagger\right) \text{Tr}\left(T_a \Sigma T_c \Sigma^\dagger\right) \\ & + \quad g_{2,b}^2 g_{1,w}^2 \sum_{a=1}^{3} \left(\text{Tr}\left(T_a \Sigma Y \Sigma^\dagger\right)\right)^2 \\ & + \quad g_{1,b}^2 g_{2,w}^2 \sum_{a=1}^{3} \left(\text{Tr}\left(Y \Sigma T_a \Sigma^\dagger\right)\right)^2 \\ & + \quad g_{1,b}^2 g_{1,w}^2 \left(\text{Tr}\left(Y \Sigma Y \Sigma^\dagger\right)\right)^2 \Big] \end{aligned} \tag{2.52}$$

where the coefficient c_{gauge} is of order one and requires knowledge of the underlying theory to compute, but is assumed to be positive. The interactions in eq. (2.52) give mass of order $g^2 f/(4\pi)$ to the $\pi^\pm$ and little Higgs fields. The field H_U gets a large finite negative contribution from the loops involving the top quark and its partners and small contributions from the other quarks, and H_D gets small negative contributions. In a simple model with two top partners, an electroweak doublet with mass m_L and an electroweak singlet with mass m_R, the one loop contribution to the Higgs mass squared would be:

$$\delta V_{\text{eff}} \supset -\frac{3\lambda_t^2 H_U^\dagger H_U}{8\pi^2} \frac{m_L^2 m_R^2}{m_L^2 - m_R^2} \log \frac{m_L^2}{m_R^2} \ . \tag{2.53}$$

In our model there are a total of six partner quarks cooperating to cancel quadratic divergences from the top loop, but we checked numerically that eq. (2.53) holds to within 10% when m_L and m_R are replaced with the masses of the two lightest exotic charge 2/3 quarks. The negative quadratic terms for the little Higgs arise from a combination of the one-loop terms and additional small symmetry breaking terms which are introduced to give masses to all the pseudo-Nambu Goldstone bosons with parameters which may be tuned to give the electroweak scale in agreement with experiment. If we assume that the 126 GeV Higgs-like

boson is the lightest boson in the Higgs sector and that it is standard model-like, then with our quark mass spectrum the various contributions to the quadratic term in Higgs potential cancel to within about 7%, a mild tuning.

Plaquette terms

In Ref. [17] four sigma fields were introduced and "plaquette" terms giving Higgs quartic interactions arose from combinations of terms involving traces of the four fields. This is obviously possible to repeat here, and there are no problems with the experimental viability of such a model. Since only one of the four sigma fields needs to couple to the fermions, introducing more fields will not affect the FCNC analysis. However, we wish to retain a more economical scalar sector for simplicity. With only a single Σ field, contributions to the Higgs potential may be introduced using symmetry breaking spurions. Note that a subset of the terms in eq. (2.52), namely

$$V_{\text{eff}} \supset c_{\text{quartic}} f^4 \left(\sum_{a=1}^{3} \left(\text{Tr} \left(T_a \Sigma Y \Sigma^\dagger \right) \right)^2 + \sum_{a=1}^{3} \left(\text{Tr} \left(Y \Sigma T_a \Sigma^\dagger \right) \right)^2 \right) \tag{2.54}$$

have the feature that they begin at quartic order in the little Higgs fields, although obtaining an $O(1)$ quartic coupling requires a coefficient which is larger than the one induced by gauge loops, by a loop factor. Other terms inducing quartic but not quadratic terms in the little Higgs fields are

$$V_{\text{eff}} \supset c'_{\text{quartic}} f^4 \left(\sum_{a=1}^{3} \left(\text{Tr} \left(T_a \Sigma X_d \Sigma^\dagger \right) \right)^2 + \sum_{a=1}^{3} \left(\text{Tr} \left(X_d \Sigma T_a \Sigma^\dagger \right) \right)^2 \right) \tag{2.55}$$

and

$$V_{\text{eff}} \supset c''_{\text{quartic}} f^4 \left(\sum_{a=1}^{3} \left(\text{Tr} \left(T_a \Sigma X_u \Sigma^\dagger \right) \right)^2 + \sum_{a=1}^{3} \left(\text{Tr} \left(X_u \Sigma T_a \Sigma^\dagger \right) \right)^2 \right) \tag{2.56}$$

These terms do an adequate job of giving a quartic potential for the neutral Higgs bosons. Unfortunately, unlike in some little Higgs models [16, 94, 168], we do not have an underlying reason based on the gauge symmetry for the inclusion of these terms and not others, which, with similar sized coefficients, could give a Higgs mass term of order f. We note however that the terms which give a Higgs mass do not preserve the same subset

of the global symmetries as the ones we have included, so their omission is technically natural. Renormalizing the theory will require the introduction of spurions that could give a Higgs mass squared term, however with coefficients which can naturally be assumed to be suppressed by loop factors.

Spurions contributing to the other scalar masses and vacuum alignment

The term

$$\mathrm{Tr}\,(X_u \Sigma X_d \Sigma^\dagger) + \mathrm{Tr}\,(X_d \Sigma X_u \Sigma^\dagger) \tag{2.57}$$

will give a mass to the $\pi^\pm$ and a quartic interaction involving charged Higgses, but no terms involving only neutral components of H_u or H_d. Each of these terms preserves different $SU(3)$ symmetries under which the Higgses transform nonlinearly, and since the divergent parts of one loop diagrams only depend on a single interaction, the interaction eq. (2.57) will not lead to one loop quadratic divergences in the Higgs potential. The term eq. (2.57) can be used to make the charged Higgs bosons relatively heavy without quadratic divergences. With an $\mathcal{O}(1)$ coefficient, this term will give masses to the $\pi^\pm$ of order f. To build other gauge invariant spurions contributing to scalar masses and vacuum alignment, consider the field combinations

$$z_a = \mathrm{Tr}\,\left[\begin{pmatrix} 0 & \\ & \sigma_a \end{pmatrix} \Sigma\right] \tag{2.58}$$

for $a = 0, \ldots, 3$, where σ_0 is the unit matrix.

The quantities

$$\mathcal{P}_1 = (|z_1|^2 + |z_2|^2)\ , \quad \mathcal{P}_2 = (z_1^2 + z_2^2)\ , \tag{2.59}$$

are gauge invariant and and begin at quartic order in the Higgs fields, and give mass to the $\pi^\pm$, but do not contribute to any quartic only involving neutral Higgses. Other gauge invariant symmetry breaking terms are

$$\mathcal{P}_3 = (|z_0|^2 + |z_3|^2)\ , \quad \mathcal{P}_4 = (z_0^2 - z_3^2)\ , \tag{2.60}$$

which begin at quadratic order in the Higgs fields. The term $\Re\mathcal{P}_4$ gives a mass to the η, since it also contributes to the Higgs masses. If we keep the coefficient of this term small enough to avoid fine-tuning the Higgs mass, the η mass will be of order the weak scale or lighter. The term $\Im\mathcal{P}_4$ violates parity and leads to a nonzero η vev; its inclusion is optional and we will omit it to avoid this complication.

2.2.6 Little flavor from extra dimensions

The model described above was motivated by earlier work on the origin of families from extra dimensions, [121]. Logically there is no need to consider the connection with extra dimensions, but we discuss the relation here on the chance that it could lead to further development of either theory.

The TI/domain wall fermion flavor mechanism

A topological insulator (TI) is a material which has massless fermion surface modes, whose existence is dictated by topological properties of the fermion dispersion relation in the bulk of the material; for references, see [91,159]. The mechanism behind topological insulators is the same as that discovered earlier in the domain wall construction for lattice field theories in 4d with chiral fermions [110]. A fascinating feature of such theories is that the number of generations of light surface modes in these lattice theories can change discontinuously (for an semi-infinite material with a single surface) as the coupling constants in the underlying Lagrangian are changed continuously, as first shown in [78, 100]. These changes occur at critical couplings for which the bulk spectrum becomes gapless, at which point a winding number associated with the fermion propagator jumps discontinuously from one value to another. In particular, it was shown in [78,100] that when the Euclidian fermion propagator $S(p)$ is suitably regulated, the number of massless surface modes is a topological invariant proportional to the integral

$$\epsilon_{abcde}\int\frac{d^5p}{(2\pi)^5)}\mathrm{Tr}\,\left[S^{-1}(p)\partial_a S(p)\cdots S^{-1}(p)\partial_e S(p)\right] \tag{2.61}$$

where the partial derivatives are with respect to the 5-momentum p, and the critical couplings at which the number of zeromodes can change are those for which the bulk gap

vanishes and $S(p)$ develops a pole. The idea presented in [121] was that the three generations of SM fermions observed in 4d could be such multiple surface modes of a single 5d bulk fermion, where this number of surface modes is determined by the topology of the 5d fermion dispersion relation, and an example was given which gave rise to three chiral families on the boundary of a semi-infinite extra dimension.

There are several difficulties in implementing a realistic theory using this idea in its simplest form. One is that while this mechanism can explain why the standard model has three families, it does not directly provide an explanation for the observed hierarchical structure of Yukawa couplings to the Higgs. Another is that flavor physics is an inherently UV phenomenon in such models, and 5d field theories are not well defined in the UV [2]. Finally, while three chiral families can arise when the 5d spacetime is semi-infinite with only one 4d surface, such a geometry is not compatible with observed gauge and gravitational interactions, as both gravitons and gauge fields necessarily live in the 5d bulk in such theories, and the bulk gauge fields are not compatible with 4d phenomenology. If the extra dimension is compactified to solve this problem, then fermion zeromodes generically appear in vector-like representations and cannot give rise to the observed chiral gauge theory of the SM at low energy.

As mentioned in [121], the problem of chirality can be solved through a conventional Z_2 orbifold projection which we discuss below; the problem of UV ambiguity may be avoided by using the technique of deconstruction [20]. Combining the two gives rise to a class of theories such as the model discussed in this paper.

The Z_2 orbifold projection

Deconstruction replaces the extra dimension with a lattice; by treating gravity (and possibly gauge interactions) as strictly four-dimensional, deconstruction yields a 4d theory with multiple copies of fields associated with the sites and links of the lattice. Five dimensional locality translates into nearest neighbor interactions on this lattice, but is not required for the 4d theory to make sense.

---

[2] It is a UV phenomenon because the number of families depends on the momentum space topology of the fermion dispersion relation, requiring knowledge of the propagator $S(p)$ at large p.

In order to ensure a chiral fermion spectrum, we require the action to be invariant under a Z_2 symmetry under which all fields ϕ transform as $\phi \to \hat{z}\phi$ where $\hat{z}^2 = 1$. The orbifold projection then consists of replacing every field ϕ in the model by

$$\phi \to \mathcal{P}_z \phi \ , \qquad P_z = \tfrac{1}{2}\left(1 - \hat{z}\right) \ . \tag{2.62}$$

The fields in our model consist of 5d (Dirac) fermions ψ and gauge fields which live on sites, as well as bosonic link fields Σ which will contain, among other mesons, the Higgs. The action of the Z_2 on fermions is

$$\hat{z}\psi_i = \mathcal{R}_{ij}\gamma_5\psi_j \tag{2.63}$$

with $\mathcal{R} = \mathcal{R}^\dagger$ and $\mathcal{R}^2 = 1$. Hopping terms in the deconstructed 5d theory appear as mass terms in the 4d interpretation,

$$\overline{\psi}_i M_{ij} P_R \psi_j + h.c. \ , \qquad P_R = \tfrac{1}{2}(1 + \gamma_5) \ , \tag{2.64}$$

where i, j are summed over sites and M can be an arbitrary finite matrix so long as it respects the Z_2 symmetry,

$$-\mathcal{R}M\mathcal{R} = M \ . \tag{2.65}$$

An index theorem proved in the appendix (§ A.2) states that

$$(\mathcal{N}_L - \mathcal{N}_R) = \mathrm{Tr}\,\mathcal{R} \ , \tag{2.66}$$

where $\mathcal{N}_L$ and $\mathcal{N}_R$ are the number of massless left-handed and right handed modes that survive the orbifold projection. If R_{ij} represents a spatial reflection in the extra dimension taking site i to site j, then nonzero diagonal elements in R must equal ± 1 and are associated with the fixed points of the Z_2 reflection. The net number of chiral families thus equals the number of fixed points minus $2k$, where k counts the number of $\{-1, 1\}$ pairs of diagonal elements of $\mathcal{R}$. Since a simply connected curve will have an even number of fixed points under reflection, to obtain three standard model chiral families will require exotic geometry in the extra dimension. For example, we can consider the configuration and pictured in Fig. 2.4 featuring an extra dimension in the shape of three circles arranged in a ring with

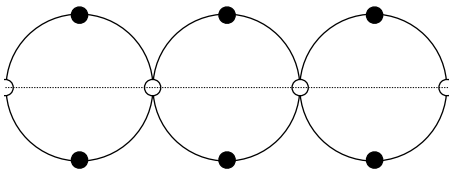

Figure 2.4: The lattice model prior to the Z_2 orbifold; the Z_2 symmetry acts as reflection about the horizontal axis and possesses three fixed points (white) and three pairs of points which transform into each other (black). The arrangement is periodic, with the first and last white points identified.

three shared points (white dots in Fig. 2.4). The action of $\mathcal{R}$ is to reflect about the horizontal axis; black sites are exchanged while white sites are fixed points.

We arrange the fermions on every site to be 4s of $SU(4)$

$$\psi = \begin{pmatrix} u \\ d \\ U \\ D \end{pmatrix} \tag{2.67}$$

where u, d form an $SU(2)$ doublet and U, D are $SU(2)$ singlets. Then we specify that the white site fermions are eigenstates of $\mathcal{R}$, with u, d having eigenvalue $+1$ and U, D having eigenvalue -1. The orbifold projection therefore leaves LH $SU(2)$ doublet zeromodes and RH $SU(2)$ singlet zeromodes at the white sites. In contrast, $\mathcal{R}$ interchanges the fermions at the pairs of black sites; the orbifold projection then reduces the two black sites to one, occupied by a single Dirac fermion. The resulting theory looks like the moose of Fig 2.2 with fermion content of eq. (2.21) and eq. (2.22).

The orbifold similarly reduces by half other fields that may live on the black sites, as well as link variables. The way we included gauge fields and link variables in the model discussed in this paper was motivated by a desire to keep the 4d model as simple as possible, and not to facilitate a 5d or higher dimensional interpretation. It is possible that other interesting models could be derived that are more faithful to a 5d spacetime interpretation, although the index theorem seems to require that the extra dimension be multiply connected if one requires three light families in the low energy theory.

2.2.7 Discussion

In this model we have tied together the large global symmetries of little Higgs models with the global flavor symmetries that arise in a deconstruction of the extra-dimensional "topological insulator" model of flavor in [121]. The role of these symmetries is different from any that have appeared previously in the flavor symmetry literature. In particular, at tree level there is a nonlinearly realized $SU(4)$ symmetry which is not chiral and which ensures that the SM fermions only have derivative couplings to the Higgs at tree level. This symmetry is broken by radiative corrections which, along with the breaking of other symmetries at the few TeV scale, allows us to generate realistic masses and mixing angles for the light fermions. Remarkably, even with the flavor physics at a few TeV, flavor changing neutral currents from the new physics are smaller than those generated radiatively in the Standard Model.

The model described in this paper only describes the quarks. We expect that leptons may be included in a similar way, with care taken to ensure that light exotic vector mesons are leptophobic. As with most flavor models involving leptons, a natural suppression mechanism for $\mu \to 3e$ will be critical. An explanation for the small size of the neutrino masses will require some new ingredient, such as a large Majorana mass for the right handed neutrinos.

We have not discussed the experimental signatures of the model, and, without having included the leptons, are not yet in a position to do so. An obvious signature is that the low energy effective theory below the TeV scale includes 2 Higgs doublets and a singlet, providing possible signatures in the usual searches for additional Higgs bosons. Unlike in the original little Higgs models, which were very constrained by precision electroweak measurements, in this model the light quarks as well as the heavy quarks are linear combinations of quarks in transforming under different SU(2) and U(1) gauge groups, giving partial cancellations in the coupling to the new gauge bosons. For example for the reference parameters considered here (such as $M = 5$ TeV, $f = 1.5$ TeV and $\gamma_{1,2} = \pi/8$, which were not fine-tuned, plus the parameters λ and $\mathcal{M}_{u,d}$ chosen to correctly reproduce the quark masses and CKM angles, which were fine-tuned), the Z' couplings to quarks are smaller than the Z couplings by a factor of around 10^{-2}, and the Z'' and W' couplings are suppressed by about an order of

magnitude relative to the Z and W couplings. These suppressions are enough to satisfy current collider bounds for jet, top quark and gauge boson final states [3–5, 39, 41, 48]. If we include the leptons in the obvious way, with Dirac neutrino masses, and no additional gauge groups, then the usual searches for new particles decaying into leptons would constrain the model. In order to evade dilepton search constraints [2, 40], the new neutral gauge bosons would have to be leptophobic, even more weakly coupled to quarks, or else heavier. The couplings to quarks could be reduced further by tuning the mixing parameters γ_i. Making the W' and Z', Z'' bosons heavier without increasing f (which would increase the fine tuning) would require introducing another sigma field with a larger decay constant, not coupled to fermions. The heavy gauge bosons would then eat the would be Nambu-Goldstone bosons from the other sigma field, leaving more scalars light. Exploring these directions in model building and collider phenomenology is interesting but beyond the scope of this paper.

This model was constructed with the aim of providing a realistic detailed description of low energy phenomenology, so that a precise quantitive analysis of FCNC could be performed. As such, we focused on a numerical fit to low energy data, rather than taking a more qualitative and analytical approach. Our fit does not predict the observed quark masses and mixing angles, as these are built into the structure of the spurions used, particularly $\mathcal{M}^u$ and $\mathcal{M}^d$ in eq. (2.35). It would be very interesting to be able to construct a more ambitious theory based on flavor symmetries which explained the structure of these spurions, and hence the SM particle spectrum, perhaps exploiting the radiative contribution to fermion masses discussed in § 2.2.4.

Chapter 3

MONOPOLES AND D-BRANE IN FIELD THEORY

3.1 monopole-electron system on a TI interface

3.1.1 Introduction

The low energy effective theory describing three dimensional topological insulators (TIs) is given by Maxwell electromagnetism augmented by an axion like $\vec{E} \cdot \vec{B}$ term [160] leading to modified constitutive relations. For the bulk material this effective theory is valid at energy scales below the gap. In the presence of interfaces the massless modes on the surface would have to be included in the effective description of the material and the low energy effective description in terms of Maxwell theory with modified constitutive relations only applies if the surface modes are gapped by an external (time reversal breaking) perturbation and furthermore the effective description is only valid at energy scales below this induced surface gap. Such an external breaking can easily be set up experimentally, e.g. by an external magnetic field. Several potential experimental consequences follow from this effective theory, such as, for an example, a non-trivial Faraday and Kerr rotation [160]. By scanning the external field, the topological contribution to the Faraday effect from the external field can be cleanly separated from the topological contribution. One of the most spectacular predictions of this effective theory is the appearance of a magnetic monopole mirror charge when solving for the static electromagnetic fields sourced by a single point charge (located inside a topological trivial insulator such as e.g. vacuum) in the presence of a TI interface [161].

For an infinitely extended planar interface, the corresponding magnetic mirror charge is a pointlike magnetic monopole (also carrying some electric charge). As always with mirror charges, this monopole of course is not physical but simply a mathematical tool to calculate the magnetic fields in the physical region (that is for calculating the fields above the interfaces, the monopole appears to be located below the interface and vice versa).

Microscopically it is surface currents on the interface that source a magnetic field with a $1/r^2$ fall-off where r is the distance to the mirror monopole. Nevertheless, the magnetic fields generated this way are, in the physical region, indistinguishable from the ones generated by a genuine monopole and so share some of its properties. In particular, it is well known that the electromagnetic fields generated by an electric point charge e and a spatially separated monopole of magnetic charge g carry a net angular momentum which has several interesting properties: it is independent of the distance between charge and monopole, pointing in the direction from the charge to the monopole and proportional to eg (see e.g. [98]). This total angular momentum of the composite dyon formed by the charge-monopole pair is the sum of the angular momenta of the two point particles and this angular momentum stored in their fields. Via the spin-statistics theorem this shift in the angular momentum of the dyon is often interpreted as a shift in the statistics angle that determines the behavior of the multi-dyon wavefuntion under the exchange of two dyons. For a genuine charge/monopole pair, the Dirac quantization of magnetic charges ensures that the resulting angular momentum is an integer multiple of $\hbar/2$. So while the statistic of the dyonic system can be changed due to angular momentum stored in the fields, the net angular momentum is still properly quantized the overall statistical angle is always an integer multiple of π. The full dyonic system is either a fermion or a boson.

As the field of the mirror monopole is indistinguishable from the field of a real monopole, the same calculation implies that the electromagnetic fields generated by a single electric point charge e above the interface of a TI carry a non-trivial angular momentum as well [161]. As the electric as well as the magnetic field below the interface (that is inside the TI) appear to be sourced by coincident charges located at the location of the actual physical charge, the contribution to the angular momentum from that region of space vanishes. By symmetry, the actual angular momentum in the system obtained from integrating over the electric and magnetic fields above the interface, sourced by the physical electric charge as well as the mirror charge, gives exactly half of the angular momentum one would get from a genuine charge/monopole pair with the same values of e and g. However the magnitude of the induced mirror charge is proportional to the finestructure constant α and furthermore depends continuously on the material properties μ and ϵ. Consequently, it generically does

not obey Dirac quantization conditions. The resulting angular momentum is not quantized. As a result, the statistics one associates with these charge carriers based on their angular momentum is no longer simply fermionic or bosonic. Instead they seem to behave as anyons with a statistical angle given by [1]

$$\theta_S = \pi \frac{L}{\hbar} = \frac{4\pi\alpha^2 P_3}{(\frac{\epsilon_1}{\epsilon_0} + \frac{\epsilon_2}{\epsilon_0})(\frac{\mu_0}{\mu_1} + \frac{\mu_0}{\mu_2}) + 4\alpha^2 P_3^2}. \tag{3.1}$$

$P_3 = \theta/(2\pi)$ is the electromagnetic polarization. It is 0 in a topologically trivial material and 1/2 inside a TI. In order to ensure that our expression for θ_S can be compared between different unit systems, we explicitly displayed factors of ϵ_0 and μ_0. For the bulk of this work we'll work with units where $\epsilon_0 = \mu_0 = 1$.

The non-trivial statistical angle was interpreted in [161] as a result of the two dimensional nature of the TI surface. It is well known that in two spatial dimensions, anyonic statistic is allowed. The authors of [161] proposed that in the vicinity of a TI surface an electric point charge indeed turns into an anyon with statistical angle θ_S and proposed an explicit experimental setup that would allow its measurement. This proposal raises one important conceptual puzzle: the angular momentum in the system and hence the inferred θ_S is entirely independent of the distance d between the point charge and the interface. While it is reasonable to assume that a point charge in close vincinity of a TI surface has anyonic character, the calculation of θ_S seems to predict that any point charge moving freely in three dimensional space would pick up a statistical angle θ_S provided there is a planar TI interface somewhere in the universe at arbitrary large distance d, which is very counter-intuitive and also seems to indicate that the anyon is truly 3+1 dimensional in character, contradicting

[1] Our expression differs by a factor of 2π from the one quoted in [161]. A factor of 4π seems to be due to the fact that in [161], which works in Gaussian units, the formula for the statistical angle has been normalized to yield $\theta_S = \pi$ for a monopole of flux hc/e. However latter has been taken to correspond to $g = hc/e$, which would be correct if $\vec{\nabla} \cdot \vec{B} = g\delta(\vec{r})$ as it is in SI units. However in Gaussian units $\vec{\nabla} \cdot \vec{B} = 4\pi g\delta(\vec{r})$ and so the formula for θ_S in [161] in terms of general e and g should be modified by a factor of 4π. The remaining factor of 2 mismatch seems to be due to the fact that in [161] the factor of 1/2 from the fact that only the half of space above the interface contributes to the angular momentum has not been taken into account. For the reader's convenience we rederive the expression of the statistical angle in SI units in the appendix, where intermediate steps can be readily compared to standard textbook expressions from e.g. [98]. This confirms the factor of 2π as we have it here. For the bulk of the paper we follow [161] and use Gaussian units. The final expression for the statistical angle has to be independent of choices of units when only expressed in terms of the fine structure constant α as well as the ratios ϵ/ϵ_0 and μ/μ_0.

the fact that 3+1 dimensional anyons should be impossible (the exception recently proposed in [174] can readily be understood in terms of a more complicated topology of configuration space in this case [65]).

One could expect the d-independence of the angular momentum to be an artifact of the special example of an infinite planar interface. After all, $L/\hbar$ is dimensionless and so could only depend on d in the form of a ration d/a, where a is another geometric scale in the problem. For the infinite plane, no such other scale is present. With this puzzle in mind, we analyze the angular momentum associated with an electric point charge in the vicinity of a TI interface for two different geometries: a TI in the shape of a sphere and a TI with a semi-infinite tube like shape inside a perfectly conducting cavity. We find that in *both* cases the statistical angle vanishes identically for any charge separated from the surface even by an infinitesimal amount. These two examples make us suspect that the statistical angle will in fact vanish for a charge close to (but not right on top) the surface of any finite size TI. In hind-sight, this result is not too surprising. After all, the microscopic description of the topological insulator is in terms of a system of electrons and protons with properly quantized charges, obeying the standard rules of quantum mechanics. Any state described by this microscopic system has to have a properly quantized angular momentum. As long as the effective theory correctly captures the long distance behavior of the system, it has to obey the quantization conditions obeyed by the microscopic constituents. So the angular momentum L for a charge close to any compact TI has to be an integer multiple of $\hbar/2$. As a consequence, L can not continuously vary as a function of d/a. As we expect $L \to 0$ for $d/a \to 0$, it should have been expected that $L = 0$ is indeed the correct answer for all finite values of d/a.

At first this result may indicate that the non-trivial θ_S identified in the planar case does not carry over to any compact sample and hence would not be measurable. But this is too naive. After all, total angular momentum of the one-particle system was only taken as a stand-in for the statistics angle of the excitations. A more careful analysis should directly analyze the two-particle system and study the change in action associated with a non-trivial loop in configuration space. Performing this analysis we find in the case of the planar inteface that θ_S as inferred from the angular momentum in the one-particle

system only describes the exchange of two particles in the limit that the size of the loop l is much larger than the separations d_1 and d_2 of the charges to the surface of the TI. This is completely consistent with the interpretation of θ_S as a topological effect. For $l \sim d_{1,2}$ short distance effects become important. In this limit details of the path matter. But for $l \gg d_{1,2}$ the only effects surviving are the topological phase (which in this limit is independent of the shape of the loop as it should be). So the statistics angle governs large loops in configuration space. However, for the realistic case of a compact TI of linear size a, we should clearly expect significant finite size effects in the case that loops are of order the sample size, $l \sim a$. Indeed this expectation is born out. For generic $d_{1,2}$ and a the change in action associated to taking particle 2 around particle 1 depends crucially on the path and has no relation to the θ_S obtained from the planar case. However, in the intermediate loop size regime

$$d_{1,2} \ll l \ll a$$

we once more are able to show that the phase is topological (independent of shape) and is given by the flat space value θ_S. While not surprising, this analysis clearly lays out that any experimental attempt at measuring θ_S e.g. as proposed in Ref. [161] has to be set up as to operate in this intermediate loop size regime.

This note is organized as follows: In the next two sections we'll review the solution for the potentials in the case of a spherical TI and construct the solution of the potentials in the case of a tube-like TI. In section 3 we analyze the distance dependence of the statistics angle. We first show that in the one particle system angular momentum vanishes identically in both examples. We then analyze explicitly the two-particle system and show, in the case of the sphere, that θ_S obtained from the flat space analysis does govern the intermediate loop size regime. We discuss the relevance of these results in section 4.

3.1.2 Electric and Magnetic Potentials in two compact examples

Spherical TI

First let us analyze the electric and magnetic fields for a spherical topological insulator and a point-like electric charge outside the sphere. The corresponding potentials have been worked

out in the supplementary material of [161]. As shown in Fig. 3.1, a spherical topological insulator of a radius a and a magneto-electric polarization P_3 is centered at the origin, and a point-like electric charge is at $(0, 0, d)$. ϵ_1 and μ_1 are the dielectric constant and the magnetic permeability outside the sphere, ϵ_2 and μ_2 the corresponding quantities inside the sphere.

Both inside and outside the sphere, the curl of electric and magnetic fields is zero, thus we can find a scalar potentials in both regions:

$$\begin{aligned} E^{(i)} &= -\nabla \Phi_E^{(i)} \\ B^{(i)} &= -\nabla \Phi_M^{(i)} \end{aligned} \tag{3.2}$$

where $i = 1, 2$ stand for inside and outside region. The most general solution for the potentials in eq. 3.2 can be written in terms of Legendre polynomials:

$$\begin{aligned} \Phi_E^{(1)} &= \tfrac{q}{\epsilon_1} \textstyle\sum \frac{r^l}{d^{l+1}} P_l(cos\theta) + \sum A_l (\frac{a}{r})^{l+1} P_l(cos\theta) \\ \Phi_E^{(2)} &= \textstyle\sum B_l (\frac{r}{a})^l P_l(cos\theta) \\ \Phi_M^{(1)} &= \textstyle\sum C_l (\frac{a}{r})^{l+1} P_l(cos\theta) \\ \Phi_M^{(2)} &= \textstyle\sum D_l (\frac{r}{a})^l P_l(cos\theta) \end{aligned} \tag{3.3}$$

Solving boundary condition for the interface between trivial and topological insulator (that is continuity of the perpendicular components of $\vec{D}$ and $\vec{B}$ as well as the parallel components of $\vec{H}$ and $\vec{E}$), one arrives at:

$$\begin{aligned} A_l &= \tfrac{q}{\epsilon_1} \tfrac{a^l}{d^{l+1}} [\tfrac{(\epsilon_1 l - \epsilon_2 l)[l/\mu_1 + (l+1)/\mu_2] - (2\alpha P_3)^2 l(l+1)}{(2\alpha P_3)^2 l(l+1) + (\epsilon_1(l+1) + \epsilon_2 l)[l/\mu_1 + (l+1)/\mu_2]}] \\ B_l &= \tfrac{q}{\epsilon_1} \tfrac{a^l}{d^{l+1}} [\tfrac{(\epsilon_1 l - \epsilon_2 l)[l/\mu_1 + (l+1)/\mu_2] - (2\alpha P_3)^2 l(l+1)}{(2\alpha P_3)^2 l(l+1) + (\epsilon_1(l+1) + \epsilon_2 l)[l/\mu_1 + (l+1)/\mu_2]} + 1] \\ C_l &= q \tfrac{a^l}{d^{l+1}} \tfrac{(2\alpha P_3)^2 l(2l+1)}{(2\alpha P_3)^2 l(l+1) + (\epsilon_1(l+1) + \epsilon_2 l)[l/\mu_1 + (l+1)/\mu_2]} \\ D_l &= q \tfrac{a^l}{d^{l+1}} \tfrac{-(2\alpha P_3)^2 (l+1)(2l+1)}{(2\alpha P_3)^2 l(l+1) + (\epsilon_1(l+1) + \epsilon_2 l)[l/\mu_1 + (l+1)/\mu_2]} \end{aligned} \tag{3.4}$$

The fields here could be considered to be generated by a point image electric charge, magnetic monopole, and a line of image electric or magnetic charges.

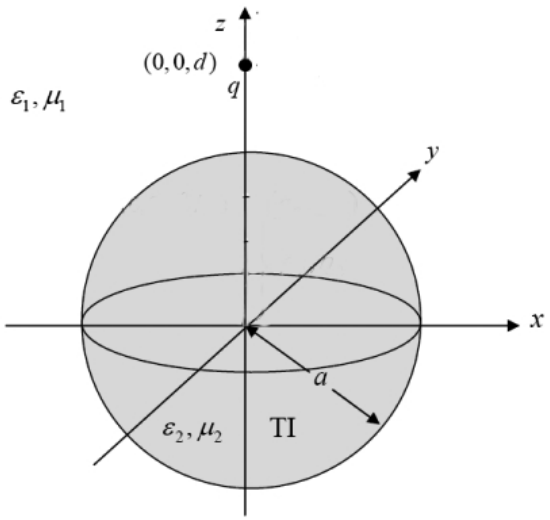

Figure 3.1: A charge q being outside of spherical TI.

Semi-infinite rectangular TI-tube in conducting cavity

Next we want to consider the case of a semi-infinite topological insulator (the TI being at $z < 0$) tube with rectangular cross section inside a conducting wall, see Fig. 3.2. An electric point-like charge is located at (x', y', z'). As in the spherical case, we can write down general forms for electric and magnetic potential:

$$\begin{aligned}
\Phi_E^{(1)} = \tfrac{q}{\epsilon_1} \textstyle\sum O_{mn} sin(k_m x) sin(k_n y) e^{\gamma_{mn}(z-z')} + \sum A_{mn} sin(k_m x) sin(k_n y) e^{-\gamma_{mn} z} \\
\Phi_E^{(2)} = \textstyle\sum B_{mn} sin(k_m x) sin(k_n y) e^{\gamma_{mn} z} \\
\Phi_M^{(1)} = \textstyle\sum C_{mn} sin(k_m x) sin(k_n y) e^{-\gamma_{mn} z} \\
\Phi_M^{(2)} = \textstyle\sum D_{mn} sin(k_m x) sin(k_n y) e^{\gamma_{mn} z}
\end{aligned} \tag{3.5}$$

with O_{mn} being the coefficients of the Green's function of a point-like charge in this system:

$$O_{mn} = \frac{2}{ab\gamma_{mn}} sin(k_m x') sin(k_n y'). \tag{3.6}$$

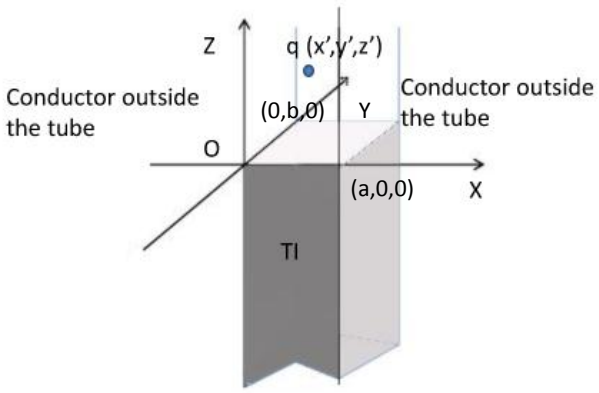

Figure 3.2: An electric charge q being inside the positive half-tube $z > 0$ with dielectric constant ϵ_1 and magnetic permeability μ_1 in the vicinity of a TI with ϵ_2 and μ_2 filling the negative half-tube $z < 0$. The tube has a width a, and length b. We assume that the walls of the tube are formed by a perfect conductor.

Solving boundary condition, we again arrive at:

$$\begin{aligned} D_{mn} &= -\frac{2qO_{mn}e^{-\gamma_{mn}z'}(2\alpha P_3)}{(\epsilon_1+\epsilon_2)(1/\mu_1+1/\mu_2)+(2\alpha P_3)^2} \\ C_{mn} &= -D_{mn} \\ B_{mn} &= \frac{2qO_{mn}e^{-\gamma_{mn}z'}(1/\mu_1+1/\mu_2)}{(\epsilon_1+\epsilon_2)(1/\mu_1+1/\mu_2)+(2\alpha P_3)^2} \\ A_{mn} &= qO_{mn}e^{-\gamma_{mn}z'}(-\frac{1}{\epsilon_1}+\frac{2(1/\mu_1+1/\mu_2)}{(\epsilon_1+\epsilon_2)(1/\mu_1+1/\mu_2)+(2\alpha P_3)^2}) \end{aligned} \tag{3.7}$$

In this case the geometry of the TI isn't really compact. However, due to the Dirichlet boundary conditions on the conducting walls from the 1d point of view all our gauge fields are massive and exponentially decay at large $|z|$. For all practical purposes, the TI is finite in extend in the z-direction.

3.1.3 Distance dependence of statistical angle

Total angular momentum as a global probe of the system

In a normal system without a topological insulator, there would not be any non-zero angular-momentum of the system in the presence of only a static point-like electric charge. The total angular momentum is defined as:

$$L = \frac{1}{4\pi c^2} \int \vec{x} \times (\vec{E} \times \vec{H}) d^3x = \frac{\epsilon}{4\pi} \int \vec{x} \times (\vec{E} \times \vec{B}) d^3x. \tag{3.8}$$

The extra factor of $1/(4\pi)$ compared to [98] is due to the fact that we follow Gaussian units. In the presence of a topological insulator, $\vec{L}$ can be non-zero. In [161] it was already calculated that for an infinite half-plane interface between TI and a trivial insulator, the angular momentum of the system has a non-zero value depending on the fine structure constant α as well as the dielectric constant and magnetic permeability, see eq. 3.1. As emphasized in the introduction, the angular momentum has no dependence on the distance between the surface and point-like electric charge. As pointed out there, this independence could be seen as an artifact of the special case of the planar geometry, where the absence of a second length scale in the problem precludes the appearance of d in the result for the angular momentum.

In both of our other examples, the spherical topological insulator as well as the rectangular tube, there is at least another length scale: the radius a and the side length a and b respectively allowing in principle for a non-trivial dependence of angular momentum on distance.

Let us start with the case of the rectangular tube. Plugging our answers from eq. 3.2, 3.5 and 3.7 into the expression for the angular momentum eq. 3.8, we see that the integral over x and y can easily be done analytically. For example, starting with the x momentum density

$$l_x = y(\partial_x \Phi_E \partial_y \phi_M - \partial_y \Phi_E \partial_x \phi_M) - z(\partial_z \Phi_e \partial_x \phi_M - \partial_x \phi_E \partial_y \phi_M) \tag{3.9}$$

we see that integrating over y first gives an expression proportional to

$$\int_0^b dy\, l_x \sim m_1 \cos(m_1 \pi x/a) \sin(m\pi x/a) + m \cos(m\pi x/a) \sin(m_1 \pi x/a)$$

for integers m, m_1 still to be summed over (as well as n and n_1 appearing in the coefficients). Further integration of this expression over dx than vanishes identically. We have confirmed that L_y and L_z similarly vanish after doing the x and y integrals using Mathematica.

The calculation in the spherical case is a little more cumbersome. Plugging eq. 3.2, 3.3 and 3.4 into eq. 3.8, we can use the recurrence relation of Legendre polynomials After performing the θ integral the double sums occuring in $\vec{E} \times \vec{B}$ collapse into a single one. Performing the integral in spherical coordinates, we once more find that the angular momentum vanishes identically as long as the electric charge is separated even an infinitesimal amount from the surface of the sphere, irrespective of the distance d. If we set the distance d to zero to begin with and then perform the integrals and sums, we get back to the result of 3.1 valid for the infinite half-plane. The fact that for $d = 0$ the sums give back this non-trivial result is a non-trivial check. For $d/a = 0$ one should clearly recover the result of the plane, which can also be thought of as $a \to \infty$. What is surprising is that this limit is not smooth. The angular momentum vanishes for any finite d.

As discussed in the introduction, this result should have been expected based on microscopic considerations. For a real finite system made of electrons and protons total angular momentum has to be quantized. So it can not continuously depend on d/a. For it to vanish at infinity it has to be zero for all d/a. Even for the topological insulator, genuine fractional angular momentum should only exist in infinite system. With the electron charge being on the surface, one can get back to infinite system result.

Finite size loop path in the two particle system

To obtain the statistical angle, the natural thing to do is to look at two particles moving around each other and study phase change of wave function. The action of two point particles at a fixed distance z_0 above a TI/insulator interface located at $z = 0$ contains the standard terms coupling the point particles to the gauge fields:

$$S = e \int A_\mu^{(2)} \frac{dx_{(1)}^\mu}{d\tau} + (1 \leftrightarrow 2) \tag{3.10}$$

where the super/sub-scripts (1) and (2) refer to the two particles, $A_\mu^{(i)}$ being the field sourced by particle i, $x_{(i)}^\mu$ its position. Let us for simplicity look at the case where particle 1 is kept

at the origin in the x-y plane and particle 2 is taken around a non-trivial loop.

- Planar interface: It is easy to work out the effect of this coupling for planar interface in detail. Note that we can write the magnetic field of the mirror monopole of magnetic charge g induced by an electric charge e at $z = -z_0$ and $x = y = 0$ in terms of a vector potential:

$$A_\phi^{(1)} = \frac{g}{4\pi}(1 - \cos\theta)$$

where ϕ and θ are the angles in a spherical coordinate system centered on the location of the mirror monopole at $(0, 0, -z_0)$. That is the 2nd particle at $(x_{(2)}, y_{(2)}, z_0)$ in this coordinate system is located at $\tan\theta_{(2)} = \rho_{(2)}/z_0$ where $\rho^2 = x^2 + y^2$. This is the standard form of the vector potential of a monopole with a Dirac string running along the negative z-axis. This is the appropriate form to use for a mirror charge located below the interface, as this mirror charge is only supposed to be used when calculating fields above the interface (for the magnetic field below the interface one would similarly use the $\vec{A}$ associated to a monopole with a Dirac string running along the positive z-axis for a monopole located at $z = +z_0$. As there is no physical charge located below the interface and so no contribution to (3.10) we will not need $\vec{A}$ in this region).

If we keep one particle fixed at $(x = 0, y = 0, z = z_0)$ and take the other particle take a loop at a fixed z_0 ($\phi_{(2)}$ goes to $\phi_{(2)} + 2\pi$ at fixed $\theta_{(2)}$), e^{iS} picks up a phase:

$$e^{iS} \to e^{iS} e^{e\int d\tau \dot{\phi}_{(2)} A_\phi^{(1)}} = e^{i\frac{e\,g}{2}(1-\cos\theta_2)}$$

We see that due to the $\theta_{(2)}$ dependence already in the case of the planar interface, the resulting statistical angle depends on path. As $\tan\theta_{(2)} = \rho_{(2)}/z_0$, we get different answers depending on the size of the loop. If z_0 is finite and we do a very small loop (that is the charge is a finite distance above the interface) we get $\theta_{(2)} = 0$ and correspondingly do not pick up any phase in the wavefunction. However, with a loop large compared to z_0, $\theta_{(2)} \to \pi/2$. In this $\theta_{(2)} \to \pi/2$ limit, or large loop limit, we get a phase in the action of $e^{ie\,g/2}$ independent of the detailed shape of the path in the x-y

plane [2]. This change in the action corresponds to $e^{2i\theta_S}$ where θ_S is the statistical angle describing the exchange of two particles. Exchanging particle 1 and 2 twice should correspond to a closed loop in configuration space as the one we have been analyzing. So $\theta_S = eg/4$. Plugging in the g obtained for the mirror charge in Ref. [161] (rederived in SI units in the appendix here) we do get back to eq.(3.1).

In conclusion, we find that for a planar interface an large loop gives a statistical angle that is half of that of a dyon made of a real electron/monopole pair in complete agreement with the angular momentum calculation in previous section. For the realistic case of a finite z_0 (so that our effective theory applies), only a large loop (compared to z_0) gives a shape independent answer governed by this statistical angle. The modification for small loops presumably should be understood as a result of short range interactions.

- Spherical TI: For the case of a spherical TI of radius a we can also obtain the vector potential associated with a single point charge at $(0, 0, z_0)$. It again only has a ϕ component with

$$A_\phi = -C_0 a \cos\theta - \sum_l^\infty \frac{C_l}{l} a^{l+1} \sin(\theta) P_l^1(\cos\theta).$$

The C_l are given in eq. (3.4). Most importantly, $C_0 = 0$ (this would be a net magnetic charge, so it has to vanish).

We use this expression for A_ϕ and study the phase change in spherical coordinates when two particles located at the same $r = z_0$ but different θ are exchanged. We take one particle fixed at $(0, 0, z_0)$ while the other one goes from ϕ to $\phi + 2\pi$ at a given θ. The action picks up a phase $2\pi A_\phi$. We plot this value for different z_0 as well as θ in a planar case below.

There are a couple of interesting features about this plot. First, this always vanishes

[2] These answers also obvious when one considers that $\vec{\nabla} \times \vec{A} = \vec{B}$, so the line integral of $\vec{A}$ we are doing is equal to the total magnetic flux through the surface enclosed by the loop. For $\theta_{(2)} = 0$ the loop has vanishing area and no flux. For $\theta_{(2)} = \pi/2$ the loop captures all the flux in the northern hemisphere.

for $\theta \to 0$ and $\theta \to \pi$, as expected after considering planar case.

Second, for intermediate θ between 0 and $\pi/2$, there is a certain non-zero plateau region. For large a, this plateau region repeats the θ behavior of planar case before finite size effect kicks in. For $z_0 \to a$, the plateau value of A_ϕ goes back to planar case result, the universal θ_s. This could also be seen analytically from the large a asymptotic behavior of A_ϕ.

To analyze the large radius limit it is convenient to rewrite the C_l in a way that makes it explicit that A_ϕ can be seen as being sourced by a point mirror charge together with a mirror line charge extending from the mirror point charge to the origin. Explicit formulas for point and line charge appear in the supplemental material of Ref. [161] for $\epsilon = \mu = 1$. We have confirmed with Mathematica that the same decomposition holds for arbitrary ϵ and μ. Taking $z_0 = a + d$ and taking a large at fixed d, one sees that every term in the potential scales as $1/a$ and so the potential seems to vanish in the large a limit. This conclusion is a little too fast as the infinite sum can alter the behavior. At $\theta = 0$ (where $P_l(1) = 1$ for all l) the sum can be performed analytically and we see that the contribution for the point charge sums up to the expected $1/(a - z_0) = -1/d$, that is it remains finite in the large a limit. At $\theta = 0$ the contribution of the line charge can also be summed up. The resulting Hypergeometric function vanishes as $1/a$ in the large a limit. As $P_l < 1$ for $\theta \neq 0$ it is clear that at non-zero θ the line charge contribution has to vanish at least as fast as for $\theta = 0$. So in the $a \to \infty$ limit, the line charge contribution can be neglected compared to the point-like one. This result has also been confirmed numerically in Ref. [161]. This shows that for loops of size $l \ll a$ we recover the planar result. However in the planar case we found that for $l \gg d$ the exchange is governed by the universal θ_S. From this we conclude that, for a compact geometry it is the intermediate size loops with $d \ll l \ll a$ which are governed by the universal topological phase of eq.(3.1).

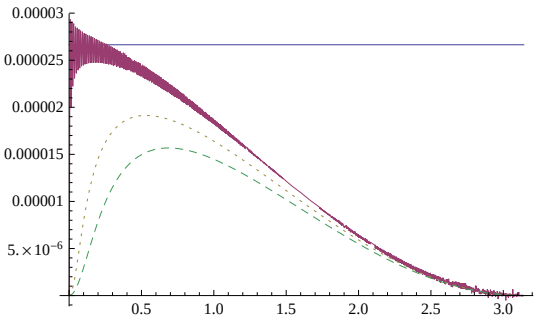

Figure 3.3: A_ϕ versus θ plot with different z_0's. z_0=1.05a for dotted line and z_0=1.1a for dashed line.z_0=1.0005a for solid curved line with straight line stands for universal angle θ_s. The thickness of line represents uncertainty due to large l truncation

3.1.4 Discussion

We find zero angular momentum for a charge outside the TI two examples. While obvious from the microscopic point of view of electrons and protons, the result looks somewhat surprising starting from Maxwell's equations of a topological insulator; in fact we haven not been able to give an analytic proof based on this effective theory that the total angular momentum always vanishes in a finite system even though the microscopic point of view strongly suggest that this is true.

By looking at the two particle system we find that the universal statistic phase governs the behavior of intermediate size loops. In realistic experiments, our results indicate that to observe such an anyon in the topological insulator set-up as suggested in [161], one should use large bulk sample with small superconductor loop close to it, to get non-zero flux. The size of the superconductor loop has to be in the intermediate regime we identified, that is much smaller than the size of the sample but much large than the distance between loop and sample. Our results are consistent with the 2+1 dimensional nature of the anyons, as the universal statistical angle ceases to accurately describe the two particle systems once the particles are removed from the surface of the TI beyond a distance of order the sample size.

3.2 matrix flavor brane and dual Wilson line in field theory

3.2.1 introduction

In string theory a pointlike object (a D0 brane) can be polarized into a membrane with a 2+1 dimensional worldvolume by an external "electric" field coupling to membrane charge. The resulting spherical membrane has zero net membrane charge, but carries the original D0 brane charge as an induced charge density on its worldvolume. This effect is usual referred to as the Myers-effect [142]. From the D0 point of view, the membrane appears as a non-Abelian configuration for the matrices representing the coordinates of the D0 branes. The Myers effect can be straightforwardly generalized to higher dimensional D-brane defects. In particular, a Dp brane, that is a defect with a $p+1$ dimensional worldvolume, can be polarized into a D$(p+2)$ brane by field strength coupling to D$(p+2)$ brane charge. Again, this brane polarization crucially relies on the non-Abelian nature of the underlying D-brane action.

In this work we show that, in the context of holography [83, 137, 180], this same brane polarization can be forced upon a D-brane, in the absence of any fluxes, by turning on certain sources in the boundary field theory. We study N_f Dp-brane probes[3] embedded in an asymptotically anti-de Sitter (AdS) space. Via holography the probe branes in AdS can be mapped to a large N_c conformal field theory coupled to N_f fundamental flavor fields [125, 127].

In general, the fundamental flavor fields can either occupy all the field theory directions or be localized on a lower dimensional defect. For our work however it is crucial that the flavor branes realize a defect field theory. This allows us to separate the defects along the field theory directions. For N_f coincident flavor branes, the field theory has a $U(N_f)$ global symmetry rotating the localized flavors into each other. There are N_f^2 different mass terms one can turn on for the N_f flavors. In the holographic dual a single mass term corresponds to geometric deformations of the flavor brane; more concretely it maps to a "slipping mode"

[3] In the limit of weak string coupling g_s, the D-brane has a negligible tension (the tension grows as $1/g_s$, but Newton's constant goes to zero as g_s^2) and so the probe does not backreact on the background geometry.

that describes how the probe D-brane in the bulk is embedded in the internal space, the S^5 of $\mathrm{AdS}_5 \times S^5$. Separating the defects breaks this global symmetry to a $U(1)^{N_f}$. In the bulk, we now have N_f well separated probe branes. Only the N_f diagonal mass terms can be realized as geometric deformations of these probe branes. They correspond to adding a fermion bilinear to the field theory action made out of fermions localized on a single defect. What we will focus on in this work is adding bilinears made from fermions localized on different defects. By gauge invariance, such non-local bilinears need to be threaded by a Wilson-line, as is well known from studies of the Sakai-Sugimoto model [167]. When these non-local mass terms are turned on, the dual probe brane system is forced into a non-Abelian configuration. A detailed quantitative study of these configurations is difficult due to the poorly understood nature of the non-Abelian action governing coincident D-branes. We are however able to reliably study the asymptotic behavior of the brane embedding. This allows us to uncover a novel UV behavior of the embedding functions due to the non-local nature of the deformation. We also are able to calculate the short-distance behavior of the 2-pt function of the Wilson-line-threaded fermion bilinears. This can be compared with a calculation of the same objects using Maldacena's description of Wilson lines via string worldsheets [138] and perfect agreement is found.

Several examples of non-Abelian D-brane configurations in AdS have previously been documented in the literature. Maybe the most famous application of non-Abelian configurations in the context of holography is the realization of confinement via the Polchinski-Strassler solution [156] - here the background D3 branes themselves puff into 5-branes. The work most closely related to what we attempt to do here is probably the recent paper [131]. The authors presented a D7 brane embedding with induced D5 brane charge which asymptotically (that is close to the AdS boundary) wraps a vanishing 2-cycle. As a consequence the dual field theory contains a defect with the matter content characteristic of a D5 brane probe, not a D7 brane. The puffing into a D7 deep in the interior of AdS corresponds to a novel state in the defect theory described by the D5 brane. While both of these papers, and others similar to them, can be thought of as holographic implementations of the Myers effect, they always allowed a description in terms of a higher dimensional probe brane with flux. Instead of describing a non-Abelian configuration of Dp-branes, the systems have an

alternative description in terms of D$(p+2)$ branes with a Dp-brane charge inducing flux. This higher-dimensional action was effectively Abelian. Even though in principle coincident probe branes are described by a non-commutative action the configurations studied did not require any genuinely non-commuting matrices when viewed from the higher dimensional perspective. As far as we can tell, the configurations we study in this paper require a genuine non-Abelian D-brane configuration in AdS. The non-Abelian nature is mandatory given the couplings we turn on in the boundary field theory. Holographic probe branes with non-Abelian gauge field configurations have been studied before e.g. in [10, 59, 143], but we believe our system is the cleanest example of a probe brane with genuinely non-Abelian scalars and hence a non-geometric embedding.

We will analyze two quite distinct setups which realize this general idea. In the first part of the paper we study a supersymmetric defect field theory with D5 brane probes with 4 "ND" directions in a D3 brane background. The defect field theory dual to this setup describes 2+1 dimensional hypermultiplets coupled to 3+1 dimensional $\mathcal{N}=4$ super Yang-Mills theory. We establish the duality between the non-local deformations of the field theory and the non-Abelian D-brane configurations. We also analyze the short-distance behavior of correlation functions in this theory and compare to a classic Wilson line calculation.

In the second part of the paper we want to analyze how the non-Abelian nature of the brane embeddings is enhanced when we turn on additional background fluxes as are present in the original Myers effect. For this purpose we analyze D5 probe branes with 6 "ND" directions. In this case the defect localized matter is purely fermionic: 2 Dirac fermions localized on 1+1 dimensional defects in the 3+1 $\mathcal{N}=4$theory. Turning on an explicit 9-form field strength in the bulk helps to polarize the D5 probe into a D7 probe brane, just as in the original Myers setup. The background flux allows us to get non-trivial commutators form the Wess-Zumino (WZ) term in the action already at cubic order in the fields, whereas commutators only entered at quartic order in the supersymmetric setup. To this order only the Abelian terms contribute to the Dirac-Born-Infeld (DBI) part of the action. We once more can reliably analyze the UV asymptotic behavior of the solution using a small field expansion of the action. The separation of the defects allows to lift some of the instabilities present in the non-supersymmetric 6 ND system above the Breitenlohner-

Freedman bound. For this stabilization to work with a small brane separation we require the 9-form flux to be significantly different from zero. Correspondingly, we need to construct the probe brane embeddings in a gravitational background where the full backreaction of the 9-form flux has been taken into account. Fortunately, such a gravitational background has been constructed recently [24, 140]. This background is dual 4D super Yang-Mills (SYM) theory with a spatially varying theta angle. In this setup we can study the non-local mass term reliably in the limit of small brane separation. While this is sufficient to stabilize the off-diagonal slipping modes, the diagonal slipping modes won't get stabilized by our construction; more ingredients are needed for a fully stabilized solution, e.g. we could turn on internal fluxes [33, 143]. Also, while the inclusion of the flux allows us to analyze stabilization of the off-diagonal modes in the UV reliably, we still need to resort to a non-linear action in the bulk in order to find a complete brane embedding. In order to numerically find a full solution for the brane embedding in this case, we make the ad-hoc assumption that commutators coming from the DBI part of the action are negligible and only the commutators from the WZ term coupling to the external flux are kept.

The paper is organized as follows: in the next section we introduce our main example: the supersymmetric D3/D5 system together with its non-Abelian deformation. In section III we calculate the 2-pt function in this system and compare to a classic Wilson line computation. In section IV we study non-supersymmetric branes in the background of polarizing fluxes. We conclude in section V.

3.2.2 Non-Abelian supersymmetric D3/D5 system without flux

Let us first review the Abelian solution for N_f D5-branes intersecting N_c D3-branes in $2+1$ dimensions as first introduced in [54,127]. The directions occupied by D3 and D5 brane are displayed in the following table.

	0	1	2	3	4	5	6	7	8	9
$D3$	×	×	×	×						
$D5$	×	×	×		×	×	×			

(3.11)

The gravity description will be studied in the probe limit, with $N_f \ll N_c$. Then for large N_c and $g_s N_c$, we can treat D5-brane as probes in the asymptotically AdS_5 geometry produced by large number of D3-branes

Let us consider the AdS/CFT dual of our D3-D5 brane system with a single D5 brane probe to warm up. The background geometry is the asymptotically flat, zero temperature D3-brane solution:

$$ds^2 = f^{-\frac{1}{2}}(-dt^2 + d\vec{x}^2) + f^{\frac{1}{2}}(dr^2 + r^2 d\Omega_5^2) \tag{3.12}$$

We can rewrite Ω_5 above as :

$$dr^2 + r^2 d\Omega_5^2 = d^2\rho + \rho^2 d\Omega_2^2 + dx_7^2 + d^2 x_8 + d^2 x_9 \tag{3.13}$$

with

$$f = \frac{R^4}{(\rho^2 + x_7^2 + x_8^2 + x_9^2)^2} = \frac{R^4}{r^4}. \tag{3.14}$$

In what follows we will usually work in units where $R = 1$. The D5 probe brane spans x_0, x_1 and wraps the S^3 above and lives on a curve $x_9(\rho)$. For the simplest solution we set $x_7 = x_8 = x_3 = 0$. The pull-back metric on the D5 brane worldvolume is:

$$\begin{aligned} ds_6^2 &= \frac{(-dt^2 + dx_1^2 + dx_2^2)}{f^{1/2}} \\ &+ f^{\frac{1}{2}}\left[(1 + x_9'^2)d\rho^2 + \rho^2 d\Omega_2^2\right] \end{aligned} \tag{3.15}$$

Without worldvolume gauge field, the action describing the embedding of the branes, the Dirac-Born-Infeld (DBI) action, is given by:

$$\begin{aligned} S_{D5} &= -N_f T_5 \int d^6\xi \sqrt{-g_6} \\ &= -N_f T_5 Vol(S^2) \int d^2x d\rho \rho^2 \sqrt{1 + x_9'^2} \end{aligned} \tag{3.16}$$

From the linearized equations of motion for x_9

$$2\rho x_9'(\rho) + \rho^2 x_9''(\rho) = 0 \tag{3.17}$$

one can read off its asymptotic behavior:

$$x_9(\rho) = C_1 + C_2 \rho^{-1}. \tag{3.18}$$

This is the right fall-off to correspond to conformal dimension $\Delta = 1$ or $\Delta = 2$, depending on the quantization scheme. For the supersymmetric D5 brane system one can see [54] that supersymmetry requires the correct dimension to be $\Delta = 2$. Another way to arrive at this result is to study the angular description of this slipping mode in terms of θ in $x_9 = r\, sin\theta$, which obeys the equations of motion of a scalar with $m^2 = -2$ in AdS_4. This fluctuation is dual to the fermion mass term on the defect.

Multi-brane solution

For N_f coincident D-branes the action (3.17) has to be generalized to the non-Abelian DBI action. In this section we'll closely follow the discussion in reference [142]. In terms of N_f by N_f matrix valued coordinates and gauge fields one has:

$$\begin{aligned} S_{D5} &= -T_5 \int d^6x \\ & \quad Tr\left(\sqrt{-det(P[G_{ab}])det(Q^i_j)}\right) \end{aligned} \tag{3.19}$$

where

$$Q^i_j \equiv \delta^i_j + \tfrac{i}{\lambda}[x^i, x^k]G_{kj}. \tag{3.20}$$

$$\lambda = 2\pi\ell_s^2 \tag{3.21}$$

In principle we have to commit to a procedure of how to deal with the ordering ambiguities of the non-Abelian action. As long as the fields remain small, we can expand the action in a power series in the fields. The first time a commutator arises from the DBI action is at quartic order in the fluctuating fields. Up to this order the action is free of ordering ambiguities. So as long as our fields are small, we have full control over the non-Abelian action. This will be sufficient for us to analyze the UV behavior of the brane fluctuations as well as for the computation of the short distance behavior of the two-point function. Expanding the non-Abelian structure to the next leading order in the embedding scalars one has for diagonal G_{ab}:

$$\sqrt{detQ^i_j} = 1 - \frac{1}{4\lambda^2}[x^i, x^j][x^i, x^j]G_{ii}G_{jj} + ... \tag{3.22}$$

To see the non-Abelian effect, we write down non-Abelian action for D5 brane as:

$$\begin{aligned} S_{D5} &= -N_f T_5 \int d^6\xi \sqrt{-g_6} \qquad (3.23) \\ &= -N_f T_5 4\pi \int d^2x d\rho \rho^2 \sqrt{1 + x_9'^2 + x_8'^2 + f^{-1} x_3'^2} \\ &\quad (1 - \frac{1}{4\lambda^2}[x^i, x^j][x^i, x^j] G_{ii} G_{jj}) \\ &\quad i, j = 3, 8, 9 \qquad (3.24) \end{aligned}$$

From now on we specialize to the case of $N_f = 2$. We wish to describe a configuration in which the two defects are separated in the field theory directions. The field theory coordinate of the two branes is given by the constant asymptotic value of the fluctuating field x_3 in the bulk. In order to have a geometric interpretation of the defect positions it is convenient to use an $SU(2)$ flavor rotation diagonalizing x_3. We can chose the origin in the x_3 direction to be in the middle between the two defects, which we take to be separated by a distance $2d$. With this we asymptotically have

$$x_3 \sim d\sigma_3. \qquad (3.25)$$

x_7, x_8 and x_9 encode the triplet of mass terms one can add for a hypermultiplet. For simplicity, we only consider the case $x_7 = 0$. The asymptotic behavior of x_8 and x_9 now encode real and imaginary part of the standard complex mass terms we add for the flavors on the defects. If the leading behavior for x_8 and x_9 is diagonal, we added only local mass terms on the two defects. However, if we chose to add non-local Wilson-line threaded mass terms, they are off-diagonal. They can not be diagonalized without ruining the geometric interpretation of x_3. The addition of these mass terms forces us to find a genuinely non-Abelian solution.

For concreteness, let us consider the following $SU(2)$ ansatz for a non-commuting solution, separating the radial parts and matrix structure as $x_3 = X_1(\rho)\sigma_3$, $x_8 = X_2(\rho)\sigma_1$, $x_9 = X_3(\rho)\sigma_2$, with $[\sigma_i, \sigma_j] = 2i\epsilon_{ijk}\sigma_k$ and $\sigma_i^2 = 1$. We insist that $X_2 = X_3$, that is we chose our off-diagonal mass to be proportional to $\sigma_1 + \sigma_2$ and assume that any condensate that forms is of the same form. Note that with this choice the radial functions are symmetric

under $x_8 \leftrightarrow x_9$. With this ansatz we can evaluate the commutators as

$$[x_i, x_j] = 2i\epsilon_{ijk}\sigma_k X_i X_j. \tag{3.26}$$

Substituting this ansatz into equation of motion, one arrives at:

$$S_{D5} = -N_f T_5 4\pi \int d^2x d\rho \rho^2 \sqrt{1 + X_2'^2 + X_3'^2 + f^{-1}X_1^2}$$
$$\left[1 + \tfrac{2}{\lambda^2}(X_1^2X_2^2 + X_1^2X_3^2 + X_2^2X_3^2 f)\right]$$

For the radial functions we now take an ansatz

$$X_1(\rho) \to d + \epsilon g(\rho)$$
$$X_{2,3}(\rho) \to \epsilon k(\rho) \tag{3.27}$$

so that g vanishes near the boundary. To determine the near boundary UV behavior of the solution we can linearize the equations of motion in ϵ:

$$-4\tfrac{d^2}{\lambda^2}\rho^2 k(\rho) + 2\rho k'(\rho) + \rho^2 k''(\rho) = 0$$
$$6g'(\rho) + \rho g''(\rho) = 0 \tag{3.28}$$

which yields solutions:

$$g(\rho) = \tfrac{C_1}{5\rho^5} + C_2$$
$$k(\rho) = C_1' e^{-m\rho}/\rho + C_2' e^{m\rho}/\rho$$
$$\text{with} \quad m = (2d)/\lambda \tag{3.29}$$

where m has dimension of energy. Since λ^{-1} is the tension of a fundamental string, m is exactly the mass of a piece of string stretched between the two defects. This behavior of x_8 and x_9 in the UV may look strange at first sight, but we will give a possible interpretation of the exponential factors in the next section. As a consistency check one should note that if one takes the limit where $m \to 0$, which corresponds to an Abelian solution with two branes on top of each other, one recovers the result from the last section.

Field theory description

The field theory dual to this probe brane setup is now easy to describe. The D3 branes themselves give the usual glue theory: $\mathcal{N} = 4$ SYM in the limit of a large number of colors N_c and large 't Hooft coupling. Each flavor brane gives rise to a single 2+1 dimensional Dirac fermion in the fundamental representation of $SU(N_c)$ and their superpartners localized along a sheet-defect inside the 3+1 dimensional SYM.

The N_f fermions do not all have to be localized on the same defect. In our construction, we separated the defects along the x_3 direction. From the holographic bulk point of view x_3 is a fluctuating scalar degree of freedom living on the worldvolume of the probe and the asymptotic value x_3 takes for the i-th brane maps to the position of the i-th defect in the field theory.

In the non-Abelian setting of $N_f = 2$ flavor branes, in the bulk all coordinates are 2 by 2 matrix. But we can always chose a gauge in the bulk in which one of them is diagonal. As x_3 has a geometric interpretation in the field theory, we chose x_3 to be diagonal; the two entries then correspond to the field theory position of the two defects. x_8 and x_9 also correspond to fluctuating degrees of freedom of the bulk probe. The operators dual to these fluctuations are the real and imaginary part of the fermion bilinear operator (that is $\bar{\psi}^i\psi_j$ and $\bar{\psi}^i\gamma_5\psi_j$). Due to the non-Abelian structure, we can not rotate away the imaginary part anymore. Real and imaginary parts will be genuinely non-commuting. Note that once we fixed x_3 to be diagonal as a 2 by 2 matrix, we no longer have the freedom to diagonalize these 2 operators. We can tag fermion 1 and fermion 2 to be the matter content localized on the two spatially separated defects respectively. Diagonal mass terms give a mass to the fermion on one or the other defect. Off-diagonal mass terms however are non-local - they mix a fermion on defect 1 with a fermion on defect 2. To be gauge invariant under $SU(N_c)$ gauge transformations, such a bi-local operator needs to include a Wilson line connecting the two defects just like the chiral condensate operator in the Sakai-Sugimoto model [167].

This origin of the non-Abelian nature of our configuration is the main contrast to the standard Myers effect. We are polarizing the brane by turning on a source for the boundary Wilson-line-threaded fermion bilinear on the field theory side rather than by a flux.

To arrive at a dictionary below for x_8 and x_9, we observe that the the UV behavior changes when going from the Abelian to the non-Abelian configuration:

$$\begin{cases} 1/\rho \\ 1 \end{cases} \rightarrow \begin{cases} e^{-m\rho}/\rho & \text{normalizable} \\ e^{m\rho}/\rho & \text{non-normalizable} \end{cases} \tag{3.30}$$

The non-normalizable mode on the field theory side will dual to a source for Wilson line operator. In the bulk the off-diagonal modes of multi-brane configuration, would normally be interpreted as open string stretched between two defects. As we will see more concretely below, the exponential factor accompanying the standard power can be seen as an avatar of the string worldsheet.

3.2.3 Wilson line two point function from two sides of Duality

Given our matrix valued brane configuration in the bulk, we can turn on a source for the Wilson-line-threaded fermion bilinear on the field theory side and can calculate the corresponding two point function. For simplicity we will refer to this Wilson-line-threaded fermion bilinear operator from now on as a short Wilson line. The first step is to find the propagator, which is described by a differential equation in the 3 field theory direction $\overrightarrow{x}$ and the AdS radial direction ρ:

$$\begin{aligned} &(\Box_G + 2 - G_{33}m^2) \qquad G(\rho', \overrightarrow{x}', \rho, \overrightarrow{x}) \\ &= \delta(\rho', \overrightarrow{x}', \rho, \overrightarrow{x}) \end{aligned} \tag{3.31}$$

For generic source this is referred to as the bulk-to-bulk propagator. In the limit that the source is taken to the boundary, it is referred to the bulk-to-boundary propagator. In the latter case, the δ-function source can be replaced by a boundary condition on G. $\Box_G$ is the scalar Laplacian for theory on the probe brane

$$\begin{aligned} \Box_G &= \frac{1}{\sqrt{g}}\partial_\mu \sqrt{g} g^{\mu\nu} \partial_\nu \\ &= \rho^2 \partial_\rho^2 + 4\rho\partial_\rho + \rho^{-2}\partial_{\overrightarrow{x}}^2 \end{aligned} \tag{3.32}$$

$G_{33}m^2 = \rho^2 m^2$ is and effective position dependent mass term due to the higher order commutators in non-Abelian DBI, which would induce non-conformal deformation to the

usual conformal defect. This is the equation for the slipping mode θ, rather than $x_9 = \rho\theta$ from the previous section. It is θ, not x_9, whose fluctuations obey a standard scalar wave equations and so its use will simplify the discussion in the section. The mass squared of -2 for this slipping mode comes from the fact that the volume of the S^2 wrapped by the D5 brane shrinks as it slips off the equator.

We were unable to find an analytical solution to this differential equation. However, we can discuss the behavior of the solution in different limits. There are two different regimes where the bulk-to-bulk correlation function behaves qualitatively different, $m\rho \gg 1$ and $m\rho \ll 1$, corresponding to whether the non-local and hence non-conformal deformation can be ignored in the equation of motion or not.

To see this in more detail, one can look at the standard solution for the bulk-to-boundary propagator without non-Abelian deformation:

$$(\Box_G + 2)G(\rho, \overrightarrow{x}) = 0 \tag{3.33}$$

$$G(\rho, \overrightarrow{x}) = \frac{1}{\rho^2} \frac{1}{(\overrightarrow{x}^2 + 1/\rho^2)^2} \tag{3.34}$$

In the second regime, $m\rho \gg 1$, one can ignore the non-Abelian deformation and so (3.34) is the correct bulk-to-boundary correlator. The equation of motion is just that for the standard slipping mode, dual to fermion bilinear in field theory side. In the field theory, its two point correlation function goes as $1/x_d^4$ with x_d being the separation between the two short Wilson lines along the defect. This corresponds to conformal dimension $\Delta = 2$ as seen above. So this $m\rho \ll 1$ regime is the Abelian regime.

The condition on the first regime, $m\rho \gg 1$, can be equivalently written as $d\rho \gg l_s^2$, using our result for m in terms of l_s, (3.29). Note that this is exactly the regime in which the standard description of the Wilson line in terms of a classical string world sheet calculation following [138] is valid. Including the warp factor, ρd is the effective width of world sheet and the condition that $d\rho \gg l_s^2$ hence guarantees that the string worldsheet is classical.

In this regime, the two point function of two spatially separated short Wilson lines can hence be captured by the area of a string world sheet connecting those two Wilson line. The world sheet, displayed in figure 3.4, ends on the two parallel branes in the bulk and connects

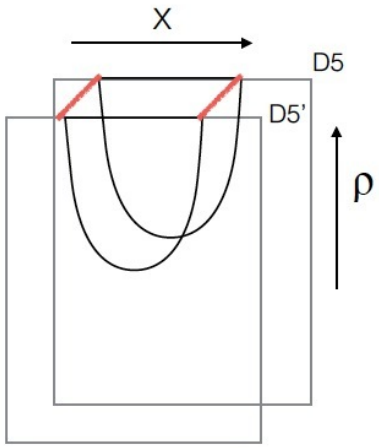

Figure 3.4: Two thick lines are the short Wilson line, with a string world sheet hanging down and stretching between them. The world sheet ends on D-branes in the bulk

the two Wilson lines on the boundary. From Maldacena's calculation [138] of the potential of two quarks, the area of this string world sheet is proportional to $1/x_d$. It follows that for the configuration of two such Wilson lines as displayed in figure 3.4 the correlation is:

$$\begin{aligned} \langle WW \rangle &\sim e^{-S} \sim e^{\frac{C}{x_d}} \\ C &= \frac{4\pi^2 (2\lambda)^{\frac{1}{2}}}{\Gamma(1/4)^4}. \end{aligned} \tag{3.35}$$

In order to confirm that our description of the system in terms of a non-Abelian brane configuration describes this physics correctly, we would like to reproduce eq. (3.35) from the non-Abelian DBI. Note that the effective mass appearing in our scalar wave equation, $M = \sqrt{m^2\rho^2 - 2} \sim m\rho$, is large in this regime and so we are asked to calculate the propagator for a very massive point particle. Furthermore, as indicated, the position independent contribution of the mass can be neglected in this regime. In the large mass limit solutions to the scalar wave equations can be reduced to the problem of finding geodesics using the WKB approximation. For a recent detailed discussion of this relation see [60]. This standard derivation also makes it clear that in the case of interest here, a scalar with a position dependent mass $M = m\rho$, we simply have to find the appropriate generalized

geodesic following from an action

$$S_{\text{particle}} = \int M(\rho) ds = m \int \rho ds. \tag{3.36}$$

with

$$ds^2 = \rho^2 (dt^2 + d\vec{x}^2) + \frac{d\rho^2}{\rho^2}. \tag{3.37}$$

In terms of the geodesic action, the 2-pt function of the Wilson lines is given by

$$\langle WW \rangle \sim e^{-S_{\text{particle}}}$$

We can take the direction of separation along the field theory directions as x, as shown in figure 3.4. With this the generalized point particle action becomes:

$$S_{\text{particle}} = \frac{2d}{\lambda} \int_{\rho_1}^{\rho_2} \sqrt{(\partial_x \rho)^2 + \rho^4}\, dx \tag{3.38}$$

$2d$ being the length of the short Wilson line or, equivalently, the width of the world sheet. But this is exactly the action for the string world sheet sourced by two parallel moving quarks as in [138]! For the string worldsheet, the determinant of the induced metric had an extra power of ρ compared to the standard geodesic simply because the worldsheet is 2-dimensional and so picked up an extra warpfactor. In the geodesic action the same factor of ρ appears due to the position dependent mass that we inherited from the leading commutator term in the non-Abelian DBI.

In the bulk we saw that the two regimes, Abelian versus WKB, are separated by

$$m\rho \sim 1. \tag{3.39}$$

The correlation function of the short Wilson loop goes as x_d^{-4} and with the exponential of eq. (3.35) respectively in those two regimes, and presumably smoothly interpolates between these two behaviors in between. We would like to know for what separation x_d these two calculations are valid. Looking at the solution for the worldsheet, one can see that the turn around point, ρ_*, and the field theory separation satisfy the relation $x_d \rho_* \sim 1$. This implies $m\rho_* \sim \frac{d}{x l_s^2}$. The two behaviors should cross over into each other when $m\rho_* \sim 1$. This implies that on the field theory side, the two behaviors are separated by $x_* \sim d\sqrt{\lambda_t}$. Here

we used that in our $R = 1$ units we have $l_s^{-2} = \sqrt{\lambda_t}$, the 't Hooft coupling, according to the standard AdS/CFT dictionary. For $x_d \gg x_*$ we see that standard x_d^{-4} fall-off of the two-point function, for $x_d \ll x_*$ the exponential behavior of eq. (3.35).

3.2.4 Non-supersymmetric D3/D5 with axion flux

We can also consider a slightly different set-up, where the non-Abelian features implied by the non-local mass terms we introduced above are enhanced by coupling to a 9-form flux via the Chern-Simon term. This time, take the N_f D5-branes to intersect the N_c D3-branes in $1+1$ dimensions. In addition, a spatially varying axion field is turned on corresponding to a constant 1-form field-strength. The dual 9-form flux can be thought of as being sourced by smeared D7 branes behind the horizon [24]. This set-up is summarized in the following table:

	0	1	2	3	4	5	6	7	8	9
$D3$	×	×	×	×						
$D5$	×	×			×	×	×	×		
$F9$	×	×	×		×	×	×	×	×	×

(3.40)

The gravity description will be once more be studied in the probe limit, with $N_f \ll N_c$.

The interpretation of the flux is best understood when writing the flux as a 1-form flux, that is a constant gradient of the string theory axion. In the solution of [24] the axion is linear in x_3 and independent of all other coordinates. This constant 1-form flux is dual to a position dependent theta angle in the field theory, where theta grows linearly with x_3. We take all our defects to live at the same x_3, so they all feel the same theta angle. The non-trivial gradient in theta still has some non-trivial effect on the defects. To impose the non-Abelian structure we separate our defects along the x_2 direction and once more turn on non-Abelian masses.

Single brane solution in pure AdS

Let us first consider the AdS/CFT dual of our second D3-D5 brane system with a single D5 brane probe and ignore 9-flux for now. In this case, the background geometry is still the

asymptotically flat, zero temperature D3-brane solution (3.12). This time we rewrite Ω_5 as:

$$dr^2 + r^2 d\Omega_5^2 = d^2\rho + \rho^2 d\Omega_3^2 + d^2x_8 + d^2x_9 \tag{3.41}$$

with

$$f = \frac{R^4}{(\rho^2 + x_8^2 + x_9^2)^2} = \frac{R^4}{r^4}. \tag{3.42}$$

In what follows we will again work in units where $R = 1$. The D5 probe brane spans x_0, x_1 and wraps the S^3 above and lives on a curve $x_9(\rho)$. For the simplest solution we set $x_5 = x_3 = 0$. The pull-back metric on the D5 brane worldvolume is:

$$ds_6^2 = \frac{(-dt^2 + dx_1^2)}{f^{1/2}} + f^{\frac{1}{2}} \left[(1 + x_9'^2)d\rho^2 + \rho^2 d\Omega_3^2\right] \tag{3.43}$$

Without worldvolume gauge field, Born-Infeld action is:

$$\begin{aligned} S_{D5} &= -N_f T_5 \int d^6\xi \sqrt{-g_6} \\ &= -N_f T_5 Vol(S^3) \int d^2x d\rho f^{\frac{1}{2}} \rho^3 \sqrt{1 + x_9'^2} \end{aligned} \tag{3.44}$$

$x_9 = 0$ is the ground state solution describing a D5 brane probe on $AdS_3 \times S^3$. From the linearized equations of motion for x_9 one can read off its asymptotic behavior:

$$x_9(\rho) = C_1 \rho^{\sqrt{2}i} + C_2 \rho^{-\sqrt{2}i}. \tag{3.45}$$

As in the supersymmetric brane configuration, this fluctuation is dual to the fermion mass term on the defect. The fact that the exponents are imaginary tells us that while this operator has dimension 1 in the free field theory, at strong coupling it has naively an imaginary dimension in contradiction with unitarity. Such an asymptotic behavior is due to the fact that the slipping mode with a mass squared of -3 in AdS unit is below the AdS_3 BF bound of -1 and so really signals an instability of the system, not a loss of unitarity. The analysis of our $AdS_3 \times S^3$ brane is very similar to the quantum hall plateau transition studied in [53]. There also the system is unstable in pure AdS. In [53] the asymptotic behavior was tamed by replacing AdS with the full D3 brane metric, that is the function f above was replaced with $f = 1 + \frac{R^4}{(\rho^2 + x_9^2 + x_5^2)^2}$. To truly stabilize the system it was later realized that internal fluxes can be turned on [33, 143]. This should also be possible here.

Interpolating Solution between AdS5 and D3-D7 Scaling Solution in Type-IIB supergravity

In this section we would like to review some of the crucial aspects of the type IIB supergravity solution with the fully backreacted 9-form flux following mostly the original presentation in [24]. The whole solution is driven by a constant axion gradient

$$F_1 = d\chi = \beta dx_3 \tag{3.46}$$

together with the standard D3-brane flux already present in $\mathrm{AdS}_5 \times S^5$. In the field theory this extra 1-form flux describes a constant gradient of the theta angle, $\theta = \beta c_3$. As the theta angle is dimensionless, β carries the dimension of energy - it sets a scale in the problem. To construct the full solution one parametrizes the (Einstein frame) metric as:

$$\begin{aligned} ds_{10}^2 &= f^{\frac{1}{2}} e^{2b(r)-2c(r)-\frac{\phi_0}{2}}(-dt^2 + d\vec{x}^2) + \\ &\quad f^{\frac{3}{2}} e^{2b(r)-6c(r)-\frac{3\phi_0}{2}} dx_3^2 + \\ &\quad e^{-\frac{\phi_0}{2}} f^{\frac{1}{2}}(d^2\rho + \rho^2 d\Omega_3^2 + d^2x_5 + d^2x_9) \end{aligned} \tag{3.47}$$

with f and r still given by eq. (3.42). The dilaton is parametrized by

$$\phi(r) = 4c(r) + 4\log r + \phi_0. \tag{3.48}$$

For

$$b(r) = \log r, \quad c(r) = -\log r, \quad \phi_0 = 0 \tag{3.49}$$

this becomes the standard $\mathrm{AdS}_5 \times S^5$ metric of eq. (3.12). At was shown in [24] a full solution to Einstein's equations with the constant axion gradient interpolates between this $\mathrm{AdS}_5 \times S^5$ solution in the UV (at large ρ) to an IR "scaling solution" in which $b \sim 7(\log r)/\sqrt{33}$ and $c \sim (\log r)/\sqrt{33}$. That is the solution describes a flow from $\mathcal{N} = 4$ SYM in the UV, which means energies much larger than β, to a scale invariant, gapless theory in the IR with an anisotropic scaling exponent (x_3 scales differently from t, x_1 and x_2). The full interpolating flow for $b(r)$ and $c(r)$ can easily be generated numerically, as described in detail in [24]. We reproduced this numerical solution and used it as a background to embed our probe branes in.

Non-Abelian double brane solution

Having reviewed all the ingredients that go into the construction, we can now present our solution for the non-Abelian embedding for multiple D5 branes. To describe multiple coincident D5-branes we once more need the non-Abelian generalization of the Born-Infeld action (3.19). The DBI part of the action is still given by

$$\begin{aligned} S_{D5} &= -T_5 \int d^6x \\ &\quad Tr\left(e^{\phi(x_i)/2}\sqrt{-det(P[G_{ab}])det(Q^i_j)}\right) \end{aligned} \tag{3.50}$$

with Q^i_j still being given by (3.22). We this time included the coupling to the dilaton, which is no longer constant in the geometry of (3.47). The standard $e^{-\phi}$ prefactor from the string brane DBI becomes $e^{\phi/2}$ in the Einstein frame. Also note that the dilaton factor now has x_i dependence from the back-reaction of the flux.

Taking x_3, x_8, and x_9 as function of ρ, the induced metric on the D5-brane is:

$$\begin{aligned} ds_6^2 &= f^{\frac{1}{2}}e^{2b(r)-2c(r)-\frac{\phi_0}{2}}(-dt^2+d^2x_1) \\ &\quad +f^{\frac{1}{2}}e^{-\frac{\phi_0}{2}}(1+x_5'^2+x_9'^2+e^{2b(r)-2c(r)}x_2'^2)d^2\rho \\ &\quad +f^{\frac{1}{2}}\rho^2 d\Omega_3^2 \end{aligned} \tag{3.51}$$

and the Abelian part of the action (3.50) yields:

$$\begin{aligned} S_{D5} &= -T_5\int d\Omega_3 d^2x d\rho e^{\frac{\phi(r)}{2}} Tr\sqrt{-g_6} \\ &= -T_5\int d\Omega_3 d^2x d\rho\, \rho^3 f^{3/2}e^{2b}r^2 \\ &\quad Tr\sqrt{1+x_5'^2+x_9'^2+e^{2b(r)-2c(r)}x_2'^2}. \end{aligned} \tag{3.52}$$

The polarization of the probe brane is aided by the background RR field. The RR field couples directly to the N_f D-branes via a Chern-Simons term.

$$S_{CS} = \frac{e^{2\phi}}{2\pi\alpha'}\frac{i}{3}\mu_5\int dt Tr(x^i x^j x^k)F^{(9)}_{tijk\mu_1\ldots\mu_5} \tag{3.53}$$

Here, and in what follows, i, j, and k will run over indices 2, 5, and 9, whereas $\mu_1,\ldots\mu_5$ run over the 5 worldvolume directions. The indices of the 9-form field strength $F^{(9)}$ in

the linear axion solution run over $x_0 \sim x_9$ without the x_3 direction. This flux promotes a polarization of the D5 brane coordinates x_2, x_5, and x_9 into matrix valued coordinates. As we mentioned before, commutator terms from the DBI action only arise at quartic order in the fields. The net-effect of the 9-form flux is to introduce the non-commutativity already at cubic order in the action. In the limit of small fields, this makes the non-commutativity more pronounced.

With $F^{(9)}_{tijk\mu_1\ldots\mu_9}$ coming from the constant 1-form from the last section it is, in components proportional to the spacetime metric $g^{33}\sqrt{-g} = \rho^3 f^{3/2} e^{2b(r)}$:

$$F^{(9)}_{tijk\mu_1\ldots\mu_5} = \beta\rho^3 f^{3/2} e^{2b(r)} \epsilon_{ijk}\epsilon_{\mu_1\ldots\mu_5} \tag{3.54}$$

As for the supersymmetric defect, we can only reliably study the non-Abelian action by keeping the first few terms of a power series expansion in small fields. As we reviewed for the supersymmetric defect, the DBI part of the action has the first commutators showing up at quartic order in the fields. The background flux introduces a cubic commutator term in the CS terms. So expanding the action to cubic order in the fields will allow us to confine the non-commutative nature of the solution to the CS term and use the Abelian action (3.52) for the DBI part. The only non-trivial commutator in the equations of motion following from the cubic action comes from the contribution of the CS term:

$$\ldots + ie^{2\phi(r)}\rho^3\beta f^{3/2} e^{2b(r)} \epsilon_{ijk}[x_j, x_k] = 0 \tag{3.55}$$

where the $\ldots$ stand for the terms from the DBI part of the action.

Let us consider the same $SU(2)$ ansatz for the non-commuting solution we used before: $x_2 = X_1(\rho)\sigma_3$, $x_8 = X_2(\rho)\sigma_1$, $x_9 = X_3(\rho)\sigma_2$, with $X_2 = X_3$. The background spacetime is asymptotic AdS in the UV, so we can use the metric eq. (3.12) for the asymptotic analysis and work with constant dilaton. We again take an ansatz $X_1(\rho) \to d + \epsilon g(\rho), X_{2,3}(\rho) \to \epsilon k(\rho)$, so that the two defects are sitting at $x_2 = \pm d$ respectively. For this solution to be captured by a small field expansion, we need to work with sufficiently small d. Expanding to first order in ϵ, one arrives at two equations:

$$\begin{aligned} -d\beta p k(\rho) + K[2pk(\rho) + p^2(k'(\rho) + \rho k''(\rho))] = 0 \\ 5g'(\rho) + \rho g''(\rho) = 0 \end{aligned} \tag{3.56}$$

which yield solutions:

$$g(\rho) = \frac{C_1}{4\rho^4} \tag{3.57}$$

$$k(\rho) = C_1'\rho^{\sqrt{-2+\frac{d}{K}\beta}} + C_2'\rho^{-\sqrt{-2+\frac{d}{K}\beta}} \tag{3.58}$$

The behavior of g is as in the Abelian case.

With

$$-2 + \frac{d}{K}\beta = -2 + \frac{m}{3}\beta > 0 \tag{3.59}$$

the equations have stable solutions. Here

$$m = \frac{2d}{2\pi\alpha'} \tag{3.60}$$

is again the mass associated with a string stretched across the distance $2d$ setting the separation of the two defects. Interestingly, the separation allows us to stabilize the slipping mode for small brane separation as long as the flux is large. Of course, for sufficiently large brane separation the slipping mode will always be stabilized by d^2 terms arising from the quartic commutator squared terms in the DBI action. But this would be outside the regime where we understand the DBI.

To find solutions that smoothly cap off in the infrared we need to consider an action where higher powers of the derivatives are non-negligible and we need to go beyond the rigorously understood aspects of the DBI. An ad-hoc ansatz we will employ for the action is to keep the full non-linear structure under the square root

$$\mathcal{L}_{DBI} = -\mathcal{F}\sqrt{(1 + x_5'^2 + x_9'^2 + e^{2b(r)-2c(r)}x_2'^2)} \tag{3.61}$$

but to neglect all commutator terms. This prescription seems to essentially agree with the adapted symmetrized trace prescription that was used in [59] to find p-wave superconductors using non-Abelian gauge fields on probe branes. Note that, in either case, with all $\sigma_i^2 = 1$, the matrix structure match between DBI and WZ term and can be scaled out from the equations of motion. We seek a solution that smoothly truncates at a finite value of the radial coordinate (a gapped or "Minkowski" embedding). Even with the ad-hoc action, finding the full brane embedding can only be done numerically. This is technically challenging since the

to be solved for functions $x_8(\rho)$ and $x_9(\rho)$ appear as arguments of the numerically obtained metric functions $b(r)$ and $c(r)$. To obtain a Minkowski embedding we start x_2 with very large derivatives (ideally infinite) at a finite value ρ_*. For an Abelian embedding this would follow from the requirement that the two separate branes dual to the two separated defects at $x_2 = \pm d$ smoothly connect into a single connected configuration $x_2(\rho)$ that close to the endpoint is given by a square root. $x_{8,9}$ on the other hand start with a finite value at ρ_*, but we require zero derivative. In the Abelian case this would correspond to the requirement that the two branches of the solution (with positive and negative x_2 respectively) are symmetric under exchange. One solution is shown in Figure 3.5: We used $\beta/K = -50$ to generate this

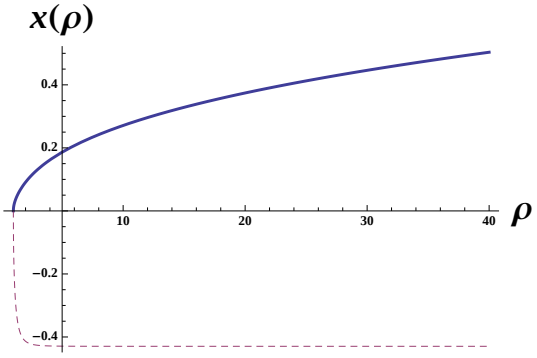

Figure 3.5: Solid line represents $x_{8,9}$ function, while dashed is x_2. For $\frac{\beta}{K} = -50$ and $d = -4.3 \times 10^{-2}$, Shooting out solution at $\rho_* = 1$, $X_5(\rho_*) = X_{8,9}(\rho_*) = 0$

plot giving rise to $d = -4.3 \times 10^{-2}$ in the asymptotic solution. The asymptotic form of the solution in the UV agrees with our analytic answer eq. (3.59). This solution mostly serves as a proof of principle.

3.2.5 Conclusion

We have shown that certain non-local mass terms in a field theory with an holographic dual in terms of probe branes can force the geometry of the probe to be non-geometric. The embedding coordinates are genuinely matrix valued. We demonstrated this basic effect in a supersymmetric defect setup, where we were also able to calculate the short-distance behavior of a two-point function using the non-Abelian DBI action. We also demonstrated

that, if we turn on in addition a brane polarizing background flux, the effect is enhanced as expected from Myers' proposal.

3.3 monopoles from intersecting branes

3.3.1 introduction

Intersecting D-branes have many applications. For example, they play a large role in top-down constructions of holographic duals. It is therefore surprising to find that the low energy field theory on D3-branes intersecting in 1+1 dimensions has several interesting features that seem not to have been previously discussed. In this paper, driven by an argument that this field theory must have magnetically charged solitons, we determine the low energy Lagrangian and discuss its properties.

To begin, consider a pair of parallel D3-branes. An F-string stretched between them is a BPS state which sources electric flux on the D3-branes. The D3-brane system is invariant under S-duality, which takes the F-string to a BPS D-string which sources magnetic flux. In the limit that the D3-branes are very close, the stretched F- and D-strings are much lighter than the string scale, and we should be able to describe them in an effective field theory. As is well-known, the F-strings become the off-diagonal components of the $\mathcal{N} = 4$ $U(2)$ fields, while the D-strings become magnetic monopole solitons in the spontaneously broken $U(2)$ theory.

Another possibility would have been for the low energy theory to contain independent magnetically charged fields. However, these would produce large nonperturbative effects due to their $1/g$ couplings, and this is not consistent. Such light nonperturbative states do arise in singular limits such as the conifold [171], but for coincident D-branes perturbation theory should be valid.

Now consider two D3-branes oriented as in Table 1. The only common spatial direction of the D3-branes is x^1, and we take them to be separated in the 8-direction. We can now ask the same question: in the limit of small separation, how does the stretched D-string, which is a BPS state, appear in the low energy effective theory?[4] This effective theory has only

[4]This issue has been raised in Ref. [49]. Related questions have been discussed in Ref. [84].

	0	1	2	3	4	5	6	7	8	9
D3	x	x			x	x				
D3′	x	x					x	x		
F/D1	x								x	

Table 3.1: The directions in which the two D3-branes and the stretched strings are extended. An x signifies extension in the indicated direction.

Abelian fields on the D3-branes, with charged hypermultiplets moving on the intersection, so it is not clear how a magnetically charged soliton could arise. But independent magnetic degrees of freedom are excluded by the same argument as before.

In this paper we resolve this puzzle. This will involve several novel properties of the intersecting brane theory. In §2 we study the effective low energy theory assuming canonical kinetic terms for the 3-3′ hypermultiplets, extending results of Ref. [49]. We show the 3-3′ fields are actually charged both electrically and magnetically under the D3 and D3′ gauge fields. While this creates the possibility of magnetic solitons, we show that the magnetic charges are actually confined, unlike the D-strings that we are trying to find.

In §3 we show that the interpretation of the hypermultiplets in terms of brane reconnection requires the $U(1)$ D-terms to be periodic variables, and this implies a nonlinear kinetic term. The hypermultiplet moduli space is a singular Gibbons-Hawking metric, with an infinite array of sources periodically identified. This periodicity produces a sine-Gordon-like potential, which supports magnetically charged kink solitons. We tentatively interpret the singularity as a breakdown of the low energy effective field theory of the intersection in regions of large field.

An interesting feature of systems with codimension-two defects, as here, is the presence of logarithmic divergences in the classical field theory. Goldberger and Wise [76] showed that these could be treated by ordinary renormalization theory. In §4 we obtain the beta functions for the Kähler potential and for the Gibbons-Hawking harmonic function V. The former is proportional to the squares of the moment maps, while the latter is simply a

constant. This renormalization mitigates, but does not remove, the singularity of the metric. We show that the same effective action is obtained from the DBI picture of the intersection.

In §5 we obtain the BPS equations, and argue that they have the desired soliton solutions. We cannot solve them analytically, but we study them in various approximations. Sec. 6 is discussion and conclusion.

	0	1	2	3	4	5	6	7	8	9
D3	x	x	x		x					
D5	x	x	x			x	x	x		
D3″	x		x			x			x	

Table 3.2: A T-dual D3-D5 system

The system we consider arises in various T-dual forms: we can dualize in one or more of the DD 2-, 3-, and 9- directions to produce higher dimensional versions, where the soliton is independent of the additional coordinates. The most well-studied intersecting brane system is probably D3-D5 intersecting in 2+1 dimensions [123]. We can reach this by T-dualities in the 2- and 5-directions, reaching the configuration shown in Table 2. However, this requires a T-dual in one of the ND-directions, and this changes the nature of the system. In particular the would-be magnetic object is not part of the brane intersection: the D1 becomes a D3″ extended in the 5-direction, so it cannot end on the D3. The various phenomena that we encounter are not present.

We were initially interested in this system as a simple field-theoretic model of S-duality, which it would inherit from the full string theory. Since the gauge fields are Abelian, the hope was that the S-duality would take a rather simple form. However, it is not clear that the brane system can be defined consistently as a field theory. The singularities of the moduli space metric apparently require embedding in the full brane DBI theory, and this in turn can only be quantized by embedding in string theory. If this is true, then there is no smaller S-dual system. Nevertheless, our work shows that intersecting D-brane systems harbor several surprising properties: the magnetic couplings of the intersection

fields, the nonlinear field space, and the classical renormalization. These may have a variety of applications.

3.3.2 Canonical action

The use of $d = 4$, $\mathcal{N} = 1$ superfields to write higher-dimensional theories has been developed in Refs. [18, 139] and applied to intersecting branes in Ref. [49]. We first give the superfield form of the action, following most closely the presentation in [18]. We then give the component form, demonstrating the magnetic couplings of the intersection fields.

Symmetries and fields

The brane system of Table 3.1 preserves eight supercharges. The bosonic symmetries are

$$SO(1,1)_{01} \times SO(2)_{45} \times SO(2)_{67} \times SO(4)_{2389} \times U(1)_V \times U(1)_{V'} \,. \tag{3.62}$$

On each D3-brane there lives the usual field content for a U(1) $d = 4$, $\mathcal{N} = 4$ gauge theory, but the supersymmetry algebras of the two branes are not the same. In order to exhibit the common supersymmetry, it is useful to label the fields in a nonstandard way. Consider the system obtained by T-duality in the 23 directions. The D3-D3$'$ become D5-D5$'$. Both D5 branes are extended in the 0123 directions, and the unbroken supersymmetry includes a $d = 4$, $\mathcal{N} = 1$ algebra in these directions. We can write the theory in terms of superfields for this algebra. The additional coordinates, $x^{4,5}$ for the D5 and $x^{6,7}$ for the D5$'$, are treated as parameters in the superfields. This follows the strategy introduced in Refs. [18, 139] for writing $d = 10$, $\mathcal{N} = 1$ SYM and other higher dimensional theories in terms of $d = 4$, $\mathcal{N} = 1$ superfields. We then dimensionally reduce in the 23 directions to obtain the system of interest. The T-dual system has different global symmetries, but the fact that the dimensionally reduced system will have an $SO(4)_{2389}$ symmetry guarantees that it has $d = 4$, $\mathcal{N} = 2$ supersymmetry.

On the D5 brane, we will call the $d = 4$, $\mathcal{N} = 1$ vector multiplet V and the scalar multiplets $Q_{1,2,3}$. After dimensional reduction to the D3, the four component gauge field will be made up of the $A_{V0,1}$ components of the vector multiplet and the real and imaginary components of Q_1, while $A_{V2,3}$ will combine to become one of the complex SYM scalars.

The D5′ brane is identical, with vector multiplet V' and scalar multiplets $S_{1,2,3}$. In this case, the components of S_2 will combine with $A_{V'0,1}$ to become the usual gauge field and $A_{V'2,3}$ becomes a complex scalar. The scalars $A_{V2,3}$ and $A_{V'2,3}$ combine with the scalars Q_3 and S_3 respectively to become $SO(4)$ vectors, since these fields will describe the transverse coordinates of the branes in the 2389 directions.

On the intersection between the branes, there are two chiral fields B and C, associated with the two orientations of F-strings stretching between the branes. B has fundamental charge $(1,-1)$ under the gauge groups $U(1)_V$ and $U(1)_{V'}$, while C has charge $(-1,1)$. These are scalars under $SO(4)$ and $SO(1,1)$. Since the $SO(4)$ is associated with the $\mathcal{N}=2$ supersymmetry, this means that the scalars B and C are not transformed into each other via the supersymmetric R-symmetry. Instead, it is fermionic superpartners of these fields that combine to form an $SU(2)_R$ doublet. This differs from the construction in [170], where the hypermultiplet scalars form an $SU(2)_R$ doublet. Under $SO(2)_{45} \times SO(2)_{67}$, B and C have charges $(\frac{1}{2}, \frac{1}{2})$. They transform as spinors because the ND boundary conditions for the 4567 directions on the string means that the corresponding RNS fermions are periodic in the NS sector and generate spinorial states.

We will discuss the transformations of the superfields further in §5, when we find the BPS equations.

Superfield action

We mostly follow the conventions of Wess and Bagger [178] and the presentation of Ref. [18]. In component form in Wess-Zumino gauge, we write

$$B = B(y) + \sqrt{2}\theta\psi_B(y) + \theta\theta F_B(y) \tag{3.63}$$

using the same symbol for the scalar component as for the superfield itself. It will be convenient to collect the spatial coordinates x_4 through x_9 into three complex coordinates z_{123} with

$$z_1 = \frac{1}{2}(x_4 + ix_5) \qquad z_2 = \frac{1}{2}(x_6 + ix_7) \qquad z_3 = \frac{1}{2}(x_8 + ix_9) \tag{3.64}$$

with derivatives denoted as $\partial_{z_1} = \partial_4 - i\partial_5$, etc. Greek indices μ, ν, etc. will run over 0123 unless otherwise specified.

The action for the 3-3 fields is then [18, 139]

$$S_{3\text{-}3} = \frac{1}{g_{\rm YM}^2}\int d^2x\, dx_4 dx_5 \Bigg\{ \int d^2\theta \left[\frac{1}{4}W_V^\alpha W_{V\alpha} + \frac{1}{2}\left(Q_3\partial_{z_1}Q_2 - Q_2\partial_{z_1}Q_3\right)\right] + \text{c.c.} \\ + \int d^4\theta \left[\left(\sqrt{2}\bar\partial_{z_1}V - \bar Q_1\right)\left(\sqrt{2}\partial_{z_1}V - Q_1\right) - \bar\partial_{z_1}V\partial_{z_1}V + \bar Q_2 Q_2 + \bar Q_3 Q_3\right]\Bigg\}. \tag{3.65}$$

As noted above, the V, Q_i are functions of the parameters $x^{4,5}$, so they represent an infinite number of $d = 4$, $\mathcal{N} = 1$ superfields. We have dimensionally reduced in $x^{2,3}$, so only the integrations over the 0145 directions remain. The terms involving z_1 derivatives of V and Q_1 are fixed by the gauge invariance[5]

$$\begin{aligned} V &\to V + \Lambda + \bar\Lambda \\ Q_1 &\to Q_1 + \sqrt{2}\partial_{z_1}\Lambda\,, \end{aligned} \tag{3.66}$$

where the superfield gauge parameter Λ is also a function of $x^{4,5}$. This choice of gauge transformation for Q_1 is consistent with its role as a gauge field,

$$Q_1 = \frac{1}{\sqrt{2}}\left(A_{V5} + iA_{V4}\right)\,. \tag{3.67}$$

The terms involving z_1 derivatives of $Q_{2,3}$ are needed to give $SO(3,1)$ invariance in the 0145 directions for this part of the action. Though both the $\mathcal{N} = 2$ supersymmetry and the Lorentz invariance in the 45 directions are obscured in this form, in component form the relationship is much clearer. This will be discussed in Section 3.3.2. Similarly the action for the $3'$-$3'$ fields is

$$S_{3'\text{-}3'} = \frac{1}{g_{\rm YM}^2}\int d^2x\, dx_6 dx_7 \Bigg\{ \int d^2\theta \left[\frac{1}{4}W_{V'}^\alpha W_{V'\alpha} + \frac{1}{2}\left(S_1\partial_{z_2}S_3 - S_3\partial_{z_2}S_1\right)\right] + \text{c.c.} \\ + \int d^4\theta \left[\left(\sqrt{2}\bar\partial_{z_2}V' - \bar S_2\right)\left(\sqrt{2}\partial_{z_2}V' - S_2\right) - \bar\partial_{z_2}V'\partial_{z_2}V' + \bar S_1 S_1 + \bar S_3 S_3\right]\Bigg\}. \tag{3.68}$$

[5]Ref. [49] gives the action in a slightly different form, which does not seem to be gauge invariant. Incidentally, our notation here follows [18], whose gauge parameter Λ is $i\Lambda_{\text{Wess\&Bagger}}$.

The fields B and C on the intersection are have charges $(1,-1)$ and $(-1,1)$ under (V,V') respectively, so their gauge transformations are

$$\begin{aligned} B &\to B e^{\Lambda'-\Lambda}\,, \\ C &\to C e^{\Lambda-\Lambda'}\,. \end{aligned} \tag{3.69}$$

Here the superfield gauge parameters Λ and Λ' are evaluated at the defect $x_{4567}=0$. The only gauge invariant combinations of B and C are then $|B|^2 e^{V-V'}$, $|C|^2 e^{V'-V}$, and BC. For a canonical kinetic term, these fields have the action

$$S_{3\text{-}3'} = \frac{1}{g_{\rm YM}^2}\int d^4x \left\{ \int d^4\theta \left(|B|^2 e^{V-V'} + |C|^2 e^{V'-V} \right) + \frac{i}{\sqrt{2}} \int d^2\theta \left(BCQ_3 - BCS_3 \right) + \text{c.c.} \right\}, \tag{3.70}$$

in which all fields living on the branes are evaluated at the defect. The superpotential

$$W = \frac{i}{\sqrt{2} g_{\rm YM}^2} \left(BCQ_3 - BCS_3 \right) \tag{3.71}$$

is fixed by $\mathcal{N}=2$ supersymmetry, since V and Q_3 combine to form a single $\mathcal{N}=2$ vector multiplet. Equivalently, this form is fixed by the requirement that we maintain the SO(4) symmetry of the original brane construction: $A_{V2,3}$ and the real components of the scalar Q_3 arise from the directions transverse to both branes, so B and C must couple identically to both.

To summarize, the full action [49] is the sum of Eqs. (3.65, 3.68, 3.70).

Component action

Integrating out all the auxiliary fields gives the bosonic sector of the component form action,

$$\begin{aligned}
S = \frac{1}{g_{\rm YM}^2}\int_{\rm D3} d^2x\, dx_4 dx_5 \Bigg\{ & -\frac{1}{4}F_V^{\mu\nu}F_{V\mu\nu} - \frac{1}{4}\left(\bar\partial_{z_1}Q_1 + \partial_{z_1}\bar Q_1 - \frac{1}{\sqrt{2}}\left(|C|^2-|B|^2\right)\delta^2(x_4,x_5)\right)^2 \\
& - \left|\partial^\mu Q_1 - \frac{i}{\sqrt{2}}\partial_{z_1}A_V^\mu\right|^2 - \partial_\mu\bar Q_2\partial^\mu Q_2 - \partial_\mu\bar Q_3\partial^\mu Q_3 - \partial_1 Q_3\bar\partial^1\bar Q_3 \\
& - \left(\bar\partial_{z_1}\bar Q_2 - \frac{i}{\sqrt{2}}\bar B\bar C\delta^2(x_4,x_5)\right)\left(\partial_{z_1}Q_2 + \frac{i}{\sqrt{2}}BC\delta^2(x_4,x_5)\right)\Bigg\} \\
+\frac{1}{g_{\rm YM}^2}\int_{\rm D3'} d^2x\, dx_6 dx_7 \Bigg\{ & -\frac{1}{4}F_{V'}^{\mu\nu}F_{V'\mu\nu} - \frac{1}{4}\left(\bar\partial_{z_2}S_2 + \partial_{z_2}\bar S_2 + \frac{1}{\sqrt{2}}\left(|C|^2-|B|^2\right)\delta^2(x_6,x_7)\right)^2 \\
& - \left|\partial^\mu S_2 - \frac{i}{\sqrt{2}}\partial_{z_2}A_{V'}^\mu\right|^2 - \partial_{z_2}S_3\bar\partial_{z_2}\bar S_3 - \partial_\mu\bar S_3\partial^\mu S_3 - \partial_\mu\bar S_1\partial^\mu S_1 \\
& - \left(\bar\partial_{z_2}\bar S_1 - \frac{i}{\sqrt{2}}\bar B\bar C\delta^2(x_6,x_7)\right)\left(\partial_{z_2}S_1 + \frac{i}{\sqrt{2}}BC\delta^2(x_6,x_7)\right)\Bigg\} \\
+\frac{1}{g_{\rm YM}^2}\int_{3\cap3'} d^2x \Bigg\{ & -\left|\left(\partial^\mu + i\frac{A_V^\mu - A_{V'}^\mu}{2}\right)B\right|^2 - \frac{|Q_3-S_3|^2}{2}|B|^2 \\
& - \left|\left(\partial^\mu - i\frac{A_V^\mu - A_{V'}^\mu}{2}\right)C\right|^2 - \frac{|Q_3-S_3|^2}{2}|C|^2\Bigg\}.
\end{aligned} \tag{3.72}$$

Here $d^2x = dx^0\,dx^1$, while the indices μ,ν run 0123. The 2-, 3-derivatives are set to zero by reduction, but terms with $A_V^{2,3}$ and $A_{V'}^{2,3}$ remain. As usual, in the intersection action all brane fields are evaluated at the defect.[6] The normalization of the intersection action can be changed by a scaling of B and C; in the next section, where the action is noncanonical, this will no longer be true.

The action (3.72) is lengthy, but this is in part because its full symmetry is obscured. First, we may check that Q_1 actually behaves like two components of the D3 gauge field, as desired. Using $Q_1 = (iA_{V4} + A_{V5})/\sqrt{2} \equiv iA_{Vz_1}/\sqrt{2}$, the kinetic terms for Q_1 become

$$-\frac{1}{4}\left(\bar\partial_{z_1}Q_1 + \partial_{z_1}\bar Q_1\right)^2 = -\frac{1}{2}\left(\partial_4 A_{V5} - \partial_5 A_{V4}\right)^2 = -\frac{1}{2}F_{V45}F_V^{45} \tag{3.73}$$

[6] We are following the conventions of Ref. [178], where covariant derivatives contain a factor $\frac{1}{2}$; the Abelian gauge fields, their scalar partners, and $g_{\rm YM}^2$ are normalized with respect to this.

and

$$-\left|\partial^\mu Q_1 - \frac{i}{\sqrt{2}}\partial_1 A_V^\mu\right|^2 = -\frac{1}{2}\left(F_{V\mu 4}F_V^{\mu 4} + F_{V\mu 5}F_V^{\mu 5}\right) . \tag{3.74}$$

Additionally we may check that, after dimensional reduction, $A_{V2,3}$, $A_{V'2,3}$, Q_3, and S_3 behave like transverse brane positions. The fields B and C couple to these as

$$-\frac{1}{2}\left(|Q_3 - S_3|^2 + |Q_0 - S_0|^2\right)\left(|B|^2 + |C|^2\right) , \tag{3.75}$$

where we have defined $Q_0 = (iA_{V2} + A_{V3})/\sqrt{2}$ and $S_0 = (iA_{V'2} + A_{V'3})/\sqrt{2}$. The separation between the branes produces a mass term for the B and C fields, from the tension of the stretched string. The expected SO(4) symmetry is manifest in this form.

The action appears to contain quadratically divergent terms, such as

$$-\frac{1}{8}\left(|C|^2 - |B|^2\right)\delta^2(0,0) , \quad -\frac{1}{4}|B|^2|C|^2\delta^2(0,0) , \tag{3.76}$$

obtained after integrating over z_1 and z_2. However, these automatically cancel. They arise from the squares of the auxiliary fields

$$D_V = -\frac{\sqrt{2}}{2}\left(\bar\partial_{z_1} Q_1 + \partial_{z_1}\bar Q_1\right) + \frac{1}{2}\left(|C|^2 - |B|^2\right)\delta^2(x_4, x_5) , \tag{3.77}$$

$$F_{Q_3} = -\bar\partial_{z_1}\bar Q_2 + \frac{i}{\sqrt{2}}\bar B\bar C\delta^2(x_4, x_5) , \tag{3.78}$$

and the corresponding terms on the other brane. Energetics requires that the other term in each auxiliary field have a compensating delta function, and so the behavior of the fields near the brane must be

$$Q_1 \approx \frac{1}{8\pi\sqrt{2}}\frac{|C|^2 - |B|^2}{z_1} , \quad Q_2 \approx -\frac{i}{4\pi\sqrt{2}}\frac{BC}{z_1} . \tag{3.79}$$

This removes the explicit squares of Dirac delta-functions, so the action is free of quadratic divergences. There are still logarithmic divergences, from the poles in the fields (3.79). Their proper treatment via renormalization will be discussed in Section 3.3.4.

The specific combination of intersection fields BC sources the derivative of Q_2 in the z_1 direction and S_1 in the z_2 direction. Noting that $Z_2 = \pi\alpha' Q_2/\sqrt{2}$ is the collective coordinate for the D3-brane,[7] we have

$$Z_1 Z_2 = -\frac{i\alpha'}{4}BC . \tag{3.80}$$

[7]The usual relation between canonical brane scalars and collective coordinates is $X = 2\pi\alpha'\Phi$. Here there is an extra $\frac{1}{2}$ from the normalization convention noted in footnote 6, and an extra $\frac{1}{\sqrt{2}}$ from the normalization (3.64) of z_2.

This is symmetric between the two branes, agreeing with the corresponding constraint from F_{S_3}. Thus BC is the modulus for the reconnection of the branes.

Electric and magnetic sources

The first three terms in the D3 part of the Lagrangian (3.72) can be nicely condensed into

$$-\frac{1}{4}\mathcal{F}_{ab}\mathcal{F}^{ab}\,. \tag{3.81}$$

Here a, b run over the D3 directions 0145 and $\mathcal{F}_{ab}$ is identified with F_{Vab} except for the component

$$\mathcal{F}_{45} = D_V = \partial_4 A_{V5} - \partial_5 A_{V4} + \frac{1}{2}\left(|C|^2 - |B|^2\right)\delta^2(x_4, x_5)\,. \tag{3.82}$$

Similarly we define on the D3′ the tensor $\mathcal{F}'_{mn}$, with m, n running over 0167 and with $\mathcal{F}'_{67} = D_{V'}$. The equations of motion for the gauge field are

$$\begin{aligned}\partial_a \mathcal{F}^{ab} =& j^b_{E,V} = \frac{i}{2}\left[\left(B\partial^b\bar{B} - \bar{B}\partial^b B\right) - \left(C\partial^b\bar{C} - \bar{C}\partial^b C\right)\right]\delta^2(x_4, x_5)\,,\\ \partial_m \mathcal{F}'^{mn} =& j^n_{E,V'} = -\frac{i}{2}\left[\left(B\partial^n\bar{B} - \bar{B}\partial^n B\right) - \left(C\partial^n\bar{C} - \bar{C}\partial^n C\right)\right]\delta^2(x_6, x_7)\,.\end{aligned} \tag{3.83}$$

Note that only the 01 components of the currents are nonzero.

For the dual tensor one finds

$$\begin{aligned}\partial_a \tilde{\mathcal{F}}^{ab} =& j^b_{M,V} = \frac{1}{2}\epsilon^{bc}\partial_c\left(|C|^2 - |B|^2\right)\delta^2(x_4, x_5)\,,\\ \partial_m \tilde{\mathcal{F}}'^{mn} =& j^n_{M,V'} = -\frac{1}{2}\epsilon^{np}\partial_p\left(|C|^2 - |B|^2\right)\delta^2(x_6, x_7)\,.\end{aligned} \tag{3.84}$$

Here $\epsilon^{01} = -\epsilon^{10} = 1$ with other components vanishing, so the current is again tangent to the intersection.

It is the square of $\mathcal{F}$ that appears in the Lagrangian and the Hamiltonian, so it is natural to identify this with the field strength. Eqs. (3.83, 3.84) thus represent electric and magnetic sources. Indeed, this kind of action for an Abelian gauge field coupled to electric and magnetic charges is well-known [36], though in the present case there is the simplification that the magnetic couplings are local because the magnetic currents are topological (curls). In particular, the total magnetic charges are

$$Q_M = -Q'_M = \frac{1}{2}\left(\mathcal{P}(x^1 = \infty) - \mathcal{P}(x^1 = -\infty)\right)\,, \tag{3.85}$$

where $\mathcal{P} = |C|^2 - |B|^2$ is the contribution of the charged fields to the D-terms. A 1+1 dimensional kink, with values of $\mathcal{P}$ differing at $\pm\infty$, will therefore carry a magnetic charge.

This somewhat surprising result, that the intersection hypermultiplets couple magnetically as well as electrically, is the first step toward identifying the D-string, but there is a complication. At nonzero brane separation, the potential (3.75) is proportional to $|C|^2+|B|^2$ and takes its minimum value only when $B = C = \mathcal{P} = 0$. A configuration of nonzero magnetic charge would necessarily have a nonzero potential energy density in at least one of the two asymptotic directions, and so an energy which diverges linearly at long distance. The lagrangian (3.72) describes a system in which magnetic charges are confined. This cannot account for the D-string, which exists as an isolated BPS particle. In the next section we resolve this issue.

3.3.3 Noncanonical action

We would obtain the expected spectrum, with unconfined monopoles of quantized charge, if the potential (3.75) were of sine-Gordon form, periodic with a series of zeroes. To see why this is the case, let us look again at the brane interpretation of the hypermultiplet fields. We have noted that the product BC sources brane bending through the F_{Q_3} potential. Similarly, $\mathcal{P}$ sources the vector potential as in Eq. (3.79),

$$A_{Vz_1} \approx -i\frac{\mathcal{P}}{8\pi z_1}\,. \tag{3.1}$$

This potential is locally pure gauge, but can have nontrivial holonomy. In particular, when the brane intersection is resolved as in Eq. (3.80), the point $z_1 = 0$ is pushed off to infinity and the remaining space is multiply connected. The holonomy is

$$\oint dz_1\, A_{Vz_1} + \text{c.c.} = \frac{1}{2}\,\text{Re}\,\mathcal{P}\,. \tag{3.2}$$

A shift of the holonomy by 4π should give a physically equivalent configuration, where the extra factor of 2 arises from the convention noted in footnote 6. Therefore,

$$\mathcal{P} \sim \mathcal{P} + 8\pi \tag{3.3}$$

must be a periodic variable. With this, the magnetic charge (3.85) has just the expected quantization.[8]

We therefore consider more general actions, in which the hypermultiplets have arbitrary Kähler potentials. This might have been anticipated, since the B and C fields on the 1+1 dimensional intersection are dimensionless. At the end of this section, we will return to the T-dual higher dimensional configurations discussed in the introduction.

General Kähler potentials

Gauge invariance and manifest $\mathcal{N} = 1$ supersymmetry restrict our general intersection action to be written in terms of a Kähler potential $K(Be^{V-V'}, \bar{B}, Ce^{V'-V}, \bar{C})$ and a superpotential of the form

$$W = \frac{i}{\sqrt{2}}(Q_3 - S_3)f(BC) \tag{3.4}$$

for some function f. Enforcing $\mathcal{N} = 2$ supersymmetry additionally requires the Kähler metric to be Ricci flat and fixes f in terms of K. The form for f is most easily determined from the component form of the action by requiring that the SO(4) symmetry associated with the $\mathcal{N} = 2$ supersymmetry remains preserved.

In order to write the action concisely in component form, collect the fields B and C into a single vector $Z^\alpha = (B, C)$. Define the Killing vector gauged by the brane gauge fields as $k^\alpha = (-iB, iC)$. Additionally, we make use of the relation

$$\partial_\alpha f(BC) = i\epsilon_{\alpha\beta}k^\beta f'(BC) \tag{3.5}$$

[8]Note that the allowed electric charges include not only the $(1, -1)$ of the intersection fields, but also $(\pm 1, 0)$ and $(0, \pm 1)$ for strings that attach only to one brane and end elsewhere.

The bosonic sector of the component form of the generalized action may be written

$$
\begin{aligned}
S = \frac{1}{g_{\rm YM}^2}\int_{\rm D3} d^2x\, dx_4 dx_5 \Bigg\{ & -\frac{1}{4}F_V^{\mu\nu}F_{V\mu\nu} - \frac{1}{4}\left(\bar\partial_{z_1}Q_1 + \partial_{z_1}\bar Q_1 - \frac{1}{\sqrt{2}}\mathcal{P}\delta^2(x_4,x_5)\right)^2 \\
& - \left|\partial^\mu Q_1 - \frac{i}{\sqrt{2}}\partial_{z_1}A_V^\mu\right|^2 - \partial_\mu\bar Q_2\partial^\mu Q_2 - \partial_\mu\bar Q_3\partial^\mu Q_3 - \partial_1 Q_3\bar\partial^1\bar Q_3 \\
& - \left(\bar\partial_{z_1}\bar Q_2 - \frac{i}{\sqrt{2}}\bar f\delta^2(z_1,\bar z_1)\right)\left(\partial_{z_1}Q_2 + \frac{i}{\sqrt{2}}f\delta^2(z_1,\bar z_1)\right)\Bigg\} \\
+\frac{1}{g_{\rm YM}^2}\int_{\rm D3'} d^2x\, dx_6 dx_7 \Bigg\{ & -\frac{1}{4}F_{V'}^{\mu\nu}F_{V'\mu\nu} - \frac{1}{4}\left(\bar\partial_{z_2}S_2 + \partial_{z_2}\bar S_2 + \frac{1}{\sqrt{2}}\mathcal{P}\delta^2(z_2,\bar z_2)\right)^2 \\
& - \left|\partial^\mu S_2 - \frac{i}{\sqrt{2}}\partial_{z_2}A_{V'}^\mu\right|^2 - \partial_{z_2}S_3\bar\partial_{z_2}\bar S_3 - \partial_\mu\bar S_3\partial^\mu S_3 - \partial_\mu\bar S_1\partial^\mu S_1 \\
& - \left(\bar\partial_{z_2}\bar S_1 - \frac{i}{\sqrt{2}}\bar f\delta^2(z_2,\bar z_2)\right)\left(\partial_{z_2}S_1 + \frac{i}{\sqrt{2}}f\delta^2(z_2,\bar z_2)\right)\Bigg\} \\
+\frac{1}{g_{\rm YM}^2}\int_{3\cap 3'} d^2x \Bigg\{ & - g_{\alpha\dot\beta}\left(\partial^\mu Z^\alpha + \frac{A_V^\mu - A_{V'}^\mu}{2}k^\alpha\right)\left(\partial_\mu\bar Z^{\dot\beta} + \frac{A_{V\mu} - A_{V'\mu}}{2}\bar k^{\dot\beta}\right) \\
& - \frac{|Q_3 - S_3|^2}{2}g^{\alpha\dot\gamma}\epsilon_{\alpha\beta}k^\beta\epsilon_{\dot\gamma\dot\delta}\bar k^{\dot\delta}|f'|^2\Bigg\}.
\end{aligned}
\tag{3.6}
$$

Here $g_{\alpha\dot\beta} = \partial_\alpha\partial_{\dot\beta}K$ is the Kähler metric, and $\mathcal{P}$ is the moment map of the Killing vector k^α,

$$
\mathcal{P} = ik^\alpha\partial_\alpha K\,. \tag{3.7}
$$

Note that Eqs. (3.85, 3.1, 3.2) continue to hold, but the relation between $\mathcal{P}$ and B, C is modified in general. Note also that the definition of $\mathcal{P}$ includes only the variations of B, C and not the term from the variation of Q_1.

It is now straightforward to determine the function f. The SO(4) symmetry mixes Q_3 into A_{V2} and A_{V3}, so demanding these terms appear identically in the action sets

$$
k^\alpha g_{\alpha\dot\beta}\bar k^{\dot\beta} = g^{\alpha\dot\gamma}\epsilon_{\alpha\beta}k^\beta\epsilon_{\dot\gamma\dot\delta}\bar k^{\dot\delta}|f'|^2 \tag{3.8}
$$

Since the Kähler metric is just a two by two matrix, it can be inverted explicitly to give the relationship $g^{\alpha\dot\gamma} = (\det g)^{-1}\epsilon^{\alpha\beta}\epsilon^{\dot\gamma\dot\delta}g_{\beta\dot\delta}$, which yields

$$
|f'|^2 = \det g\,. \tag{3.9}
$$

The condition that the Kähler metric be Ricci flat is

$$0 = R_{\alpha\dot{\beta}} = -\partial_\alpha \partial_{\dot{\beta}} \ln (\det g) \ , \tag{3.10}$$

which is equivalently that the requirement that $\det g$ split into a holomorphic and anti-holomorphic part. Therefore, for any Kähler potential preserving $\mathcal{N} = 2$ supersymmetry, we are guaranteed to be able to solve Eq. 3.9 to find a superpotential that also preserves the supersymmetry.

As an aside, it is worth noting that to make the preservation of supersymmetry apparent in the fermionic sector, it is necessary to also make a field redefinition of the fermion fields. For the vector multiplet fermion λ_V, the Q_3 chiral multiplet fermion ψ_{Q_3}, and the Z^α fermions ψ_Z^α, we expect (λ_V, ψ_{Q_3}) and $(\psi_Z^1, \bar{\psi}_Z^2)$ to transform as $SU(2)$ doublets. However, the relevant Yukawa couplings

$$\sqrt{2}\bar{\lambda}_V \psi_Z^\alpha g_{\alpha\dot{\beta}} \bar{k}^{\dot{\beta}} \qquad\qquad - i\sqrt{2}\bar{\psi}_{Q_3} \bar{\psi}_Z^\alpha \bar{\partial}_\alpha \bar{f} \tag{3.11}$$

are not singlets under this $SU(2)$ transformation. By demanding the new fields obey this condition, the necessary field redefinition takes the form

$$\psi_Z'^\alpha = -i \left(k^\beta g_{\beta\dot{\gamma}} \bar{k}^{\dot{\gamma}} \right)^{-1/2} \bar{f}' \epsilon^{\alpha\sigma} \left(g_{\sigma\dot{\lambda}} \bar{k}^{\dot{\lambda}} \psi_Z^B - \partial_\sigma f \psi_Z^C \right) \ . \tag{3.12}$$

This gives the Yukawa couplings

$$\begin{aligned} &\bar{\lambda}_V \psi_Z'^B \sqrt{2k^\delta g_{\delta\dot{\lambda}} \bar{k}^{\dot{\lambda}}} \\ &\bar{\psi}_{Q_3} \bar{\psi}_Z'^C \sqrt{2k^\delta g_{\delta\dot{\lambda}} \bar{k}^{\dot{\lambda}}} \\ &\lambda_V \bar{\psi}_Z'^C \cdot 0 \\ &\psi_{Q_3} \psi_Z'^B \cdot 0 \end{aligned} \tag{3.13}$$

Thus in order to preserve $\mathcal{N} = 2$ supersymmetry in the fermion sector, half the Yukawa couplings must vanish.

We need a Kähler potential which satisfies the conditions for $\mathcal{N} = 2$ supersymmetry and for which $\mathcal{P}$ is periodic. In §3.2 we will construct this explicitly, but first we can deduce how the periodic identification must act on the (B, C) fields. First, we claim that the function $f(BC)$ must remain equal to BC. The product BC transforms as $(+1, +1)$ under the

$SO(2)_{45} \times SO(2)_{67}$ R-symmetries, so a more general superpotential would not transform properly. Then the periodicity must be

$$B \to B/(\beta BC)\,, \quad C \to C(\beta BC) \tag{3.14}$$

for some constant β. First, this preserves the holomorphicity and gauge quantum numbers of the fields. Second, it leaves invariant $BC = f$, which has a physical interpretation (3.80) in terms of the brane configuration. Finally, this identification would seem not to commute with $SO(2)_{45} \times SO(2)_{67}$. However, the shift of the A_{Vz_1} holonomy requires a gauge transformation $e^{i\theta} = \sqrt{z_1/\bar{z}_1}$. This adds a gauge piece to the rotation generator in the 45 plane, exactly cancelling the effect of the transformation (3.14); corresponding arguments apply in the 67 plane.

Gibbons-Hawking geometry

We want to construct a specific Kähler metric that both preserves $\mathcal{N} = 2$ supersymmetry and provides the correct periodicity for the topological charge $\mathcal{P}$. The Gibbons-Hawking metrics provide a large class of $\mathcal{N} = 2$ supersymmetric theories with in two complex dimensions, and we will see that there is a natural metric in of this type.

The Gibbons-Hawking metrics are of the form

$$ds^2 = V(\vec{x}) d\vec{x} \cdot d\vec{x} + \frac{1}{V(\vec{x})}\omega^2\,, \tag{3.15}$$

where $\vec{x} = (x, y, z)$ and

$$\omega = d\theta + \vec{A}(\vec{x}) \cdot d\vec{x}\,, \quad d\omega = dA = *dV\,, \quad \vec{\partial} \cdot \vec{\partial} V = 4\pi \sum_i \delta^3(\vec{x} - \vec{x}_i)\,. \tag{3.16}$$

To express these in Kähler form we follow Lebrun [133], with the function u from that reference set to zero. Define

$$U = x + iy\,, \quad \phi = V dz + i\omega\,, \tag{3.17}$$

so that

$$ds^2 = V dU d\bar{U} + \frac{1}{V}\phi\bar{\phi}\,. \tag{3.18}$$

Then one finds that

$$d\phi = d(x+iy) \wedge [(\partial_x - i\partial_y)V dz - \tfrac{1}{2}\partial_z V d(x-iy)] \,. \tag{3.19}$$

Since the right-hand side is closed it follows that locally we can write

$$V dz + i\omega = \phi = dW + \sigma dU \,, \tag{3.20}$$

where

$$d\sigma = -(\partial_x - i\partial_y)V dz + \tfrac{1}{2}\partial_z V d(x-iy) + O(d(x+iy)) \,. \tag{3.21}$$

We can regard Eqs. (3.23, 3.21) as differential equations determining W and σ. Picking out the dz components gives

$$\partial_z W = V \,, \quad \partial_z \sigma = (-\partial_x + i\partial_y)V \,. \tag{3.22}$$

These hold in an axial gauge, $\omega_z = 0$. The real part of Eq. 3.23 is

$$2V dz = dW + d\bar{W} + \sigma dU + \bar{\sigma} d\bar{U} \,, \tag{3.23}$$

which determines the partial derivatives of z with respect to the complex coordinates.[9]

Then U and $W \equiv W_1 + iW_2$ are the appropriate complex coordinates on the space. The metric is Hermitian,

$$ds^2 = V dU d\bar{U} + \frac{1}{V}(dW + \sigma dU)(d\bar{W} + \bar{\sigma} d\bar{U}) \,. \tag{3.24}$$

It is also Kähler, from $d\Omega = 0$ where

$$\Omega = V dU \wedge d\bar{U} + \frac{1}{V}\phi \wedge \bar{\phi} = -2iV dx \wedge dy - 2i dz \wedge \omega \,. \tag{3.25}$$

We see that $\det g = 1$ so it is Ricci-flat.

A special case is $V = 1/r$ where $r = |\vec{x}|$. We have

$$W = \sinh^{-1}\left(\frac{z}{\sqrt{x^2+y^2}}\right) + i\theta \equiv W_1 + iW_2 \,, \quad \sigma = \frac{z}{(x+iy)r} \,. \tag{3.26}$$

---

[9] There are two natural sets of independent variables, the Gibbons-Hawking coordinates (x, y, z, θ) and the complex $(U, \bar{U}, W, \bar{W})$. Which we are using is determined by context: which derivatives appear in a given equation. Also, when we differentiate with respect to W_1 we hold fixed x, y, θ or equivalently $U, \bar{U}, W_2$, so the change of variables between z and W_1 is one-dimensional.

The metric in complex coordinates is then

$$ds^2 = \sqrt{U\bar{U}}\cosh W_1 \left(dW d\bar{W} + \frac{dU d\bar{U}}{U\bar{U}} \right) + \sqrt{U\bar{U}}\sinh W_1 \left(\frac{dW dU}{U} + \frac{dW d\bar{U}}{\bar{U}} \right) . \quad (3.27)$$

This is obtained from the Kähler potential

$$K = 4\sqrt{U\bar{U}}\cosh W_1 . \quad (3.28)$$

This metric is actually flat: let

$$U = BC/2 , \quad e^W = B/C , \quad (3.29)$$

and then $K = B\bar{B} + C\bar{C}$. In fact these identifications could have been anticipated, up to c-number normalization, in terms of the $U(1)$ symmetries by shifts of θ and rotations of $x + iy$. Thus they continue to hold in the nonlinear case.

Returning to the general case, the $U(1)$ invariance on θ, implies that the Käher potential K is a function of W_1 but not W_2. Then

$$\frac{1}{V} = g_{W\bar{W}} = \partial_W \partial_{\bar{W}} K = \frac{1}{4}\partial^2_{W_1} K . \quad (3.30)$$

From (3.22), $\partial_z W_1 = V$, and we can write

$$4 = \partial^2_{W_1} K \partial_z W_1 = \partial_z \partial_{W_1} K \;\Rightarrow\; \partial_{W_1} K = 4(z + d(x, y)) . \quad (3.31)$$

Further,

$$\frac{\bar{\sigma}}{V} = g_{\bar{U}W} = \partial_{\bar{U}}\partial_W K = \frac{1}{2}\partial_{\bar{U}}\partial_{W_1} K = 2\partial_{\bar{U}}(z + d(x, y)) = \frac{\bar{\sigma}}{V} + 2\partial_{\bar{U}} d(x, y) , \quad (3.32)$$

so that $d(x, y)$ is a constant that can be set to zero. Noting that $k^\alpha \partial_\alpha W = k^B - k^C = -2i$, the moment map is then

$$\mathcal{P} = ik^\alpha \partial_\alpha \partial_W K = \partial_{W_1} K = 4z . \quad (3.33)$$

To obtain the periodicity (3.3), Eq. (3.33) suggests that we should take

$$V \stackrel{?}{=} \sum_{n=-\infty}^{\infty} \frac{1}{\sqrt{x^2 + y^2 + (z + 2\pi n)^2}} , \quad (3.34)$$

but this diverges. We therefore regulate and subtract,

$$V = c + \lim_{N\to\infty} \left(-\frac{1}{\pi}\ln N + \sum_{n=-N}^{N} \frac{1}{\sqrt{x^2 + y^2 + (z + 2\pi n)^2}} \right) . \quad (3.35)$$

The parameter c must be fixed by a stringy calculation, but its precise value will not matter. For any c the renormalized V becomes negative for large enough x^2+y^2,

$$V \sim c - \frac{1}{2\pi} \ln \frac{x^2+y^2}{4\pi^2} \,. \tag{3.36}$$

This implies a singularity in the metric, whose implications we will discuss later. The $U(1)$ symmetries are as before, and so the identification (3.29) is the same.

The differential equation for W implies that

$$W = i\theta + cz + \lim_{N\to\infty} \left(-\frac{z}{\pi} \ln N + \sum_{n=-N}^{N} \sinh^{-1} \frac{z+2\pi n}{\sqrt{x^2+y^2}} \right) + h(U,\bar{U}) \,. \tag{3.37}$$

for some function h. Shifting by one period $z \to z+2\pi$ removes the $n=-N$ term and adds a term $n=N+1$, with the net effect $W \to W + c\pi + \ln(16\pi^2/U\bar{U})$. This cannot be correct, as it does not respect the holomorphy, but we note that this can be repaired if the shift of z is accompanied by a shift $\theta \to \theta - i\ln(\bar{U}/U)$. The full periodicity is then

$$W \to W + c\pi + \ln \frac{16\pi^2}{U^2} \,. \tag{3.38}$$

One could use as complex coordinates U and $Y = W/\ln(U^2/16\pi^2 e^{\pi c})$, for which the periodicity is simply $(U,Y) \to (U, Y-2)$. Using the relation (3.29) of W to B, C, the periodicity of (B,C) is precisely (3.14), with $\beta = e^{-\pi c/2}/8\pi$.

T-dual configurations

We might have anticipated the need for a nonlinear kinetic term, since the fields B, C are dimensionless in two dimensions. However, we have noted that the soliton persists if we T-dual on k DD directions, leading to a higher dimensional theory in which B, C have units of $m^{k/2}$. The point is that while the nonlinear terms are irrelevant in the renormalization sense, as two-derivative terms they are important on the moduli space. Note that the D-string has mass $|Q_3|/g$ (for separation in the z_3-direction), but the D$(1+k)$ monopole in the T-dual theory has tension $|Q_3|(2\pi\alpha')^{-k/2}/g$, corresponding to a mass scale of order $|Q_3|^{1/(k+1)}\alpha'^{-k/2(k+1)}$. This does go to zero with the separation, but it retains a dependence on the UV scale, which enters into the low energy theory through the couplings of the irrelevant terms.

For the D3-D5 theory shown in Table 2, the interpretation of the hypermultiplets is different. The D5-brane bisects the D3 on the line $x^4 = x^5 = x^6 = x^7 = 0$. The two halves of the D3 can be shifted independently in the 567 directions, since D3's can end on D5's. The hypermultiplet moments correspond to the separation of the D3 endings along the D5 [89]. In this case the moduli space is R^3 and there is no periodicity.

3.3.4 Renormalization

We have noted that there will be logarithmic divergences in the classical action. These arise in theories with codimension-two defects, because the fall-off of a point-sourced massless field in two dimensions is logarithmic. Ref. [76] addressed this issue, showing that these classical divergences fit naturally into the framework of renormalization theory. In particular, they induce a flow of the effective action with scale.[10]

Procedurally, the renormalization is calculated no differently than in quantum field theory, except we work with tree level Feynman diagrams instead of loop diagrams. Consider tree-level diagrams whose external lines are all Z^α or $\bar{Z}^{\dot{\alpha}}$. Internal exchanges of $A_{V0,1}$, Q_1, or Q_2 can all lead to logarithmic divergences. The tree-level vertices in diagrams for these fields are localized to the defect, and so their Fourier transforms are independent of the transverse momenta. This means that the momentum of an internal line is unconstrained in two of the dimensions and must be integrated over, similar to the more usual loop integral over momentum. This calculation may be done in either with superfields or with components and we will present both.

Superfield calculation

Begin by introducing sources $J_{1,2,3}$ for the chiral fields $Q_{1,2,3}$ and J_V for the vector field V. First we integrate out $Q_{2,3}$. We have

$$S_{Q_{2,3}} = \int d^4x\, d^4\theta \left(\bar{Q}_i Q_i + Q_i J_i + \bar{Q}_i J_i\right) + \int d^4x\, d^2\theta\, Q_3 \partial_1 Q_2 + \text{c.c.}\,. \tag{3.1}$$

[10] This is also similar to the renormalization of the Schrödinger equation with a delta-function potential in 2+1 dimensions [95].

Now shift, $Q_i = Q'_i + q_i$. The terms linear in Q' are

$$\begin{aligned} S_{O(Q')} &= \int d^4x\, d^4\theta\, Q'_i(q_i + J_i) - \int d^4x\, d^2\theta\, \epsilon_{ij} Q'_i \partial_1 q'_j \\ &= \int d^4x\, d^2\theta\, Q'_i \left[\bar{D}^2(q_i + J_i)/4 - \epsilon_{ij}\partial_1 q'_j\right]. \end{aligned} \tag{3.2}$$

Here $\epsilon_{23} = 1$. In the second line we have combined terms, noting that $\int d\theta = \partial_\theta$ implies that $\bar{D}^2 X/4 = \int d^2\bar{\theta}\, X$ for any X, up to total x derivatives (there is an implicit $\frac{1}{4}$ in the integral so that $\int d^2\theta\, \theta^2 = 1$). The condition that the linear term vanish gives

$$\begin{bmatrix} q_2 \\ \bar{q}_3 \end{bmatrix} = \frac{1}{p^2} \begin{bmatrix} \bar{D}^4/4 & \partial_1 \\ -\partial_1 & D^2/4 \end{bmatrix} \begin{bmatrix} D^2 J_2/4 \\ \bar{D}^2 J_3/4 \end{bmatrix}. \tag{3.3}$$

Here we have gone to momentum space, and $p^2 = p_\parallel^2 + p_\perp^2 = p_\mu p^\mu + p_1 \bar{p}_1$. We only need the propagator for Q_3 so can set $J_2 = 0$. The source-dependence of the action is then given as usual by $\frac{1}{2}$ of the source terms with classical background inserted,

$$S_{V,Q} \to \int \frac{d^4p}{(2\pi)^4} d^4\theta\, q_3 J_3 = \int \frac{d^4p}{(2\pi)^4} d^4\theta\, \bar{J}_3 \frac{D^2\bar{D}^2}{16p^2} J_3\,. \tag{3.4}$$

The propagator is then

$$\langle Q_3(p,\theta)\bar{Q}_3(p',\theta')\rangle = -i(2\pi)^4\delta^4(p+p')\frac{\bar{D}^2 D^2}{16p^2}\delta^4(\theta-\theta')\,. \tag{3.5}$$

The interaction is

$$S_{\rm int} = \frac{i}{\sqrt{2}}\int d^2x\, d^2\theta\, Q_3 f + \text{c.c.} = -\frac{i}{\sqrt{2}}\int d^2x\, d^2\theta\, Q_3 \frac{\bar{D}^2 D^2}{16p_\parallel^2} f + \text{c.c.} \tag{3.6}$$

$$= -\frac{i}{\sqrt{2}}\int d^2x\, d^4\theta\, Q_3 \frac{D^2}{4p_\parallel^2} f + \text{c.c.}\,. \tag{3.7}$$

The graph from exchanging a Q_3 is then

$$i\int \frac{d^4p}{(2\pi)^4} f(p_\parallel) \frac{D^2\bar{D}^2 D^2\bar{D}^2}{512 p_\parallel^2 p_\parallel^2 p^2} \bar{f}(-p_\parallel) = \frac{i}{2}\int \frac{d^4p}{(2\pi)^4}\frac{1}{p^2} f(p_\parallel)\bar{f}(-p_\parallel)\,. \tag{3.8}$$

We see that the integral over $p_\perp^2$ generates a log divergence, which is canceled by an $\bar{f}f$ correction to the Kähler potential. The effective Kähler potential is given by integrating out $p_\perp$ between a UV cutoff Λ and the scale μ,[11]

$$i\Delta K = \frac{i}{8\pi}\ln\left(\frac{\Lambda^2}{\mu^2}\right)\bar{f}f\,. \tag{3.9}$$

[11] To extract the log divergence we do not need the details of the cutoff, but in fact a simple transverse momentum cutoff preserves both supersymmetry and gauge invariance.

This contributes $-\frac{1}{4\pi}\bar{f}f$ to $\mu\partial_\mu K$; the second brane makes an equal contribution.

Now we integrate out V and Q_1. The action is

$$S_{V,Q_1} = \int d^4x\, d^2\theta\, \frac{1}{4} W_V^\alpha W_{V\alpha} + \text{c.c.} \\ + \int d^4x\, d^4\theta\, \left(\bar{\partial}_1 V \partial_1 V - \sqrt{2}(Q_1 \bar{\partial}_1 V + \bar{Q}_1 \partial_1 V) + \bar{Q}_1 Q_1 + J_V V) \right) . \tag{3.10}$$

With the gauge transformation $Q_1 \to Q_1 + \partial_1 \Lambda$ we can go to the unitary gauge $Q_1 = 0$, in which

$$S_{V,Q_1} = -\int d^4x\, d^4\theta\, V(P_T \partial_\mu \partial^\mu + \bar{\partial}_1 \partial_1) V\,. \tag{3.11}$$

We use the projection operators defined in Ref. [178], chap. IX. The propagator is then

$$\langle V(p,\theta) \bar{V}(p',\theta') \rangle = -i(2\pi)^4 \delta^4(p+p') \left(\frac{P_T}{p^2} + \frac{P_1 + P_2}{p_\perp^2} \right) \delta^4(\theta - \theta')\,. \tag{3.12}$$

The first order coupling of the field V is $V\delta_\Lambda K = -V\delta_{\bar{\Lambda}} K \equiv -V\mathcal{P}$, where K is the hypermultiplet Kähler potential and δ_Λ is the holomorphic part of the gauge transformation. At large $p_\perp$, where the divergence enters, the projection operators just add to unity. We thus obtain the divergence

$$-\frac{i}{4} \int \frac{d^4p}{(2\pi)^4} \frac{1}{p^2} \mathcal{P}(p_\parallel) \bar{\mathcal{P}}(-p_\parallel)\,, \tag{3.13}$$

and so

$$i\Delta' K = -\frac{i}{16\pi} \ln\left(\frac{\Lambda^2}{\mu^2} \right) \mathcal{P}^2\,. \tag{3.14}$$

In all,

$$\mu\partial_\mu K = \frac{1}{4\pi} (\mathcal{P}^2 - 2\bar{f}f)\,, \tag{3.15}$$

including the contribution of the second brane.

It can be shown that this renormalization preserves $d = 4$, $\mathcal{N} = 2$ supersymmetry. We illustrate this with the simple case

$$K = \bar{B}B + \bar{C}C\,, \quad f = BC \tag{3.16}$$

at the initial point $\mu = \mu_0$. Then $\mathcal{P} = (\bar{C}C - \bar{B}B)$ and

$$\mu\partial_\mu K = \frac{1}{4\pi} (\bar{B}^2 B^2 - 4\bar{B}B\bar{C}C + \bar{C}^2 C^2)\,; \tag{3.17}$$

we are working to linear order in the flow, so quantities on the right are evaluated at μ_0. The flow of the metric is

$$\mu\partial_\mu g_{B\bar{B}} = \frac{1}{\pi}(\bar{B}B - \bar{C}C) = -\mu\partial_\mu g_{C\bar{C}}, \tag{3.18}$$

which is traceless. So to this linear order the $\mathcal{N} = 2$ condition $\det g = 1$ is preserved.

Component calculation

Consider first exchange of a Q_2. The relevant interaction is

$$-\left(\bar{\partial}^1\bar{Q}_2 - \frac{i}{\sqrt{2}}\bar{f}\delta^2(x_4, x_5)\right)\left(\partial^1 Q_2 + \frac{i}{\sqrt{2}}f\delta^2(x_4, x_5)\right). \tag{3.19}$$

This leads to a Feynman diagram equation of the form

$$\frac{(-i)^3}{2}f^{[n]}\bar{f}^{[m]}\delta^2\left(\sum_{i=1}^{n+m}\vec{k}_i\right)\int\frac{d^2p_\perp}{(2\pi)^2}\frac{p_\perp^2}{p_\perp^2 + p_\parallel^2} \tag{3.20}$$

for external momenta $\vec{k}_i$, transverse (to the intersection space) internal momenta $\vec{p}_\perp$, and parallel internal momenta $\vec{p}_\parallel$. The expression $f^{[n]}$ corresponds to the coefficient of some term of f with n total fields. The parallel momentum is set by total momentum on either side of the graph:

$$\vec{p}_\parallel = \sum_{i=1}^{n}\vec{k}_{fi} = -\sum_{i=1}^{m}\vec{k}_{\bar{f}i}\,. \tag{3.21}$$

If we regulate the momentum integral by a cut-off Λ and integrate, we get

$$\frac{(-i)^3}{8\pi}f^{[n]}\bar{f}^{[m]}\delta^2\left(\sum_{i=1}^{n+m}\vec{k}_i\right)\left(\Lambda^2 - p_\parallel^2\ln\left(\frac{\Lambda^2}{p_\parallel^2}\right)\right). \tag{3.22}$$

The quadratic divergence is cancelled by the explicit $|f|^2(\delta^2(x_4, x_5))^2$ term in the action. For the logarithmic term, a finite renormalization scale μ can be introduced, and then we can ignore the non-infinite piece, giving

$$-\frac{(-i)^3}{8\pi}f^{[n]}\bar{f}^{[m]}\delta^2\left(\sum_{i=1}\vec{k}_i\right)p_\parallel^2\ln\left(\frac{\Lambda^2}{\mu^2}\right). \tag{3.23}$$

Since we may write

$$p_\parallel^2 = -\left(\sum_{i=1}^{n}\vec{k}_{fi}\right)\cdot\left(\sum_{i=1}^{m}\vec{k}_{\bar{f}i}\right), \tag{3.24}$$

the diagram is proportional to all pairs of momenta, one taken from f and one from $\bar{f}$. This is equivalent to the contribution that would come from a Lagrangian term of the form

$$-\frac{1}{8\pi}\ln\left(\frac{\Lambda^2}{\mu^2}\right)\partial^\mu Z^\alpha\left(\partial_\alpha f\right)\left(\partial_{\dot\beta}\bar{f}\right)\partial_\mu\bar{Z}^{\dot\beta}\,. \tag{3.25}$$

Since the Kähler potential enters the Lagrangian as $\partial^\mu Z^\alpha\left(\partial_\alpha\partial_{\dot\beta}K\right)\partial_\mu\bar{Z}^{\dot\beta}$, we can conclude that the correction to the Kähler potential from an internal Q_2 is

$$\Delta K=\frac{|f|^2}{8\pi}\ln\left(\frac{\Lambda^2}{\mu^2}\right)\,. \tag{3.26}$$

Now we calculate the remaining contributions to the renormalization. Since Q_1 is really the gauge field, consider the contribution from it and $A_{V0,1}$ together. First rewrite the Q_1 interaction

$$-\frac{1}{4}\left(\bar\partial^1 Q_1+\partial^1\bar{Q}_1-\frac{1}{\sqrt{2}}\mathcal{P}\delta^2(x_4,x_5)\right)^2 \tag{3.27}$$

in terms of A_4 and A_5 using $Q_1=(iA_4+A_5)/\sqrt{2}$ and $\partial_1=\partial_4-i\partial_5$ to get

$$-\frac{1}{4}\left(\frac{2}{\sqrt{2}}\partial_4 A_5-\frac{2}{\sqrt{2}}\partial_5 A_4-\frac{1}{\sqrt{2}}\mathcal{P}\delta^2(x_4,x_5)\right)^2\,. \tag{3.28}$$

This leads to the usual $F_{45}^2/2$ kinetic term for the gauge field, as well as giving the interactions

$$-\frac{1}{2}\left(A_5\mathcal{P}\partial_4\delta^2(x_4,x_5)-A_4\mathcal{P}\partial_5\delta^2(x_4,x_5)\right)\,. \tag{3.29}$$

The $A_{0,1}$ couple to $(1/2)k^\alpha g_{\alpha\dot\beta}\partial_\mu\bar{Z}^{\dot\beta}=(-i/2)\partial_{\dot\beta}\mathcal{P}\partial_\mu\bar{Z}^{\dot\beta}$ and its complex conjugate, so we can now write a valid but unusual source for A_μ as

$$J^\mu=\begin{pmatrix}-\frac{i}{2}\partial_{\dot\beta}\mathcal{P}\partial^0\bar{Z}^{\dot\beta}\delta^2(x_4,x_5)+\text{c.c.}\\ -\frac{i}{2}\partial_{\dot\beta}\mathcal{P}\partial^1\bar{Z}^{\dot\beta}\delta^2(x_4,x_5)+\text{c.c.}\\ -\frac{1}{2}\mathcal{P}\partial^5\delta^2(x_4,x_5)\\ \frac{1}{2}\mathcal{P}\partial^4\delta^2(x_4,x_5)\end{pmatrix} \tag{3.30}$$

for $\mu=0,1,4,5$. We can then use the usual $-i\eta_{\mu\nu}/(p_\perp^2+p_\parallel^2)$ propagator for A_μ and calculate $J^\mu\Delta_{\mu\nu}J^\nu$. At this point, it is easier to consider the $0,1$ and $4,5$ terms separately. Starting with the $4,5$ terms together, we get a $p_\perp^2$ in momentum space from the ∂_4^2 and ∂_5^2. The

calculation is then almost identical to the previous case for Q_2. Regulate and then integrate to get

$$\frac{(-i)^3}{32\pi}\mathcal{P}^{[n]}\mathcal{P}^{[m]}\delta^2\left(\sum_{i=1}^{n+m}\vec{k}_i\right)\left(\Lambda^2 - p_\parallel^2\ln\left(\frac{\Lambda^2}{p_\parallel^2}\right)\right). \tag{3.31}$$

The quadratic piece is cancelled by $\delta^2(0)$ as expected. Introducing the RG scale in place of p, the corresponding term in the effective Lagrangian is

$$-\frac{1}{32\pi}\ln\left(\frac{\Lambda^2}{\mu^2}\right)\left(\partial_\mu Z^\alpha\partial^\mu Z^\beta\partial_\alpha\mathcal{P}\partial_\beta\mathcal{P} + 2\partial_\mu Z^\alpha\partial^\mu\bar{Z}^{\dot\beta}\partial_\alpha\mathcal{P}\partial_{\dot\beta}\mathcal{P} + \partial_\mu\bar{Z}^{\dot\alpha}\partial^\mu\bar{Z}^{\dot\beta}\partial_{\dot\alpha}\mathcal{P}\partial_{\dot\beta}\mathcal{P}\right), \tag{3.32}$$

where the extra terms have arisen since $\mathcal{P}$ is not holomorphic, unlike f. This term does not appear to preserve the Kähler structure of the metric, but we should first combine it with contribution from $A_{V0,1}$ before handling this issue.

The contribution from an internal $A_{V0,1}$ is more straightforward. The internal integral yields only a logarithmic divergence as $A_{V0,1}$ already couples to the form $\mathcal{P}\partial^\mu\bar{Z}^{\dot\beta}$. We will then get

$$-\frac{1}{32\pi}\ln\left(\frac{\Lambda^2}{\mu^2}\right)\left(\partial_\mu Z^\alpha\partial^\mu Z^\beta\partial_\alpha\mathcal{P}\partial_\beta\mathcal{P} - 2\partial_\mu Z^\alpha\partial^\mu\bar{Z}^{\dot\beta}\partial_\alpha\mathcal{P}\partial_{\dot\beta}\mathcal{P} + \partial_\mu\bar{Z}^{\dot\alpha}\partial^\mu\bar{Z}^{\dot\beta}\partial_{\dot\alpha}\mathcal{P}\partial_{\dot\beta}\mathcal{P}\right), \tag{3.33}$$

where the minus sign arises from the leading i's in the vertex. These combine to give

$$-\frac{1}{16\pi}\ln\left(\frac{\Lambda^2}{\mu^2}\right)\left(\partial_\mu Z^\alpha\partial^\mu Z^\beta\partial_\alpha\mathcal{P}\partial_\beta\mathcal{P} + \partial_\mu\bar{Z}^{\dot\alpha}\partial^\mu\bar{Z}^{\dot\beta}\partial_{\dot\alpha}\mathcal{P}\partial_{\dot\beta}\mathcal{P}\right). \tag{3.34}$$

This is still not in the form of a hermitian metric. In order to restore the Kähler form, we need to renormalize the fields as well. Make the coordinate transform $Z^\alpha \to Z^\alpha + \xi^\alpha$ with with

$$\xi^\alpha = -\frac{1}{16\pi}\ln\left(\frac{\Lambda^2}{\mu^2}\right)\mathcal{P}\partial^\alpha\mathcal{P}\,. \tag{3.35}$$

The metric transforms as

$$\begin{aligned}\delta g_{\alpha\beta} &= \nabla_\alpha\xi_\beta + \nabla_\beta\xi_\alpha\\ \delta g_{\alpha\dot\beta} &= \nabla_\alpha\bar{\xi}_{\dot\beta} + \nabla_{\dot\beta}\xi_\alpha\,,\end{aligned} \tag{3.36}$$

which corrects Equation 3.34 to give

$$\frac{1}{16\pi}\ln\left(\frac{\Lambda^2}{\mu^2}\right)\partial_\mu Z^\alpha\partial^\mu\bar{Z}^{\dot\beta}\partial_\alpha\partial_{\dot\beta}\mathcal{P}^2 \tag{3.37}$$

or

$$\Delta K = -\frac{1}{16\pi}\mathcal{P}^2 \ln\left(\frac{\Lambda^2}{\mu^2}\right) . \tag{3.38}$$

Combining the with the results from an internal Q_2 and doubling to include contributions from both branes gives the overall beta functions

$$\mu\partial_\mu K = \frac{1}{4\pi}\left(\mathcal{P}^2 - 2|f|^2\right) , \tag{3.39}$$

$$\mu\partial_\mu Z^\alpha = -\frac{i}{4\pi}k^\alpha\mathcal{P} . \tag{3.40}$$

Here we have used $\partial^\alpha\mathcal{P} = g^{\alpha\dot{\beta}}\partial_{\dot{\beta}}(ik^\gamma\partial_\gamma K) = ik^\alpha$.

The nonholomorphic renormalization of Z^α arises because of the nonlinearity of the supersymmetry transformation in Wess-Zumino gauge. In the superfield gauge used in §4.1 holomorphy is preserved.

Renormalized Gibbons-Hawking potential

With the RG flow of the Kähler potential in hand, we can ask how it affects the specific Kähler potential given by Eq. (3.35). In terms of the Gibbons-Hawking coordinates the flow is

$$\mu\frac{\partial K}{\partial\mu}\bigg|_{W,\bar{W},U,\bar{U}} = \frac{2}{\pi}(2z^2 - x^2 - y^2) . \tag{3.41}$$

It is important to be careful that the derivative is taken with the chiral fields held fixed. Then using $g_{W\bar{W}} = \partial_W\partial_{\bar{W}}K = 1/V$ and the earlier result $\partial_{W_1}z = 1/V$,

$$\mu\frac{\partial(1/V)}{\partial\mu}\bigg|_{W,\bar{W},U,\bar{U}} = \frac{1}{\pi V^2}\partial^2_{\bar{W}_1}(z^2) = \frac{2}{\pi V^3}(V - z\partial_z V) . \tag{3.42}$$

Now

$$\mu\frac{\partial}{\partial\mu}\bigg|_{W,\bar{W},U,\bar{U}} = \mu\frac{\partial}{\partial\mu}\bigg|_{x,y,z,\theta} + \mu\frac{\partial z}{\partial\mu}\bigg|_{W,\bar{W},U,\bar{U}}\frac{\partial}{\partial z} . \tag{3.43}$$

Using the earlier $z = \partial_W K/2$ gives

$$\mu\frac{\partial z}{\partial\mu}\bigg|_{W,\bar{W},U,\bar{U}} = \frac{2}{\pi}\partial_W(z^2) = \frac{2z}{\pi V} , \tag{3.44}$$

and so

$$\mu\frac{\partial V}{\partial\mu}\bigg|_{x,y,z,\theta} = \mu\frac{\partial V}{\partial\mu}\bigg|_{W,\bar{W},U,\bar{U}} - \frac{2z\partial_z V}{\pi V} = -\frac{2}{\pi} . \tag{3.45}$$

Thus the whole effect of the flow for any metric is on the constant term in the Gibbons-Hawking potential, in such a direction that it becomes more positive in the IR. This partly offsets the singularity (3.36) found previously: in combination the two give

$$V(\mu) \sim -\frac{1}{\pi} \ln \left[\alpha' \mu^2 \sqrt{x^2 + y^2} \right] . \tag{3.46}$$

One consequence is that the metric on moduli space, give by the $\mu \to 0$ limit, is positive and in fact infinite. In other words, the moduli are frozen due to IR divergences, a phenomenon encountered previously in Ref. [179]. Thus the renormalization removes one of the potentially unphysical properties of our field theory.

The metric on field space still breaks down if $x^2 + y^2$ is too large, for given μ. This suggests a simple interpretation: if we probe the resolved intersection on scales shorter than the resolution, then the effective field theory of the resolution in terms of the fields B and C breaks down and we must use the full DBI brane action. Thus the complete formulation of the intersection requires embedding in string theory.

However, if we work at finite Q_3, we would expect the fluctuations of the B, C fields to be of order $-g_{\rm YM} \ln \alpha' |Q_3|$, and the product of this with $\mu \sim |Q_3|$ can be made parametrically small. Thus it may be that there is a regime in which the effective field theory can be quantized, and S-duality studied in the field theory.

DBI action

When $z_1 z_2 \gg \alpha'$, the brane curvature is small and the DBI action should be an effective description of the system. This gives us an alternate means of calculating the moduli space metric, which should agree with that found above. Thus we insert into the DBI action the t, x-dependent

$$z_1 z_2 = -i \frac{\alpha'}{4} f(t, x) , \tag{3.47}$$

where in the field theory $f(t, x) = BC$ is a function of the intersection fields. With all other fields zero, we will assume this form in the DBI action and find the resulting effective action for $f(t, x)$.

With only metric fields turned on, the D3-brane DBI action is just

$$-\frac{T_p}{g_c}\int d^4\zeta\sqrt{|\det G_{ab}|}\,, \tag{3.48}$$

where G_{ab} is the induced metric on the brane given in the coordinates ζ^a. A convenient choice of coordinates is $\zeta^a = (t, x, w_1, w_2)$ with

$$z_1 = \sqrt{\alpha'}e^{w_1+iw_2} \qquad z_2 = i\frac{\sqrt{\alpha'}}{4}f(t,x)e^{-w_1-iw_2}\,. \tag{3.49}$$

The DBI action is then

$$S = -\frac{8\pi T_p\alpha'}{g_c}\int dt\,dx\,dw_1\left|\left[\left(e^{2w_1}+\frac{1}{16}e^{-2w_1}|f|^2\right)+\frac{\alpha'}{8}\partial_\mu f\partial^\mu\bar{f}\right]^2-\frac{\alpha'^2}{64}\left|\partial_\mu f\partial^\mu f\right|^2\right|^{1/2}, \tag{3.50}$$

with $\mu = t, x$. As expected, dependence on the phase of z_1 drops out of the metric, and the integral in the w_2 direction has been done. The remaining integral in w_1 is divergent as $w_1 \to \pm\infty$, corresponding to contributions far out on the branes in the z_1 and z_2 directions. This corresponds to an IR divergence associated with the infinite surface area of the extended D-branes, and should ultimately be f-independent. To regulate symmetrically, set a cut-off at $|z_1| = |z_2| = L$, which restricts the integral to

$$-\frac{1}{2}\ln\left(\frac{16L^2}{\alpha'|f|^2}\right) < w_1 < \frac{1}{2}\ln\left(\frac{L^2}{\alpha'}\right)\,. \tag{3.51}$$

To find the effective action we expand in derivatives. With only 8 supersymmetries, we expect the DBI action to match the gauge theories for terms with two or fewer derivatives, so expand to second order in derivatives of f, integrate out w_1, and drop terms that vanish for $L^2/\alpha' \to \infty$ to get the effective action for f:

$$S = -\frac{8\pi T_p}{g_c}\int dtdx\left\{L^2+\frac{\alpha'^2}{8}\ln\left(\frac{4L^2}{\alpha'|f|}\right)\partial_\mu f\partial^\mu\bar{f}\right\}\,. \tag{3.52}$$

The potential term is independent of f, consistent with the masslessness of the deformation modes. The cutoff L should be identified with μ^{-1}. For example, if we consider ripples of wavelength λ then $L \sim \lambda$. Noting that $f = BC = 2(x+iy)$, we see that metric for f corresponds to a Gibbons-Hawking potential

$$V(\mu) \propto \text{constant} - \ln\left[\alpha'\mu^2\sqrt{x^2+y^2}\right]\,. \tag{3.53}$$

This is precisely as found in Eq. (3.46) from the combination of classical renormalization and Gibbons-Hawking gymnastics, confirming our picture.

The DBI action gives a result that corresponds to the smearing of the Gibbons-Hawking sources into a line source, independent of the GH coordinate z. This action cannot be sensitive to z because this corresponds to a pure gauge excitation. The leading effect that would be sensitive to z would be string disk instantons: the resolution of the singularity pushes the point $z_1 = 0$ to infinity, producing a nontrivial circle which can bound a disk. The world-sheet action $\mathrm{Re}\, I \propto |z_1 z_2|/2\pi\alpha' \propto |BC|$, $\mathrm{Im}\, I = z$, is of the correct parametric form.

The full DBI action is stable, but the action (3.52) has the wrong sign for perturbations of sufficiently short wavelength. For these the higher-derivative terms must be included in order to have a stable configuration. This will result in the breakdown of the associated effective field theory, as argued in §4.3.

3.3.5 Magnetic soliton solution

Given the correct Kähler metric with the proper periodicity conditions, we should be able to solve for the magnetic soliton solution that corresponds to a D1-string connecting the two intersecting D-branes. The monopole is a half-BPS solution, so we can determine it by requiring that half the supersymmetry transformations still vanish. We need to choose a BPS state whose unbroken supersymmetry is contained within the manifest $\mathcal{N} = 1$. The $\mathcal{N} = 1$ supersymmetry algebra is the usual $\{Q_\alpha, \bar{Q}_{\dot\beta}\} = 2\sigma^\mu_{\alpha\dot\beta} P_\mu$, and so potential BPS states will have charges T-dual to $P_{2,3}$. Thus we take the D3-branes to be separated in the 2-direction, implying expectation value for $A_{V2} - A_{V'2}$. This is $SO(4)$-equivalent to the 8-direction depicted in Table 1, but has a different orientation with respect to the manifest $\mathcal{N} = 1$.

Enforcing this, and demanding a static solution gives the following first order differential

equations in x^1 for the monopole solution:

$$\begin{aligned}
\partial_1 Q_1 &= \frac{1}{\sqrt{2}}\partial_{z_1} A_{V2}\,,\\
\partial_1 Q_2 &= i\bar\partial_{z_1}\bar Q_3\,,\\
\partial_1 Q_3 &= -i\bar\partial_{z_1}\bar Q_2 - \frac{1}{\sqrt{2}}\bar f\delta^2(x_4,x_5)\,,\\
\partial_1 A_{V2} &= -\frac{\sqrt{2}}{2}\left(\bar\partial_{z_1} Q_1 + \partial_{z_1}\bar Q_1\right) + \frac{1}{2}\mathcal{P}\delta^2(x_4,x_5)\,,\\
\partial_1 Z^\alpha &= \frac{1}{\sqrt{2}} g^{\alpha\dot\beta}\partial_{\dot\beta}\bar f(\bar Q_3(0,0) - \bar S_3(0,0)) + \frac{i}{2}k^\alpha(A_{V2}(0,0) - A_{V'2}(0,0))\,,
\end{aligned} \tag{3.1}$$

with $A_{V0} = A_{V1} = A_{V3} = 0$; similar equations hold for the $3'$-$3'$ fields. These field equations contain ln(0)'s from the D3 fields evaluated at the defect. As usual, these are canceled by renormalization. For example, $A_{V2}(0,0) \sim \mathcal{P}\ln(0)$, which cancels against the field renormalization (3.40).

To get some understanding of these equations, let us change the theory by taking the coefficients of the 3-3 and $3'$-$3'$ actions to be large while holding fixed the 3-$3'$ action. The 3+1 fields are now sourceless and we can set $A_{V2} = v$ with the others vanishing. This leads to the simple differential equations

$$\partial_1 B = \frac{v}{2}B \quad \partial_1 C = -\frac{v}{2}C\,. \tag{3.2}$$

The solutions are exponentials, which appear to blow up in one direction or the other. To see that the solution is well-behaved, we must take into account the periodicity of (B,C). On the covering space, we have smooth coordinates (B_n, C_n) in the neighborhood of the pole of the Gibbons-Hawking potential at $z = 2\pi n$. The identification is $B_n = B_{n+1}/(\beta B_{n+1}C_{n+1}) = 1/\beta C_{n+1}$. The solution $B_n = e^{vx^1/2}$ thus connects smoothly onto $C_{n+1} = e^{-vx^1/2}/\beta$ at large positive x^1.

We can also write this in terms of the W, U coordinates. The BPS equation is

$$\partial_1 Z^\alpha = \frac{iv}{2}k^\alpha\,, \quad k^W = -2i\,, \quad k^U = 0\,. \tag{3.3}$$

The solution is

$$U(x) = U_0\,, \quad W = vx^1\,. \tag{3.4}$$

Noting the periodicity (3.38) of W, this describes an infinite chain of solitons, spaced in x^1 by $c\pi + \ln(4\pi^2/|U_0^2|)$. In the limit $U_0 \to 0$ the spacing becomes infinite, and we obtain a single D1.

Let us also evaluate the solition mass in this model. Defining $\partial_w = \partial_1 - i\partial_2$, the relevant term in the energy is proportional to

$$\begin{aligned} &\int dx\, g_{\alpha\dot\beta} \left\{ (\partial_w Z^\alpha + iA_w \delta_\Lambda Z^\alpha)(\partial_{\bar w} Z^{\dot\beta} - iA_{\bar w}\delta_{\bar\Lambda} Z^{\dot\beta}) + (w \leftrightarrow \bar w) \right\} \\ &= \int dx\, 2g_{\alpha\dot\beta} (\partial_w Z^\alpha + iA_w \delta_\Lambda Z^\alpha)(\partial_{\bar w} Z^{\dot\beta} - iA_{\bar w}\delta_{\bar\Lambda} Z^{\dot\beta}) + 2v\partial_1 \mathcal{P}\,. \end{aligned} \tag{3.5}$$

Thus the energy of a BPS state, for which the first term vanishes, is proportional to the magnetic charge.

We have not found a simple treatment of the actual case of dynamical D3-brane fields. However, by continuity the BPS soliton should continue to exist as the D3-brane $g_{\rm YM}$ is increased.

3.3.6 Discussion

Our study of the D3-D3 intersection has led to a number of surprises. The first is the magnetic couplings of the hypermultiplets. In one sense this has a simple origin. The hypermultiplet bosons are spinors in the ND directions, and so it is not surprising that they have magnetic dipole couplings. In a sense, a line of dipoles is like a separated monopole-antimonopole pair. (This is similar to the kink construction of fermions in bosonization, in that $\partial_\pm \phi$ produce dipoles of fermion number.) The dipole density is $\mathcal{P}$, and the monopole density is $\mathcal{P}'$. This does not seem to be a useful way to make magnetic monopoles in nature, but here when the dipole density $\mathcal{P}$ reaches a multiple of 8π, the line disappears and we are left with unconfined monopoles.

The essential role of the nonlinear hypermultiplet kinetic term and the periodicity of the hypermultiplet moduli space is the second interesting feature. Again, this is relevant only for intersections with two ND and two DN directions. With three plus one the moduli space is R^3, and with four plus zero it is R^4 (in noncompact spaces). This is for the Abelian case; we have not considered intersections of stacks of branes.

The third interesting feature is the need for classical renormalization. Our results highlight the importance of this phenomenon [76], which may be useful for understanding other brane intersections, and brane self-interactions.

The final surprising feature is the inconsistency of the intersection theory as a field theory. Note that the metric on moduli space is infinite, so the usual logarithmic exploration of the space of vacua will be absent. Nevertheless, any attempt to define this theory via a path integral will run into the regions of negative metric.

Our consideration of this system was originally motivated by the construction of top-down AdS/CM models. The magnetic source terms appeared implicitly in Refs. [49, 101], but the present interpretation was not noted. It seems unlikely that these terms have relevance for condensed matter duals; rather, they exemplify some of the rigidity of top-down constructions.

Another motivation for this work was the exploration of simple models of electric-magnetic duality. The lack of a UV completion in field theory complicates this question, but there may still be interesting questions in the effective field theory.

Chapter 4

FINITE TEMPERATURE FIELD THEORY FOR NON-RELATIVESTIC VIRAL EXPANSION

4.1 Introduction

The virial expansion allows one to express the equation of state of a non-ideal gas in a density expansion, and is equivalent to a fugacity expansion of the grand potential density at nonzero chemical potential:

$$-\frac{\beta\Omega}{V} = \beta P = \frac{2}{\lambda^3}\left[z + b_2 z^2 + b_3 z^3 + \ldots\right] \tag{4.1}$$

or $\partial\Omega/\partial\mu = -2(V/\lambda^3)\sum_n n\, b_n z^n$. Here V, P and β are the volume, pressure and inverse temperature respectively, $z = e^{\beta\mu}$ is the fugacity, and $\lambda = \sqrt{2\pi\beta/M}$ is the thermal wavelength; the b_n are dimensionless quantities directly related to the virial coefficients. The $O(z)$ contribution is independent of interactions, and therefore the ideal gas term $2/\lambda^3$ has been factored out front (we assume here a gas of spin 1/2 fermions). The thermal wavelength provides a natural length scale, and the fugacity expansion is expected to be valid when λ is short compared to the average inter-particle distance, and long compared to the range of interactions. This expansion is of current interest because of experimental focus on the properties of dilute atomic gases; and the case of fermionic atoms at a Feshbach resonance — where the two-body scattering length diverges — is of particular interest to both theorists and experimentalists. Such examples of "unitary fermions" are strongly interacting conformal systems interpolating between the BCS and BEC regimes, with universal properties that serve (on a completely different length scale) as an interesting starting point for effective field theory treatments of interacting nucleons [117,118]. There has been extensive theoretical interest in computing the parameter b_3 in the fugacity expansion for unitary fermions [31, 165], culminating in a high accuracy determination $b_3 = -0.29095295$ from a spectral study of the 3-fermion system, solving for the lowest 10,000 energy levels for three unitary fermions in a harmonic trap [134], a value that appears to agree with experimental

results [135, 147].

It would be convenient to have a method for computing the b_n coefficients directly using field theory techniques, particularly if accurate results could be obtained by computing a small set of diagrams. Despite the fact that Ω is directly related to the sum of one particle irreducible Feynman diagrams in a finite temperature field theory, the theory is not ideally suited to this task for several reasons: interparticle potentials are not in general readily described by Feynman rules; the sum of multiple interparticle interactions cannot typically be computed analytically or numerically without resorting to solving the corresponding Schrödinger or Lippman-Schwinger equation; the Feynman graphs are functions of arbitrary μ and there is no simplification gained by the expansion in z.

In this Letter we devise a graphical expansion that circumvents these difficulties, and demonstrate its utility by performing analytic calculations of b_3 for unitary fermions; it has some features in common with the approach of refs. [31, 165]. The calculation is mostly analytical, with some integrals performed numerically, and we will show that an extremely accurate determination of b_3 can be obtained. The two components of our general procedure are (i) to perform the "dual" of the Matsubara sum over discrete frequencies — in the sense of a Poisson resummation — which directly leads to a fugacity expansion; (ii) to use a dimer field as in [111], which is designed to reproduce the continuum 2-body phaseshift, thereby bypassing discussion of potentials and leading to purely local interactions in space. We consider these two innovations in turn, first addressing the case of free fermions, then including two-body interactions.

4.2 Chronographs

We consider a dilute gas comprised of a single species of nonrelativistic spin half fermion; generalization to bosons or more species is straight forward, but we have not considered the relativistic case. In the Euclidian time formulation of finite temperature field theory, Ω is given by sum of 1PI vacuum Feynman diagrams, where the theory is analyzed for Euclidian time τ compactified with period β and antiperiodic (periodic) boundary conditions imposed for fermions (bosons). For a free spin $\frac{1}{2}$ fermion, Ω is given by the one loop diagram on the

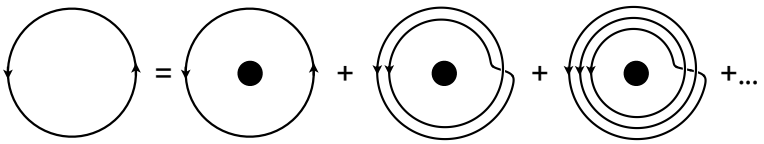

Figure 4.1: The free fermion contribution to Ω. The conventional finite temperature Feynman diagram on the left is expanded as a sum over worldline loops about the compact time direction ("chronographs") with winding number ν making a contribution proportional to z^ν. The black dot indicates the nontrivial topology, and Euclidian time increases in the counterclockwise direction.

left in Fig. 4.1. It is convenient instead to compute $\partial\Omega/\partial\mu$ with the result

$$\frac{\partial\Omega}{\partial\mu} = -\frac{1}{\beta}\mathrm{Tr}\, G_0^E = -\frac{2V}{\beta}\int\frac{d^3\mathbf{p}}{(2\pi)^3}\sum_n \widetilde{G}_0^E(\omega_n,\mathbf{p}) \tag{4.2}$$

where $\widetilde{G}_0^E(\omega,\mathbf{p}) = e^{i\omega\,0^+}/(i\omega-(\varepsilon_{\mathbf{p}}-\mu))$ is the free Euclidian propagator, $\varepsilon_{\mathbf{p}} = \mathbf{p}^2/2M$, and $\omega_n = 2\pi(n+\frac{1}{2})/\beta$; the factor of 2 is from the two spin states, and the minus sign from the fermion loop. The frequency sum is trivial to compute and the result can be subsequently expanded in powers of the fugacity, but it is interesting to note that a Poisson resummation yields the fugacity expansion directly (see also appendix B of Ref. [37]):

$$\begin{aligned}\frac{1}{\beta}\sum_n \widetilde{G}_0^E(\omega_n,\mathbf{p}) &= \sum_\nu (-1)^\nu G_0^E(\nu\beta,\mathbf{p}) \\ &= \sum_{\nu=1}^{\infty}(-1)^{(\nu+1)} z^\nu e^{-\nu\beta\varepsilon_{\mathbf{p}}}\end{aligned} \tag{4.3}$$

where $G_0^E(\tau,\mathbf{p}) = -\theta(\tau-0^+)e^{-\tau(\varepsilon_{\mathbf{p}}-\mu)}$ is the Fourier transform of $\widetilde{G}_0^E(\omega,\mathbf{p})$. The Poisson formula exchanges the sum over Matsubara frequencies for a sum over the winding number ν of worldlines wrapping around the compact time direction, each term proportional to z^ν, as shown graphically in Fig. 4.1. We therefore immediately read off the b_n coefficients for a free fermion:

$$b_n^{(1)} = (-1)^{n+1}\frac{\lambda^3}{n}\int\frac{d^3\mathbf{p}}{(2\pi)^3}\,e^{-n\beta\varepsilon_{\mathbf{p}}} = \frac{(-1)^{n+1}}{n^{5/2}}\ . \tag{4.4}$$

Note this result includes both the (-1) from the Feynman graph, as well as a factor of $(-1)^\nu$ from fermion worldline loops due to antiperiodic boundary conditions.

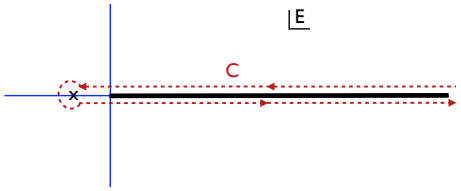

Figure 4.2: The contour C in eq. (4.5) is designed to pick up contributions from all cuts and poles along the real energy axis.

We will refer to the diagrams on the right in Fig. 4.1 as "chronographs", which allow one to compute directly the n^{th} term in the fugacity expansion of Ω or $\partial\Omega/\partial\mu$. The rules for chronographs can be easily generalized for computing the fugacity expansion in interacting systems: (i) Chronograph propagators $\mathcal{G}(\tau, \mathbf{p})$ can be defined in terms for the Minkowski propagator $\widetilde{G}^M(E, \mathbf{p}) = i/(E - \varepsilon_{\mathbf{p}} + i\epsilon)$ at $\mu = 0$ via the contour integral along the path C shown in Fig 4.2, which simply picks up all the physical poles and cuts:

$$\mathcal{G}(\tau, \mathbf{p}) \equiv \theta(\tau - 0^+) \int_C \frac{dE}{2\pi}\, e^{-E\tau} \widetilde{G}^M(E, \mathbf{p}) \tag{4.5}$$

$\mathcal{G}$ should be thought of as a multi-valued function of τ living on a compact manifold of circumference β. For a free fermion, $\mathcal{G}_0(\tau, \mathbf{p}) = -\theta(\tau) e^{-\tau\varepsilon_{\mathbf{p}}}$; (ii) vertices (from the Euclidian action) are located on the circle at Euclidian time τ_i, each with a 3-momentum conserving δ-function; (iii) one integrates over all vertex positions τ and all propagator 3-momenta $\mathbf{p}$; (iv) a factor of $(-1)^{\nu_F}$ is included where ν_F is the winding number carried by fermions in the diagram, with an additional (-1) for each closed fermion loop in the parent Feynman diagram; (v) symmetry factors are computed as in Feynman diagrams, with the caveat that two propagators connecting the same two vertices do not warrant a symmetry factor when their length differs by $n\beta$; (vi) the winding number about compact Euclidian time, weighted by particle charge, is the order of the graph; all graphs of order p are included in a fugacity expansion to order z^p. For example, a dimer loop with $\nu = 1$ contributes to order z^2 since the dimer has particle number 2.

4.3 Interactions and b_2

To include 2-particle interactions it is convenient to represent the interaction not in terms of a potential, but by s-channel dimer exchange, a technique introduced in [111]. The advantage is that the dimer — with a dispersion relation constructed to exactly reproduce the two particle phase shift δ — has a separable contact interaction with the fermions. This phase shift is assumed to be given, either directly from scattering data, or previously calculated from a potential model. That one can take this simplifying approach is due to the fact that the virial coefficients depend on interactions only through the S-matrix [52].

We focus on the case of s-wave scattering, commenting below on its generalization to other partial waves. Consider the Minkowski spacetime Lagrangian

$$\mathcal{L} = \psi^\dagger(i\partial_t + \nabla^2/2M)\psi + \phi^\dagger K\phi + \tfrac{1}{2}\phi^\dagger\psi^T\sigma_2\psi + \text{h.c.} \tag{4.6}$$

where K is a function of the Galilean invariant operator $D = (i\partial_t + \nabla^2/4M)$. It is important to recognize that this is *not* a conventional effective field theory (EFT); in an EFT, one would perform a low energy expansion and express K as a polynomial in D, as was done to subleading order in [111] and to leading order in [31]; such an expansion of K in powers of D corresponds directly to the effective range expansion of $p\cot\delta(p)$. However, here we consider K to be a more general function of D (e.g, nonlocal) chosen so that the full dimer Green's function given by the sum in Fig. 4.3 results in the exact 2-fermion scattering amplitude:

$$\widetilde{G}^M_\phi(E,\mathbf{P}) \;=\; \frac{4\pi}{M}\frac{-i}{k\cot\delta(k)+\sqrt{-k^2}}\ , \tag{4.7}$$

where $k^2 = [M(E+2\mu) - \mathbf{P}^2/4 + i\epsilon]$, E and $\mathbf{P}$ being the total energy and momentum of the fermion pair. In Fig. 4.3 the geometric sum of loop diagrams creates the correct 2-fermion cut appearing as the $\sqrt{-k^2}$ term in the amplitude; the loops are linearly divergent, and the divergence is absorbed into a constant counterterm in K, so that the renormalized operator is $K_R = K - \text{const.}$ (see, for example [117, 118]). This theory is valid beyond the radius of convergence of the effective range expansion, up to energies where inelastic processes set in, such as pion production in the case where the fermions are nucleons.

The chronographs in this theory for $b_{1,2,3}$ are shown in Fig. 4.4. The second coefficient b_2 gets the contribution $b_2^{(1)} = -1/4\sqrt{2}$ computed in eq. (4.4) from free fermions, as well as

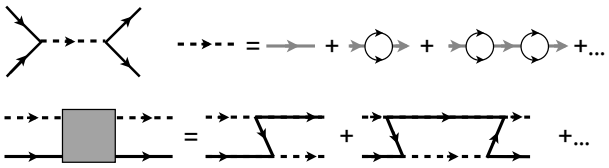

Figure 4.3: Feynman graphs for dimer mediated two-body scattering, and the integral equation relevant for three-body scattering (dashed line = fully dressed dimer, solid line = fermion; gray = K^{-1}).

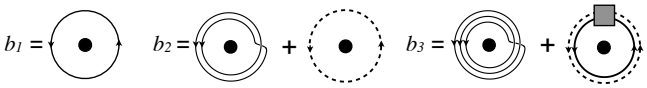

Figure 4.4: Chronograph expansion for the virial coefficients b_n. Dashed line: fully dressed dimer propagator, shaded box: summed three-body interaction from Fig. 4.3. For b_3, bosons or multiple fermion species would require introduction of a trimer field as well.

the dimer contribution computed from $\partial\Omega/\partial\mu$:

$$b_2^{(2)} = \frac{\lambda^3}{4}\int \frac{d^3\mathbf{P}}{(2\pi)^3}\int_C \frac{dE}{2\pi} e^{-\beta E}\widetilde{G}_\phi^M \frac{\partial (i\widetilde{G}_\phi^M)^{-1}}{\partial\mu}\bigg|_{\mu=0} \tag{4.8}$$

where $\widetilde{G}_\phi^M$ and k are given in eq. (4.7). The contour integration picks up contributions both from poles and from the cut along the positive real E axis from $\sqrt{-k^2}$ in eq. (4.7). If the theory has bound states with binding energy ε_n, then $\widetilde{G}_\phi^M$ has poles at $E_n \equiv (\epsilon_n + \mathbf{P}^2/4M - 2\mu)$ and the integrand in brackets has poles at $E = E_n$ with residue 2. To compute the contribution from the cut, one substitutes eq. (4.7) for $\widetilde{G}_\phi^M$ accounting for $\sqrt{-k^2}$ flipping sign across the cut. Combining the cut and pole contributions and performing the $\mathbf{P}$ integration we immediately recover the well-known result [35, 151]

$$b_2^{(2)} = \sqrt{2}\left[\sum_n e^{-\beta\epsilon_n} + \frac{1}{\pi}\int_0^\infty dk\, \frac{d\delta(k)}{dk} e^{-\beta\frac{k^2}{M}}\right] . \tag{4.9}$$

This analysis can be extended to other partial waves by introducing new dimer fields with appropriate couplings to fermions.

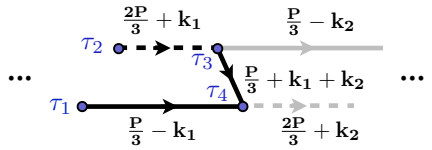

Figure 4.5: The three propagator subgraph (in black) contributing to b_3 and corresponding to the expression L appearing in eqs. (4.10,4.11).

4.4 Computing b_3

At third order we need to compute the new chronographs for Ω shown in Fig. 4.4, the first graph yielding the free fermion contribution, $b_3^{(1)} = 1/9\sqrt{3}$ as computed in eq. (4.4). The second graph for $b_3^{(3)}$ sums all dimer-fermion and three fermion interactions, barring additional three-body forces; for a single species of fermion renormalizability does not require three-body forces and we shall ignore them here; however, in principle a trimer could be introduced to generate fundamental three-body forces. This diagram can be expressed in a loop expansion as

$$b_3^{(3)} = \lambda^3 \sum_n \mathrm{Tr}\, \frac{L^n}{n} \tag{4.10}$$

where L corresponds to the subdiagram in Fig. 4.5 with

$$\begin{aligned} L_{12\mathbf{k}_1,34\mathbf{k}_2} &= \mathcal{G}_0(\tau_4-\tau_1, \mathbf{P}/3-\mathbf{k}_1) \\ &\times \mathcal{D}(\tau_3-\tau_2, 2\mathbf{P}/3+\mathbf{k}_1)\mathcal{G}_0(\tau_4-\tau_3, \mathbf{P}/3+\mathbf{k}_1+\mathbf{k}_2)\ , \end{aligned} \tag{4.11}$$

$\mathcal{G}_0$ being the fermion chronograph propagator and $\mathcal{D}$ being the dimer propagator computed from eqs. (4.5,4.7), and we include a symmetry factor of $1/n$, a spin factor of $\mathrm{Tr}\,\sigma_2^{2n} = 2$ from the vertices and a factor of (-1) due to $\nu_F = 3$; there is no overall fermion sign from the parent Feynman diagram. In this expression, a product of L's corresponds to the integral

$$L^2_{12\mathbf{k}_1,56\mathbf{k}_2} = \int_0^\beta d\tau_3 d\tau_4 \int \frac{d^3\mathbf{q}}{(2\pi)^3}\, L_{12\mathbf{k}_1,34\mathbf{q}} L_{34\mathbf{q},56\mathbf{k}_2} \tag{4.12}$$

with an integral over the center of mass momentum $\mathbf{P}$ implied in the trace; this $\mathbf{P}$ integral is gaussian and contributes a factor of $(3\sqrt{3}/\lambda^3)$. Then the n^{th} term in eq. (4.10) corresponds to the $(n+1)$-loop contribution to the last diagram in Fig. 4.4.

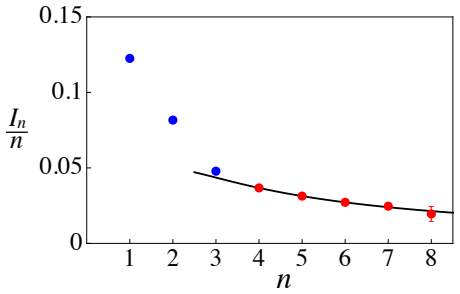

Figure 4.6: Results for I_n/n, including error estimate from numerical integration for $n = 3, \ldots, 8$. The solid line is the large-n fit to the last five data points by the function $(c_0/n + c_1/n^2)$, as described in the text.

At this point in order to be concrete we will narrow our focus to computing $b_3^{(3)}$ for unitary fermions, for which $p \cot \delta = 0$ identically. From eqs. (4.5,4.7) we find the dimer propagator $\mathcal{D}(\tau, \mathbf{q}) = -\theta(\tau)\sqrt{16\pi/M^3}\, e^{-\tau \mathbf{q}^2/4M}/\sqrt{\tau}$. In this case the expansion takes the form

$$b_3^{(3)} = 3^{3/2} \sum_{n=1}^{\infty} \frac{(-1)^n I_n}{n} \tag{4.13}$$

where I_n is given by the integral

$$\begin{aligned} &(16\pi)^{n/2} \int_{\mathcal{T}} \prod_{i=1}^{n} \frac{d\tau_{2i-1} d\tau_{2i}}{\sqrt{\tau_{2i+1} - \tau_{2i}}} \int \prod_{j=1}^{n} \frac{d^3\mathbf{k}_j}{(2\pi)^3} e^{-\mathbf{k}_a \cdot A_{ab} \mathbf{k}_b} \\ &= (2\pi)^{-n} \int_{\mathcal{T}} \prod_{i=1}^{n} \frac{d\tau_{2i-1} d\tau_{2i}}{\sqrt{\tau_{2i+1} - \tau_{2i}}} \, (\det A)^{-\frac{3}{2}} \end{aligned} \tag{4.14}$$

which is positive and independent of β and M, A being the $n \times n$ matrix

$$\begin{aligned} A_{ab} = \delta_{ab} &\frac{4\tau_{2a+2} - \tau_{2a+1} + \tau_{2a} - 4\tau_{2a-1}}{4} \\ &+ \left(\hat{\delta}_{a,b+1} \frac{\tau_{2a} - \tau_{2a-1}}{2} + a \leftrightarrow b \right) \end{aligned} \tag{4.15}$$

with $\hat{\delta}_{ab}$ is the Kronecker δ-function with indices defined modulo n, so that $\hat{\delta}_{n+a,b} = \hat{\delta}_{a,n+b} = \delta_{ab}$ for $1 \le a, b \le n$, and $\int_{\mathcal{T}}$ represents a $2n$-dimensional time ordered integral over τ_i with $0 \le \tau_1 \le \tau_2 < \ldots < \tau_{2n} \le 1$ and $\tau_{2n+j} \equiv 1 + \tau_j$ for $j = 1, 2$.

The integral I_n can be performed analytically for $n = 1, 2$ with the result $I_1 = 2/(3\sqrt{3}\pi)$, $I_2 = 8/(9\sqrt{3}\pi)$; for $n = 3, \ldots, 8$ we have computed the integrals numerically. We find that I_n

is apparently a smooth function of n for large n and we perform a large-n extrapolation, fitting our results for $n = 4, \ldots, 8$ to the function $I_n \sim (c_0 + c_1/n)$ finding $c_0 = 0.1955 \pm 0.0011$, $c_1 = -0.1943 \pm 0.0044$ (with highly correlated errors); the results are shown in Fig. 4.6. We estimate our errors by also fitting to the function $(c_0 + c_1/n + c_2/n^2)$, and varying the range of points used in the fit, finding a very stable result. Our final result for the interacting contribution to b_3 is $b_3^{(3)} = -0.3573 \pm 0.0005$, or for the full answer, $b_3 = -0.29315 \pm 0.0005$, to be compared with the recent computation $b_3 = -0.29095295$ by Liu, Hu and Drummond [134], which involved summing over energy levels for three unitary fermions in a harmonic trap [177]. It is remarkable that an expansion and extrapolation of chronographs is able to arrive at such a precise number for what is essentially a nonperturbative system; however, we do not have an explanation for why our procedure leads to an estimated error for b_3 (± 0.0005) which is significantly smaller than our discrepancy with Liu et al. (0.0021).

To our knowledge, this is the first time b_3 was calculated by analytical means for a strongly interacting system, and it suggests that the graphical techniques presented here for the virial expansion may prove powerful for applications to other systems as well.

Chapter 5

CONCLUSION

Modern quantum field theory has been a very useful tool to many subfields of theoretical physics: condensed matter, atomic, nuclear, particle and string theory. In this thesis, I present the work on a few related topics, some of them have experiments behind them while some do not. It is in the very nature of physics to always have experiment to motivate the theory, however sometimes the theory is way in front of experiments.

The recent running of LHC has discovered Higgs boson, and measured most of its decay channels. It opens a door toward higher energies, and severely raises the question of Naturalness of quantum field theory. There is no concrete discovery beyond the standard model so far, albeit most of the theory have predicted new physics at current energy scale. This is a very interesting time for high energy physics. Theories like supersymmetry and Little Higgs, face great challenges in the coming couple of years, with LHC probing the TeV physics.

The model Little Flavor I presented in chapter 2 is an attempt to alleviate the Naturalness problem while giving a testable flavor theory framework. It is all about TeV physics, has the relevant energy scale for LHC and possible next generation machine ILC.

String theory has been a rich resource for theoretical physics and mathematics. The top-down approach is very elegant but hard to test in experiments. However it leads to many surprising results and deepens our understanding of nature. Among all that, the AdS/CFT correspondence is one of the most dramatic results, which also renewed the interest in condensed matter physics among particle theorists. The active field of topological insulator/order in condensed matter these days also finds its deep connection to the long-developed topological field theory. The studies of supersymmetric gauge theory have made an impact on the field of mathematics.

The three topics about D-branes and monopoles in this thesis are in the string/particle

theory interface, and may have implication for broader fields.

BIBLIOGRAPHY

[1] Georges Aad et al. ATLAS search for a heavy gauge boson decaying to a charged lepton and a neutrino in *pp* collisions at $\sqrt{s} = 7$ TeV. *Eur.Phys.J.*, C72:2241, 2012.

[2] Georges Aad et al. Search for high-mass resonances decaying to dilepton final states in pp collisions at s**(1/2) = 7-TeV with the ATLAS detector. *JHEP*, 1211:138, 2012.

[3] Georges Aad et al. A search for $t\bar{t}$ resonances in the lepton plus jets final state with ATLAS using 4.7 fb^{-1} of *pp* collisions at $\sqrt{s} = 7$ TeV. 2013.

[4] Georges Aad et al. Search for resonances decaying into top-quark pairs using fully hadronic decays in *pp* collisions with ATLAS at $\sqrt{s} = 7$ TeV. *JHEP*, 1301:116, 2013.

[5] Georges Aad et al. Search for resonant diboson production in the $WW/WZ \to l\nu jj$ decay channels with the ATLAS detector at $\sqrt{s} = 7$ TeV. 2013.

[6] Kaustubh Agashe and Roberto Contino. The Minimal composite Higgs model and electroweak precision tests. *Nucl.Phys.*, B742:59–85, 2006.

[7] S. Aguilar and D. Singleton. Fermion generations, masses, and mixings in a 6D brane model. *PRD*, 73(8):085007, April 2006.

[8] Silvestre Aguilar and Douglas Singleton. Fermion generations, masses and mixings in a 6D brane model. *Phys. Rev.*, D73:085007, 2006.

[9] Guido Altarelli and Ferruccio Feruglio. Discrete Flavor Symmetries and Models of Neutrino Mixing. *Rev.Mod.Phys.*, 82:2701–2729, 2010. * Temporary entry *.

[10] Martin Ammon, Johanna Erdmenger, Matthias Kaminski, and Patrick Kerner. Flavor Superconductivity from Gauge/Gravity Duality. *JHEP*, 0910:067, 2009.

[11] F. P. An, J. Z. Bai, A. B. Balantekin, H. R. Band, D. Beavis, W. Beriguete, M. Bishai, S. Blyth, K. Boddy, R. L. Brown, and et al. Observation of Electron-Antineutrino Disappearance at Daya Bay. *Physical Review Letters*, 108(17):171803, April 2012.

[12] F.P. An et al. Observation of electron-antineutrino disappearance at Daya Bay. 2012.

[13] F.P. An et al. Observation of electron-antineutrino disappearance at Daya Bay. 2012.

[14] N. Arkani-Hamed, A. G. Cohen, and H. Georgi. (De)Constructing Dimensions. *Physical Review Letters*, 86:4757–4761, May 2001.

[15] N. Arkani-Hamed, A. G. Cohen, and H. Georgi. Electroweak symmetry breaking from dimensional deconstruction. *Physics Letters B*, 513:232–240, July 2001.

[16] N. Arkani-Hamed, A.G. Cohen, E. Katz, and A.E. Nelson. The Littlest Higgs. *JHEP*, 0207:034, 2002.

[17] N. Arkani-Hamed, A.G. Cohen, E. Katz, A.E. Nelson, T. Gregoire, et al. The Minimal Moose for a Little Higgs. *JHEP*, 0208:021, 2002.

[18] N. Arkani-Hamed, T. Gregoire, and J. Wacker. Higher dimensional supersymmetry in 4D superspace. *Journal of High Energy Physics*, 3:55, March 2002.

[19] Nima Arkani-Hamed, Andrew G. Cohen, and Howard Georgi. (De)constructing dimensions. *Phys.Rev.Lett.*, 86:4757–4761, 2001.

[20] Nima Arkani-Hamed, Andrew G. Cohen, and Howard Georgi. Electroweak Symmetry Breaking from Dimensional Deconstruction. *Phys.Lett.*, B513:232–240, 2001.

[21] Nima Arkani-Hamed, Andrew G. Cohen, David B. Kaplan, Andreas Karch, and Lubos Motl. Deconstructing (2,0) and little string theories. *JHEP*, 0301:083, 2003.

[22] Nima Arkani-Hamed, Lawrence J. Hall, David Tucker-Smith, and Neal Weiner. Flavor at the TeV scale with extra dimensions. *Phys.Rev.*, D61:116003, 2000.

[23] Nima Arkani-Hamed, Massimo Porrati, and Lisa Randall. Holography and phenomenology. *JHEP*, 0108:017, 2001.

[24] Tatsuo Azeyanagi, Wei Li, and Tadashi Takayanagi. On String Theory Duals of Lifshitz-like Fixed Points. *JHEP*, 0906:084, 2009.

[25] Riccardo Barbieri, Dario Buttazzo, Filippo Sala, David M. Straub, and Andrea Tesi. A 125 GeV composite Higgs boson versus flavour and electroweak precision tests. 2012.

[26] C. Beasley, J. J. Heckman, and C. Vafa. GUTs and exceptional branes in F-theory I. *Journal of High Energy Physics*, 1:58, January 2009.

[27] C. Beasley, J. J. Heckman, and C. Vafa. GUTs and exceptional branes in F-theory II. Experimental predictions. *Journal of High Energy Physics*, 1:59, January 2009.

[28] Chris Beasley, Jonathan J. Heckman, and Cumrun Vafa. GUTs and Exceptional Branes in F-theory - I. *JHEP*, 01:058, 2009.

[29] Chris Beasley, Jonathan J. Heckman, and Cumrun Vafa. GUTs and Exceptional Branes in F-theory - II: Experimental Predictions. *JHEP*, 01:059, 2009.

[30] Paulo F. Bedaque, H. W. Hammer, and U. van Kolck. Renormalization of the three-body system with short-range interactions. *Phys. Rev. Lett.*, 82:463–467, 1999.

[31] Paulo F. Bedaque and Gautam Rupak. Dilute resonating gases and the third virial coefficient. *Phys.Rev.*, B67:174513, 2003.

[32] Paulo F. Bedaque and Ubirajara van Kolck. Effective field theory for few-nucleon systems. *Ann. Rev. Nucl. Part. Sci.*, 52:339–396, 2002.

[33] Oren Bergman, Niko Jokela, Gilad Lifschytz, and Matthew Lippert. Quantum Hall Effect in a Holographic Model. *JHEP*, 1010:063, 2010.

[34] J. Beringer, J. F. Arguin, R. M. Barnett, K. Copic, O. Dahl, D. E. Groom, C. J. Lin, J. Lys, H. Murayama, C. G. Wohl, W. M. Yao, P. A. Zyla, C. Amsler, M. Antonelli, D. M. Asner, H. Baer, H. R. Band, T. Basaglia, C. W. Bauer, J. J. Beatty, V. I. Belousov, E. Bergren, G. Bernardi, W. Bertl, S. Bethke, H. Bichsel, O. Biebel, E. Blucher, S. Blusk, G. Brooijmans, O. Buchmueller, R. N. Cahn, M. Carena, A. Ceccucci, D. Chakraborty, M. C. Chen, R. S. Chivukula, G. Cowan, G. D'Ambrosio, T. Damour, D. de Florian, A. de Gouvêa, T. DeGrand, P. de Jong, G. Dissertori, B. Dobrescu, M. Doser, M. Drees, D. A. Edwards, S. Eidelman, J. Erler, V. V. Ezhela, W. Fetscher, B. D. Fields, B. Foster, T. K. Gaisser, L. Garren, H. J. Gerber, G. Gerbier, T. Gherghetta, S. Golwala, M. Goodman, C. Grab, A. V. Gritsan, J. F. Grivaz, M. Grünewald, A. Gurtu, T. Gutsche, H. E. Haber, K. Hagiwara, C. Hagmann, C. Hanhart, S. Hashimoto, K. G. Hayes, M. Heffner, B. Heltsley, J. J. Hernández-Rey, K. Hikasa, A. Höcker, J. Holder, A. Holtkamp, J. Huston, J. D. Jackson, K. F. Johnson, T. Junk, D. Karlen, D. Kirkby, S. R. Klein, E. Klempt, R. V. Kowalewski, F. Krauss, M. Kreps, B. Krusche, Yu. V. Kuyanov, Y. Kwon, O. Lahav, J. Laiho, P. Langacker, A. Liddle, Z. Ligeti, T. M. Liss, L. Littenberg, K. S. Lugovsky, S. B. Lugovsky, T. Mannel, A. V. Manohar, W. J. Marciano, A. D. Martin, A. Masoni, J. Matthews, D. Milstead, R. Miquel, K. Mönig, F. Moortgat, K. Nakamura, M. Narain, P. Nason, S. Navas, M. Neubert, P. Nevski, Y. Nir, K. A. Olive, L. Pape, J. Parsons, C. Patrignani, J. A. Peacock, S. T. Petcov, A. Piepke, A. Pomarol, G. Punzi, A. Quadt, S. Raby, G. Raffelt, B. N. Ratcliff, P. Richardson, S. Roesler, S. Rolli, A. Romaniouk, L. J. Rosenberg, J. L. Rosner, C. T. Sachrajda, Y. Sakai, G. P. Salam, S. Sarkar, F. Sauli, O. Schneider, K. Scholberg, D. Scott, W. G. Seligman, M. H. Shaevitz, S. R. Sharpe, M. Silari, T. Sjöstrand, P. Skands, J. G. Smith, G. F. Smoot, S. Spanier, H. Spieler, A. Stahl, T. Stanev, S. L. Stone, T. Sumiyoshi, M. J. Syphers, F. Takahashi, M. Tanabashi, J. Terning, M. Titov, N. P. Tkachenko,

N. A. Törnqvist, D. Tovey, G. Valencia, K. van Bibber, G. Venanzoni, M. G. Vincter, P. Vogel, A. Vogt, W. Walkowiak, C. W. Walter, D. R. Ward, T. Watari, G. Weiglein, E. J. Weinberg, L. R. Wiencke, L. Wolfenstein, J. Womersley, C. L. Woody, R. L. Workman, A. Yamamoto, G. P. Zeller, O. V. Zenin, J. Zhang, R. Y. Zhu, G. Harper, V. S. Lugovsky, and P. Schaffner. Review of particle physics. *Phys. Rev. D*, 86:010001, Jul 2012.

[35] E. Beth and G. Uhlenbeck. The quantum theory of the non-ideal gas. II. Behaviour at low temperatures. *Physica*, 4:915–924, 1937.

[36] R. A. Brandt, F. Neri, and D. Zwanziger. Lorentz invariance from classical particle paths in quantum field theory of electric and magnetic charge. *PRD*, 19:1153–1167, February 1979.

[37] Lowell S. Brown and Laurence G. Yaffe. Effective field theory for quasiclassical plasmas. *Phys.Rept.*, 340:1–164, 2001.

[38] C. G. Callan and J. A. Harvey. Anomalies and fermion zero modes on strings and domain walls. *Nuclear Physics B*, 250:427–436, 1985.

[39] Serguei Chatrchyan et al. Search for exotic resonances decaying into WZ/ZZ in pp collisions at $\sqrt{s} = 7$ TeV. *JHEP*, 1302:036, 2013.

[40] Serguei Chatrchyan et al. Search for heavy narrow dilepton resonances in pp collisions at $\sqrt{s} = 7$ TeV and $\sqrt{s} = 8$ TeV. *Phys.Lett.*, B720:63–82, 2013.

[41] Serguei Chatrchyan et al. Search for narrow resonances using the dijet mass spectrum in pp collisions at sqrt(s) = 8 TeV. 2013.

[42] Serguei Chatrchyan et al. Search for new physics in final states with a lepton and missing transverse energy in pp collisions at the LHC. *Phys. Rev. D*, 87:072005, 2013.

[43] R. Sekhar Chivukula and Howard Georgi. Composite Technicolor Standard Model. *Phys.Lett.*, B188:99, 1987.

[44] A. G. Cohen, D. B. Kaplan, and A. E. Nelson. Progress in electroweak baryogenesis. *Ann.Rev.Nucl.Part.Sci.*, 43:27–70, 1993.

[45] A. G. Cohen, D. B. Kaplan, and A. E. Nelson. Progress in electroweak baryogenesis. *Annual Review of Nuclear and Particle Science*, 43:27–70, 1993.

[46] Andrew G. Cohen, David B. Kaplan, and Ann E. Nelson. Counting 4 pis in strongly coupled supersymmetry. *Phys.Lett.*, B412:301–308, 1997.

[47] Andrew G. Cohen, D.B. Kaplan, and A.E. Nelson. The More minimal supersymmetric standard model. *Phys.Lett.*, B388:588–598, 1996.

[48] CMS Collaboration. Search for high-mass resonances decaying to top quark pairs in the lepton+jets channel. *CERN Report No. CMS-PAS-EXO-11-093*, 2012.

[49] N. R. Constable, J. Erdmenger, Z. Guralnik, and I. Kirsch. Intersecting D3-branes and holography. *PRD*, 68(10):106007, November 2003.

[50] Roberto Contino, Thomas Kramer, Minho Son, and Raman Sundrum. Warped/composite phenomenology simplified. *JHEP*, 0705:074, 2007.

[51] Csaba Csaki, Witold Skiba, and Martin Schmaltz. Exact results and duality for SP(2N) SUSY gauge theories with an antisymmetric tensor. *Nucl.Phys.*, B487:128–140, 1997.

[52] Roger Dashen, Shang-Keng Ma, and Herbert J. Bernstein. S Matrix formulation of statistical mechanics. *Phys.Rev.*, 187:345–370, 1969.

[53] Joshua L. Davis, Per Kraus, and Akhil Shah. Gravity Dual of a Quantum Hall Plateau Transition. *JHEP*, 0811:020, 2008.

[54] O. Dewolfe, D. Z. Freedman, and H. Ooguri. Holography and defect conformal field theories. *PRD*, 66(2):025009, July 2002.

[55] L. Dixon, J. A. Harvey, C. Vafa, and E. Witten. Strings on orbifolds. *Nuclear Physics B*, 261:678–686, 1985.

[56] Lance J. Dixon, Jeffrey A. Harvey, C. Vafa, and Edward Witten. Strings on Orbifolds. *Nucl.Phys.*, B261:678–686, 1985.

[57] Lance J. Dixon, Jeffrey A. Harvey, C. Vafa, and Edward Witten. Strings on Orbifolds. 2. *Nucl.Phys.*, B274:285–314, 1986.

[58] Michael J. Dugan, Howard Georgi, and David B. Kaplan. Anatomy of a Composite Higgs Model. *Nucl.Phys.*, B254:299, 1985.

[59] Johanna Erdmenger, Matthias Kaminski, and Felix Rust. Holographic vector mesons from spectral functions at finite baryon or isospin density. *Phys.Rev.*, D77:046005, 2008.

[60] Guido Festuccia and Hong Liu. Excursions beyond the horizon: Black hole singularities in Yang-Mills theories. I. *JHEP*, 0604:044, 2006.

[61] A. L. Fitzpatrick, G. Perez, and L. Randall. Flavor Anarchy in a Randall-Sundrum Model with 5D Minimal Flavor Violation and a Low Kaluza-Klein Scale. *Physical Review Letters*, 100(17):171604, May 2008.

[62] A. Liam Fitzpatrick, Gilad Perez, and Lisa Randall. Flavor from Minimal Flavor Violationa Viable Randall- Sundrum Model. 2007.

[63] G. L. Fogli, E. Lisi, A. Marrone, A. Palazzo, and A. M. Rotunno. Evidence of theta13 from global neutrino data analysis. *PRD*, 84(5):053007, September 2011.

[64] G.L. Fogli, E. Lisi, A. Marrone, A. Palazzo, and A.M. Rotunno. Evidence of theta13 from global neutrino data analysis. *Phys.Rev.*, D84:053007, 2011.

[65] M. Freedman, M. B. Hastings, C. Nayak, X.-L. Qi, K. Walker, and Z. Wang. Projective ribbon permutation statistics: A remnant of non-Abelian braiding in higher dimensions. *PRD*, 83(11):115132–+, March 2011.

[66] C. D. Froggatt and H. B. Nielsen. Hierarchy of quark masses, cabibbo angles and CP violation. *Nuclear Physics B*, 147:277–298, January 1979.

[67] C.D. Froggatt and Holger Bech Nielsen. Hierarchy of Quark Masses, Cabibbo Angles and CP Violation. *Nucl.Phys.*, B147:277, 1979.

[68] Howard Georgi and David B. Kaplan. Composite Higgs and Custodial SU(2). *Phys.Lett.*, B145:216, 1984.

[69] Howard Georgi, David B. Kaplan, and Peter Galison. CALCULATION OF THE COMPOSITE HIGGS MASS. *Phys.Lett.*, B143:152, 1984.

[70] T. Gherghetta and A. Pomarol. Bulk fields and supersymmetry in a slice of AdS. *Nuclear Physics B*, 586:141–162, October 2000.

[71] Tony Gherghetta and Alex Pomarol. Bulk fields and supersymmetry in a slice of AdS. *Nucl. Phys.*, B586:141–162, 2000.

[72] G.W. Gibbons and D.L. Wiltshire. Space-Time as a Membrane in Higher Dimensions. *Nucl.Phys.*, B287:717, 1987.

[73] S. L. Glashow and S. Weinberg. Natural conservation laws for neutral currents. *PRD*, 15:1958–1965, April 1977.

[74] Sheldon L. Glashow and Steven Weinberg. Natural Conservation Laws for Neutral Currents. *Phys.Rev.*, D15:1958, 1977.

[75] M. L. Goldberger. On the second virial coefficient. *Physics of Fluids*, 2(3):252–255, 1959.

[76] W. D. Goldberger and M. B. Wise. Renormalization group flows for brane couplings. *PRD*, 65(2):025011, January 2002.

[77] M. F. L. Golterman, K. Jansen, and D. B. Kaplan. Chern-Simons currents and chiral fermions on the lattice. *Physics Letters B*, 301:219–223, March 1993.

[78] Maarten F.L. Golterman, Karl Jansen, and David B. Kaplan. Chern-Simons currents and chiral fermions on the lattice. *Phys.Lett.*, B301:219–223, 1993.

[79] P. G. Grinevich and G. E. Volovik. Topology of gap nodes in superfluid^{3}He: π_4 Homotopy group for^{3}He-B disclination. *Journal of Low Temperature Physics*, 72:371–380, September 1988.

[80] PG Grinevich and GE Volovik. Topology of gap nodes in superfluid 3 he: π 4 homotopy group for 3 he-b disclination. *J. Low Temp. Phys.*, 72(5):371–380, 1988.

[81] Y. Grossman and M. Neubert. Neutrino masses and mixings in non-factorizable geometry. *Physics Letters B*, 474:361–371, February 2000.

[82] Yuval Grossman and Matthias Neubert. Neutrino masses and mixings in non-factorizable geometry. *Phys. Lett.*, B474:361–371, 2000.

[83] S.S. Gubser, Igor R. Klebanov, and Alexander M. Polyakov. Gauge theory correlators from noncritical string theory. *Phys.Lett.*, B428:105–114, 1998.

[84] S. Gukov and E. Witten. Gauge Theory, Ramification, And The Geometric Langlands Program. *ArXiv High Energy Physics - Theory e-prints*, December 2006.

[85] Z.-q. Guo and B.-Q. Ma. Fermion families from two layer warped extra dimensions. *Journal of High Energy Physics*, 8:65, August 2008.

[86] Z.-Q. Guo and B.-Q. Ma. A model of fermion masses and mixings triggered by family problem in warped extra dimensions. *Journal of High Energy Physics*, 9:91, September 2009.

[87] Zhi-Qiang Guo and Bo-Qiang Ma. Fermion Families from Two Layer Warped Extra Dimensions. *JHEP*, 08:065, 2008.

[88] Zhi-Qiang Guo and Bo-Qiang Ma. A Model of Fermion Masses and Mixings Triggered by Family Problem in Warped Extra Dimensions. *JHEP*, 09:091, 2009.

[89] A. Hanany and E. Witten. Type IIB superstrings, BPS monopoles, and three-dimensional gauge dynamics. *Nuclear Physics B*, 492:152–190, May 1997.

[90] M. Z. Hasan and C. L. Kane. Colloquium: Topological insulators. *Reviews of Modern Physics*, 82:3045–3067, October 2010.

[91] M.Z. Hasan and C.L. Kane. Topological Insulators. *Rev.Mod.Phys.*, 82:3045, 2010.

[92] J. J. Heckman and C. Vafa. Flavor hierarchy from F-theory. *Nuclear Physics B*, 837:137–151, September 2010.

[93] Jonathan J. Heckman and Cumrun Vafa. Flavor Hierarchy From F-theory. *Nucl. Phys.*, B837:137–151, 2010.

[94] Anson Hook and Jay G. Wacker. Collective Quartics from Simple Groups. *JHEP*, 1006:041, 2010.

[95] R. Jackiw. Delta function potentials in two-dimensional and three-dimensional quantum mechanics,. *Jackiw, R.: Diverse topics in theoretical and mathematical physics*, pages 35–53.

[96] R. Jackiw and C. Rebbi. Solitons with Fermion Number 1/2. *Phys.Rev.*, D13:3398–3409, 1976.

[97] R. Jackiw and C. Rebbi. Solitons with fermion number 1/2. *PRD*, 13:3398–3409, June 1976.

[98] John David Jackson. *Classical electrodynamics*. Wiley, New York, NY, 3rd ed. edition, 1999.

[99] K. Jansen and M. Schmaltz. Critical momenta of lattice chiral fermions. *Physics Letters B*, 296:374–378, December 1992.

[100] Karl Jansen and Martin Schmaltz. Critical momenta of lattice chiral fermions. *Phys.Lett.*, B296:374–378, 1992.

[101] K. Jensen, S. Kachru, A. Karch, J. Polchinski, and E. Silverstein. Towards a holographic marginal Fermi liquid. *PRD*, 84(12):126002, December 2011.

[102] Theodor Kaluza. On the Problem of Unity in Physics. *Sitzungsber.Preuss.Akad.Wiss.Berlin (Math.Phys.)*, 1921:966–972, 1921.

[103] C. L. Kane and E. J. Mele. Quantum Spin Hall Effect in Graphene. *Physical Review Letters*, 95(22):226801, November 2005.

[104] CL Kane and EJ Mele. Quantum spin hall effect in graphene. *Phys. Rev. Lett.*, 95(22):226801, 2005.

[105] D. B. Kaplan. A method for simulating chiral fermions on the lattice. *Physics Letters B*, 288:342–347, August 1992.

[106] D. B. Kaplan, F. Lepeintre, and M. Schmaltz. Flavor from strongly coupled supersymmetry. *PRD*, 56:7193–7206, December 1997.

[107] D. B. Kaplan and S. Sun. New Field-Theoretic Method for the Virial Expansion. *Physical Review Letters*, 107(3):030601, July 2011.

[108] D. B. Kaplan and S. Sun. Spacetime as a Topological Insulator: Mechanism for the Origin of the Fermion Generations. *Physical Review Letters*, 108(18):181807, May 2012.

[109] David B. Kaplan. Flavor at SSC energies: A New mechanism for dynamically generated fermion masses. *Nucl.Phys.*, B365:259–278, 1991. Revised version.

[110] David B. Kaplan. A Method for simulating chiral fermions on the lattice. *Phys.Lett.*, B288:342–347, 1992.

[111] David B. Kaplan. More effective field theory for nonrelativistic scattering. *Nucl.Phys.*, B494:471–484, 1997.

[112] David B. Kaplan. Chiral Symmetry and Lattice Fermions. 2009.

[113] David B. Kaplan. Chiral Symmetry and Lattice Fermions. In L. Lellouch, R. Sommer, B. Svetitsky, A. Vladikas, and L.F. Cugliandolo, editors, *Modern Perspectives in Lattice QCD Quantum Field Theory and High Performance Computing: Lecture Notes of the Les Houches Summer School*. Oxford Univ Pr, 2011.

[114] David B. Kaplan and Howard Georgi. SU(2) x U(1) Breaking by Vacuum Misalignment. *Phys.Lett.*, B136:183, 1984.

[115] David B. Kaplan, Howard Georgi, and Savas Dimopoulos. Composite Higgs Scalars. *Phys.Lett.*, B136:187, 1984.

[116] David B. Kaplan, Francois Lepeintre, and Martin Schmaltz. Flavor from strongly coupled supersymmetry. *Phys.Rev.*, D56:7193–7206, 1997.

[117] David B. Kaplan, Martin J. Savage, and Mark B. Wise. A New expansion for nucleon-nucleon interactions. *Phys.Lett.*, B424:390–396, 1998.

[118] David B. Kaplan, Martin J. Savage, and Mark B. Wise. Two nucleon systems from effective field theory. *Nucl.Phys.*, B534:329–355, 1998.

[119] David B. Kaplan and Martin Schmaltz. Flavor unification and discrete nonAbelian symmetries. *Phys.Rev.*, D49:3741–3750, 1994.

[120] David B. Kaplan and Martin Schmaltz. Domain wall fermions and the eta invariant. *Phys.Lett.*, B368:44–52, 1996.

[121] David B. Kaplan and Sichun Sun. Spacetime as a topological insulator: Mechanism for the origin of the fermion generations. *Phys.Rev.Lett.*, 108:181807, 2012.

[122] JI Kapusta. *Finite-temperature Field Theory*. Cambridge University Press, Cambridge, UK, 1989.

[123] A. Karch and L. Randall. Localized Gravity in String Theory. *Physical Review Letters*, 87(6):061601, August 2001.

[124] A. Karch and S. Sun. Matrix flavor brane and dual Wilson line. *PRD*, 89(6):066008, March 2014.

[125] Andreas Karch and Emanuel Katz. Adding flavor to AdS / CFT. *JHEP*, 0206:043, 2002.

[126] Andreas Karch, Joseph Maciejko, and Tadashi Takayanagi. Holographic fractional topological insulators in 2+1 and 1+1 dimensions. *Phys.Rev.*, D82:126003, 2010.

[127] Andreas Karch and Lisa Randall. Open and closed string interpretation of SUSY CFT's on branes with boundaries. *JHEP*, 0106:063, 2001.

[128] S. Katz and C. Vafa. Matter from geometry. *Nuclear Physics B*, 497:146–154, February 1997.

[129] Sheldon H. Katz and Cumrun Vafa. Matter from geometry. *Nucl. Phys.*, B497:146–154, 1997.

[130] O. Klein. Quantum Theory and Five-Dimensional Theory of Relativity. (In German and English). *Z.Phys.*, 37:895–906, 1926.

[131] Charlotte Kristjansen and Gordon W. Semenoff. Giant D5 Brane Holographic Hall State. 2012.

[132] M. Le Bellac. *Thermal field theory*.

[133] C. Lebrun. Explicit self-dual metrics on CP_2, CP_2,. *J. Diff. Geom.*, 34:223, 1991.

[134] X.J. Liu, H. Hu, and P.D. Drummond. Virial expansion for a strongly correlated Fermi gas. *Phys. Rev. Lett.*, 102(16):160401, 2009.

[135] L. Luo et al. Measurement of the entropy and critical temperature of a strongly interacting fermi gas. *Phys. Rev. Lett.*, 98(8):080402, Feb 2007.

[136] Martin Luscher. Two particle states on a torus and their relation to the scattering matrix. *Nucl. Phys.*, B354:531–578, 1991.

[137] Juan Martin Maldacena. The Large N limit of superconformal field theories and supergravity. *Adv.Theor.Math.Phys.*, 2:231–252, 1998.

[138] Juan Martin Maldacena. Wilson loops in large N field theories. *Phys.Rev.Lett.*, 80:4859–4862, 1998.

[139] N. Marcus, A. Sagnotti, and W. Siegel. Ten-dimensional supersymmetric Yang-Mills theory in terms of four-dimensional superfields. *Nuclear Physics B*, 224:159–179, August 1983.

[140] David Mateos and Diego Trancanelli. The anisotropic N=4 super Yang-Mills plasma and its instabilities. *Phys.Rev.Lett.*, 107:101601, 2011.

[141] E. Mintun, J. Polchinski, and S. Sun. The Field Theory of Intersecting D3-branes. *ArXiv e-prints*, February 2014.

[142] Robert C. Myers. Dielectric branes. *JHEP*, 9912:022, 1999.

[143] Robert C. Myers and Matthias C. Wapler. Transport Properties of Holographic Defects. *JHEP*, 0812:115, 2008.

[144] K. Nakamura et al. Review of particle physics. *J. Phys. G: Nucl. Part. Phys.*, 37:075021, 2010.

[145] K. Nakamura et al. Review of particle physics. *J.Phys.G*, G37:075021, 2010.

[146] K. Nakamura and Particle Data Group. Review of Particle Physics. *Journal of Physics G Nuclear Physics*, 37(7):075021, July 2010.

[147] S. Nascimbène et al. Exploring the thermodynamics of a universal Fermi gas. *Nature*, 463:1057–1060, February 2010.

[148] Ann E. Nelson. A FERMION MASS HIERARCHY WITHOUT FLAVOR CHANGING NEUTRAL CURRENTS IN A TECHNICOLOR MODEL. *Phys.Rev.*, D38:2875, 1988.

[149] Ann E. Nelson and Matthew J. Strassler. Suppressing flavor anarchy. *JHEP*, 0009:030, 2000.

[150] Axel Orgogozo and Slava Rychkov. The S parameter for a Light Composite Higgs: a Dispersion Relation Approach. 2012.

[151] A. Pais and G.E. Uhlenbeck. On the Quantum Theory of the Third Virial Coefficient. *Phys.Rev.*, 116:250–269, 1959.

[152] Giuliano Panico, Michele Redi, Andrea Tesi, and Andrea Wulzer. On the Tuning and the Mass of the Composite Higgs. 2012.

[153] G. Perez and L. Randall. Natural neutrino masses and mixings from warped geometry. *Journal of High Energy Physics*, 1:77, January 2009.

[154] Gilad Perez and Lisa Randall. Natural Neutrino Masses and Mixings from Warped Geometry. *JHEP*, 01:077, 2009.

[155] Joseph Polchinski. Dirichlet Branes and Ramond-Ramond charges. *Phys.Rev.Lett.*, 75:4724–4727, 1995.

[156] Joseph Polchinski and Matthew J. Strassler. Hard scattering and gauge / string duality. *Phys.Rev.Lett.*, 88:031601, 2002.

[157] A. Pomarol and M. Quiros. The Standard model from extra dimensions. *Phys.Lett.*, B438:255–260, 1998.

[158] A. Pomarol and M. Quirós. The standard model from extra dimensions. *Physics Letters B*, 438:255–260, October 1998.

[159] X.-L. Qi, T. L. Hughes, and S.-C. Zhang. Topological field theory of time-reversal invariant insulators. *PRB*, 78(19):195424, November 2008.

[160] X.-L. Qi, T. L. Hughes, and S.-C. Zhang. Topological field theory of time-reversal invariant insulators. *PRD*, 78(19):195424–+, November 2008.

[161] X.-L. Qi, R. Li, J. Zang, and S.-C. Zhang. Inducing a Magnetic Monopole with Topological Surface States. *Science*, 323:1184–, February 2009.

[162] L. Randall and D. Simmons-Duffin. Quark and Lepton Flavor Physics from F-Theory. *ArXiv e-prints*, April 2009.

[163] Lisa Randall and David Simmons-Duffin. Quark and Lepton Flavor Physics from F-Theory. 2009.

[164] V.A. Rubakov and M.E. Shaposhnikov. Do We Live Inside a Domain Wall? *Phys.Lett.*, B125:136–138, 1983.

[165] G. Rupak. Universality in a 2-component Fermi system at finite temperature. *Phys. Rev. Lett.*, 98(9):90403, 2007.

[166] S. Ryu et al. *New J. Phys.*, 12:065010, 2010.

[167] Tadakatsu Sakai and Shigeki Sugimoto. Low energy hadron physics in holographic QCD. *Prog.Theor.Phys.*, 113:843–882, 2005.

[168] Martin Schmaltz and Jesse Thaler. Collective Quartics and Dangerous Singlets in Little Higgs. *JHEP*, 0903:137, 2009.

[169] Martin Schmaltz and David Tucker-Smith. Little Higgs Review. *Ann.Rev.Nucl.Part.Sci.*, 55:229–270, 2005.

[170] N. Seiberg and E. Witten. Electric-magnetic duality, monopole condensation, and confinement in N=2 supersymmetric Yang-Mills theory. *Nuclear Physics B*, 426:19–52, September 1994.

[171] A. Strominger. Massless black holes and conifolds in string theory. *Nuclear Physics B*, 451:96–108, February 1995.

[172] S. Sun, D. B. Kaplan, and A. E. Nelson. Little flavor: A model of weak-scale flavor physics. *PRD*, 87(12):125036, June 2013.

[173] S. Sun and A. Karch. Finite-size effects on the statistical angle of an electron induced dyon in proximity to a topological insulator. *PRB*, 84(19):195115, November 2011.

[174] J. C. Y. Teo and C. L. Kane. Majorana Fermions and Non-Abelian Statistics in Three Dimensions. *Physical Review Letters*, 104(4):046401–+, January 2010.

[175] G.E. Uhlenbeck and E. Beth. The quantum theory of the non-ideal gas I. Deviations from the classical theory. *Physica*, 3(8):729–745, 1936.

[176] G. E. Volovik. Topology of quantum vacuum. *ArXiv e-prints*, November 2011.

[177] Felix Werner and Yvan Castin. The Unitary three-body problem in a trap. *Phys.Rev.Lett.*, 97:150401, 2006.

[178] J. Wess and J. Bagger. Supersymmetry and supergravity. *Princeton, USA: Univ. Pr.*, page 259, 1992.

[179] E. Witten. Solutions of four-dimensional field theories via M-theory. *Nuclear Physics B*, 500:3–42, February 1997.

[180] Edward Witten. Anti-de Sitter space and holography. *Adv.Theor.Math.Phys.*, 2:253–291, 1998.

[181] Zhi-zhong Xing, He Zhang, and Shun Zhou. Updated Values of Running Quark and Lepton Masses. *Phys.Rev.*, D77:113016, 2008.

[182] Tsutomu Yanagida. HORIZONTAL SYMMETRY AND MASS OF THE TOP QUARK. *Phys.Rev.*, D20:2986, 1979.

Appendix A

APPENDIX TO LITTLE FLAVOR THEORY

A.1 Gauge boson couplings

Here we give the gauge boson couplings to quarks, assuming the $[SU(2) \times U(1)]^2$ angles $\gamma_1 = \gamma_2 = \pi/8$ (see eq. (2.8)), using the fit parameters described in the text. For these parameters, the masses of the gauge bosons are as given in eq. (2.40), with $M_{Z'} = 750$ GeV and $M_{Z''} = 1.4$ TeV.

A.1.1 Neutral gauge boson couplings

We parametrize the SM family parts of the neutral gauge boson currents in terms of four 3×3 matrices for each vector meson as $\mathcal{L}_V^{u,d}$ and $\mathcal{R}_V^{u,d}$ where $V = \{Z, Z', Z''\}$ specifies the vector meson, $\mathcal{L}$, $\mathcal{R}$ indicates whether the current is LH or RH, and u, d specifies up-type versus down-type currents. The results for our phenomenological fit are as follows, where the basis is $\{u, c, t\}$ for the up-type quarks, and $\{d, s, b\}$ for the down-type quarks:

$$|\mathcal{L}_Z^u| = \begin{pmatrix} 2.6 \times 10^{-1} & 0 & 1.9 \times 10^{-6} \\ 0 & 2.6 \times 10^{-1} & 9.7 \times 10^{-6} \\ 1.9 \times 10^{-6} & 9.7 \times 10^{-6} & 2.6 \times 10^{-1} \end{pmatrix}, \quad |\mathcal{R}_Z^u| = \begin{pmatrix} 1.1 \times 10^{-1} & 0 & 2.3 \times 10^{-6} \\ 0 & 1.1 \times 10^{-1} & 1.0 \times 10^{-5} \\ 2.3 \times 10^{-6} & 1.0 \times 10^{-5} & 1.1 \times 10^{-1} \end{pmatrix},$$

$$|\mathcal{L}_Z^d| = \begin{pmatrix} 3.2 \times 10^{-1} & 1.0 \times 10^{-6} & 5.0 \times 10^{-6} \\ 1.0 \times 10^{-6} & 3.2 \times 10^{-1} & 2.3 \times 10^{-5} \\ 5.0 \times 10^{-6} & 2.3 \times 10^{-5} & 3.2 \times 10^{-1} \end{pmatrix}, \quad |\mathcal{R}_Z^d| = \begin{pmatrix} 5.5 \times 10^{-2} & 0 & 0 \\ 0 & 5.5 \times 10^{-2} & 3.6 \times 10^{-6} \\ 0 & 3.6 \times 10^{-6} & 5.5 \times 10^{-2} \end{pmatrix}, \tag{A.1}$$

$$|\mathcal{L}^u_{Z'}| = \begin{pmatrix} 2.6\times10^{-3} & 0 & 0 \\ 0 & 2.6\times10^{-3} & 3.4\times10^{-5} \\ 0 & 3.4\times10^{-5} & 3.8\times10^{-3} \end{pmatrix}, \quad |\mathcal{R}^u_{Z'}| = \begin{pmatrix} 1.4\times10^{-2} & 0 & 4.0\times10^{-4} \\ 0 & 1.5\times10^{-2} & 1.7\times10^{-3} \\ 4.0\times10^{-4} & 1.7\times10^{-3} & 3.7\times10^{-1} \end{pmatrix},$$

$$|\mathcal{L}^d_{Z'}| = \begin{pmatrix} 5.\times10^{-3} & 1.9\times10^{-5} & 8.9\times10^{-5} \\ 1.9\times10^{-5} & 4.9\times10^{-3} & 4.1\times10^{-4} \\ 8.9\times10^{-5} & 4.1\times10^{-4} & 3.7\times10^{-3} \end{pmatrix}, \quad |\mathcal{R}^d_{Z'}| = \begin{pmatrix} 6.7\times10^{-3} & 0 & 2.6\times10^{-5} \\ 0 & 6.6\times10^{-3} & 2.0\times10^{-4} \\ 2.6\times10^{-5} & 2.0\times10^{-4} & 8.8\times10^{-3} \end{pmatrix}, \tag{A.2}$$

$$|\mathcal{L}^u_{Z''}| = \begin{pmatrix} 1.9\times10^{-2} & 0 & 7.9\times10^{-5} \\ 0 & 1.9\times10^{-2} & 2.8\times10^{-4} \\ 7.9\times10^{-5} & 2.8\times10^{-4} & 2.9\times10^{-2} \end{pmatrix}, \quad |\mathcal{R}^u_{Z''}| = \begin{pmatrix} 1.4\times10^{-3} & 0 & 0 \\ 0 & 1.4\times10^{-3} & 0 \\ 0 & 0 & 1.3\times10^{-3} \end{pmatrix},$$

$$|\mathcal{L}^d_{Z''}| = \begin{pmatrix} 2.0\times10^{-2} & 1.0\times10^{-4} & 5.0\times10^{-4} \\ 1.0\times10^{-4} & 1.9\times10^{-2} & 2.3\times10^{-3} \\ 5.0\times10^{-4} & 2.3\times10^{-3} & 2.9\times10^{-2} \end{pmatrix}, \quad |\mathcal{R}^d_{Z''}| = \begin{pmatrix} 1.6\times10^{-3} & 0 & 0 \\ 0 & 1.6\times10^{-3} & 0 \\ 0 & 0 & 9.7\times10^{-4} \end{pmatrix}, \tag{A.3}$$

For legibility we have set to zero all entries smaller than 10^{-6}, and only give the absolute values of the entries in the vector meson coupling matrices. These couplings depend on the choice of $\gamma_{1,2}$; for $\gamma_{1,2} = \pi/5$ we find that the largest flavor diagonal coupling of the Z' is bigger by about a factor of six, but remains smaller than the Z diagonal couplings by about a factor of eight.

A.1.2 Charged current couplings

The W boson mass has been fit to experiment, while the W' boson is degenerate with the Z'', with a mass of 1.4 TeV for $\gamma_1 = \gamma_2 = \pi/8$. We write the charged current couplings as

$$-\frac{g_2}{\sqrt{2}}\left(W^+_\mu \bar{u}_i \left[\mathcal{L}^W_{ij} P_L + \mathcal{R}^W_{ij} P_R\right] d_j + {W'}^+_\mu \bar{u}_i \left[\mathcal{L}^{W'}_{ij} P_L + \mathcal{R}^{W'}_{ij} P_R\right] d_j\right). \tag{A.4}$$

For the parameters given in the text, we find for the couplings

$$|\mathcal{L}_W| = \begin{pmatrix} 9.7\times10^{-1} & 2.3\times10^{-1} & 3.8\times10^{-3} \\ 2.3\times10^{-1} & 9.7\times10^{-1} & 4.2\times10^{-2} \\ 8.9\times10^{-3} & 4.1\times10^{-2} & 1.0 \end{pmatrix}, \quad |\mathcal{R}_W| = \begin{pmatrix} 2.2\times10^{-3} & 2.7\times10^{-5} & 0 \\ 2.7\times10^{-5} & 2.2\times10^{-3} & 3.1\times10^{-5} \\ 0 & 2.4\times10^{-5} & 1.1\times10^{-3} \end{pmatrix}$$

$$|\mathcal{L}_{W'}| = \begin{pmatrix} 5.7\times10^{-2} & 1.3\times10^{-2} & 1.4\times10^{-5} \\ 1.3\times10^{-2} & 5.6\times10^{-2} & 3.3\times10^{-3} \\ 1.0\times10^{-3} & 4.4\times10^{-3} & 8.9\times10^{-2} \end{pmatrix}, \quad |\mathcal{R}_{W'}| = \begin{pmatrix} 5.2\times10^{-3} & 6.5\times10^{-5} & 0 \\ 6.4\times10^{-5} & 5.3\times10^{-3} & 7.4\times10^{-5} \\ 0 & 5.9\times10^{-5} & 2.9\times10^{-3} \end{pmatrix} \tag{A.5}$$

where we have set to zero all entries smaller than 10^{-5}. This normalization gives $\mathcal{L}_W = V_{\rm CKM}$.

We see that the model predicts small W couplings to right-handed currents; such couplings can lead to an m_t/m_b enhancement relative to the SM in the weak penguin graph contributing to $b \to s\gamma$, but the above $|\mathcal{R}_W|_{33}$ element is small enough to ensure that this enhancement does not cause conflict with experiment. We see also see that the W' couplings to the SM fermions are quite small and will not lead to problems with precision electroweak corrections. Note that when every gauge field is rescaled by its coupling constant, the W wavefunction is constant around the moose in Fig. 2.2, while the W' wavefunction alternates in sign between white and black sites; it is this sign alternation which causes strong cancellations in the coupling of the W' to SM fermions.

A.2 Index theorem

We prove here the assertion in eq. (2.66), which was also stated without proof in [121]. Define LH and RH eigenmodes

$$MM^\dagger \phi_L^i = \lambda_i \phi_L^i \ , \qquad M^\dagger M \phi_R = \lambda_i \phi_R^i \ , \tag{A.6}$$

where M is the Z_2 invariant mass of eq. (2.64) and eq. (2.65), and the eigenmodes are assumed to be normalized. The set of eigenvalues $\{\lambda_i\}$ are real and non-negative. Then for

$\lambda_i \neq 0$, we can choose $\phi^i_{L,R}$ to satisfy

$$\phi^i_R = \frac{1}{\sqrt{\lambda_i}} M^\dagger \phi^i_L \ , \qquad \phi^i_L = \frac{1}{\sqrt{\lambda_i}} M \phi^i_R \ . \tag{A.7}$$

From eq. (2.65) it follows that $[\mathcal{R}, M^\dagger M] = [\mathcal{R}, M M^\dagger] = 0$; therefore we can choose $\mathcal{R}$ to be diagonal in this same basis; furthermore, since $\mathcal{R}^2 = 1$, its eigenvalues r equal ± 1.

The fermion fields $\psi_{L,R}$ are expanded in the eigenstates $\phi_{L,R}$ times LH or RH spinors. Consider $\lambda_i \neq 0$ and $\hat{z}\psi^i_L = -r_i \psi^i_L$ with $r_i^2 = 1$ (recall that $\hat{z} = \mathcal{R}\gamma_5$); it follows from eq. (2.65) and eq. (A.7) that $\hat{z}\psi^i_R = -r_i \psi^i_R$. Therefore if we define

$$z_L \equiv \mathrm{Tr}\, \hat{z} P_L \big|_{\lambda \neq 0} \ , \qquad z_R \equiv \mathrm{Tr}\, \hat{z} P_R \big|_{\lambda \neq 0} \ , \tag{A.8}$$

we know that

$$z_L = z_R \ . \tag{A.9}$$

Now consider the zeromode solutions to eq. (A.6), with $\lambda_i = 0$. Let $\mathcal{N}^\pm_{L,R}$ be the number of LH or RH zeromodes with $\hat{z} = \pm 1$ respectively. Since M is a finite matrix we have equal number of LH and RH zeromodes,

$$\mathcal{N}^+_L + \mathcal{N}^-_L = \mathcal{N}^+_R + \mathcal{N}^-_R \equiv \mathcal{N} \tag{A.10}$$

We also have

$$\begin{aligned} \mathrm{Tr}\, \mathcal{R} &= -\mathrm{Tr}\, \hat{z} P_L = -\left(z_L + \mathcal{N}^+_L - \mathcal{N}^-_L \right) \\ &= +\mathrm{Tr}\, \hat{z} P_R = +\left(z_R + \mathcal{N}^+_R - \mathcal{N}^-_R \right) \ . \end{aligned} \tag{A.11}$$

Making use of eq. (A.9), eq. (A.10), and eq. (A.11), we arrive at our index theorem eq. (2.66),

$$\left(\mathcal{N}^-_L - \mathcal{N}^-_R \right) = \mathrm{Tr}\, \mathcal{R} \ . \tag{A.12}$$

VITA

Sichun Sun obtained her B.S. in physics and applied mathematics from Peking University, Beijing in 2008. She has been working towards her Ph.D at University of Washington, Seattle since then. She will be a postdoctoral fellow in Hong Kong University of Science and Technology upon graduation. Email: `sichun@uw.edu`